Department of Obstetrics and Gynecology, Ulm University

Prof. Dr. Wolfgang Janni

Roles of p53 isoforms in the POLι dependent DNA damage tolerance pathway

Dissertation submitted to Faculty of Medicine of Ulm University for the degree of "Doctor of Medicine" (Dr. med.)

Yitian Guo

Born in Shaanxi, China

2021

Acting Dean: Prof. Dr. Thomas Wirth

1. Reviewer: Prof. Dr. Lisa Wiesmüller
2. Reviewer: PD. Dr. Mike-Andrew Westhoff

Date of doctoral examination: 16th December 2021

Parts of this work have already been published elsewhere:

Guo Yitian, Rall-Scharpf Melanie, Bourdon Jean-Christophe, Wiesmüller Lisa, Biber Stephanie: p53 isoforms differentially impact on the POLι dependent DNA damage tolerance pathway. Cell Death & Disease 12**:** 941 (2021). https://doi.org/10.1038/s41419-021-04224-3.

Table of content

List of Abbreviations

%	percentage
µg	microgram
µl	microliter
µM	micromolar
ALDH2	Aldehyde Dehydrogenase 2 Family Member
ANXA5	Annexin A5
AP	Apurinic-apyrimidinic Site
ADP	Adenosine Diphosphate
APS	Ammoniumpersulfate
ASPP2	Apoptosis-stimulating of p53 protein 2
ATM	Ataxia Telangiectasia Mutated
ATR	ATM-Related
BAX	Bcl2-Associated X protein
BCA	Bicinchoninic Acid
Bcl-2	B-cell Lymphoma 2
BCL2L	Bcl-2-like 1
BER	Base Excision Repair
bp	Base Pair
BIRC5	Baculoviral inhibitor of apoptosis repeat-containing 5
BrdU	Bromodeoxyuridine
BSA	Bovine Serum Albumin
°C	Degree Celsius
CCT5	Chaperonin containing TCP1 subunit 5
CD28	Cluster of Differentiation 28
CD57	Cluster of Differentiation 57
CD62L	L-selectin
CDC20	Cell division cycle protein 20 homolog
CDK	Cyclin Dependent Kinases

CDKN1A	Cyclin Dependent Kinase Inhibitor 1A
CD34	Cluster of Differentiation 34
cDNA	Complementary Desoxyribonucleic Acid
CETN2	Centrin 2
ChK	Checkpoint Kinase
CldU	5`-Chloro-2`-deoxyuridine
cm	Centimeter
CTD	C-terminal domain
Co-IP	Co-immunoprecipitation
CXCL10	C-X-C motif chemokine ligand 10
DAPI	4',6-Diamidino-2-phenylindole Dihydrochloride
DBD	DNA binding domain
DDR	DNA Damage Response
DDT	DNA Damage Tolerance
DNA LIG	DNA Ligase
ddH_2O	Double-Distilled Water
DFS	Disease-free survival
dH_2O	Distilled H_2O
DNA	Deoxyribonucleic Acid
dNTPs	Deoxynucleotide triphosphates (dATP, dCTP, dGTP and dTTP)
DSB	DNA Double Strands Break
DTT	Dithiothreitol
EDTA	Ethylenediaminetetraacetic Acid
EIF2α	Eukaryotic Initiation Factor 2α
EGFP	Enhanced Green Fluorescent Protein
EGR1	Early growth response protein 1
EGTA	Ethylene-glycol-bis(2-aminoethylether)-N,N,N',N'
ESC	Embryonic stem cell
EXO1	Exonuclease 1

FACS	Fluorescence-Activated Cell Sorting
FANCD2	Fanconi Anemia Complementation Group D2
FBS	Fetal Bovine Serum
FCM	Flow cytometry
FSC	Forward Scatter Channel
FLp53	Full length protein 53
g	Gram
GADD45	Growth Arrest And DNA-Damage-Inducible 45 Alpha
h	Hour(s)
HASMC	Human Aortic Smooth Muscle Cell
HCl	Hydrochloric acid
HD	Hinge domain
HGPS	Hutchinson-Gilford progeria syndrome
HIV-1	Immunodeficiency Virus 1
HLTF	Helicase-like Transcription Factor
HMW	High Molecular Weight
hTERT	Human telomerase reverse transcriptase
hpt	hour(s) post transfection
HR	Homologous Recombination
HRP	Horseradish Peroxidase
IdU	5`-Iodo-2`-deoxyuridine
IF	Immunofluorescence
IFI47	Interferon gamma inducible protein 47
IFIT2	Interferon-induced protein with tetratricopeptide repeats 2
IGF	Insulin-like growth factor
IgG	Immunoglobulin G
IGFBP-3	Insulin-like growth factor-binding protein 3
IGFBP7	Insulin-like growth factor-binding protein 7
IL	Interleukin

IFN-g	Interferon-gamma
IP	Immunoprecipitation
IR	Ionizing Radiation
ITGB7	Integrin Subunit Beta 7
JAK	Janus kinase
JUNB	Transcription factor jun-B
kDa	kilodalton
KLF5	Kruppel Like Factor 5
l	Liter
LAG-3	Lymphocyte-activation gene 3
LB-media	Lysogeny Broth-Media
LOH	Loss of Heterozygosity
LIG	DNA Ligase
M	Molar
mA	Mili-Ampere
MDM2	Mouse Double Minute 2
min	Minute(s)
miR	microRNA
MLV	Murine Leukemia Virus
ml	Milliliter
mm	Millimeter
mM	Millimolar
MMC	Mitomycin C
MMP-3	Matrix metalloproteinase-3
MMR	Mismatch Repair
MMS	Methyl Methanesulfonate
MRE11	Meiotic Recombination 11 Homolog
MRN	Mre11/Rad50/Nibrin; Meiotic recombination 11 homolog-radiation sensitive 50-Nibrin

NER	Nucleotide Excision Repair
NHEJ	Non-Homologous End-Joining
NES	Nuclear Export Signal
NTD	N-terminal domain
nM	Nanomolar
nm	Nanometer
NLS	Nuclear Localization Signal
NOXA	Phorbol-12-myristate-13-acetate-induced protein 1
NPM1	Nucleophosmin
NP40	Nonidet P40
OD	Oligomerization domain
PRIMPOL	Primase And DNA Directed Polymerase
PAI-1	Plasminogen activator inhibitor-1
PAR	Poly(ADP-ribose)
PARI	PCNA-associated Recombination Inhibitor
PARP	Poly(ADP-ribose) Polymerase
PBS	Phosphate-Buffered Saline
PCNA	Proliferating Cell Nuclear Antigen
PCR	Polymerase Chain Reaction
PD-1	Programmed cell death protein 1
PLA	Proximity Ligation Assay
PNK	Polynucleotide Kinase
POL	Polymerase
POLβ	DNA polymerase β
p-PKR	Phospho protein kinase R
PRD	Proline rich domain
PFS	Progression-free survival
PTEN	Phosphatase and tensin homolog
PTM	Posttranslational modifications

PUMA	p53 Up-Regulated Modulator of Apoptosis
p53RE	p53 Response Element
p53WT	Protein 53 wild-type
p21	Protein 21
p53	Protein 53
PIDD	p53-induced protein with a death domain
PMSF	Phenylmethylsulfonyl fluoride
Ras	Rat Sarcoma
RE	Restriction Enzyme
RFS	Recurrence-free survival
RIPA	Radioimmunoprecipitation Assay Puffer
RhoA	Ras Homolog Family Member A
RhoB	Ras Homolog Family Member B
ROCK	Rho-associated protein kinase
ROS	Reactive Oxygen Species
RPA	Replication Protein A
RT	Room Temperature
Saos-2	Human Osteosarcoma Cells
SD	Standard Deviation
SDS	Sodium Dodecyl sulphate
SDS-PAGE	Sodium Dodecyl sulphate Polyacrylamide Gel Electrophoresis
SEM	Standard Error of Mean
SHPRH	SNF2 Histone Linker PHD RING Helicase
SMARCAL1	SWI/SNF Related, Matrix Associated, Actin Dependent Regulator Of Chromatin, Subfamily A Like 1
SOX2	Sex determining region Y box 2
SRS2	Saccharomyces Cerevisiae Helicase 2
SRSF3	Serine/Arginine Rich Splicing Factor 3

SSA	Single Strand Annealing
SSC	Side Scatter Channel
ssDNA	Single Stranded DNA
STAT	Signal transducer and activator of transcription
STAT3	Signal transducer and activator of transcription 3
STIP1	Stress-induced-phosphoprotein 1
STUB1	STIP1 homology and U-Box containing protein 1
SUMO	Small Ubiquitin-like Modifier
SV40	Simian Vaculoating Virus 40
TAD	Transactivation Domain
TEMED	N,N,N',N'- Tetramethylethylenediamine
TGFβ	Transforming Growth Factor Beta
TIAL1	Nucleolysin TIAR
TLS	Translesion Synthesis
TNF	Tumor necrosis factor
TP53	Tumor Protein 53 gene
TPT1	Translationally-controlled tumor protein
TRAF1	TNF receptor-associated factor 1
TS	Template switch
Ub	Ubiquitin
UBC13	Ubiquitin-conjugated Enzyme E2 13
UV	Ultraviolet Light
V	Volt
VCP	Valosin-containing protein
VCAM1	Vascular cell adhesion protein 1
XPA	Xeroderma Pigmentosum, Complementation group A
ZRANB3	Zinc Finger Ran-Binding Domain-Containing Protein

1 Introduction

1.1 The discovery and function of p53

1.1.1 The discovery of p53

Human *Tumor protein p53* (*TP53*) gene, located on chromosome 17p13.1 [97], consists of 13 exons, among them are 11 exons and 2 alternatively spliced exons [5]. Anyone who is interested in cancer research has clearly recognized existence of p53 and its impact on almost every aspect of tumor biology. Despite being discovered 40 years ago, new functions, activities or interactions are still being discovered.

Lionel Crawford and David Lane discovered a non-viral protein that has a molecular weight of around 53 kDa when they immunoprecipitated Simian Vacuolating Virus 40 (SV40) large T-antigen about 40 years ago. Further studies showed that this protein was complexed with the SV40 large T antigen physically [114]. In parallel, Daniel Linzer and Arnold Levine basically made the same observation that a complex of SV40 large T antigen and a 53 kilodalton (kDa) protein exists in SV40-transformed cells [120]. Several other groups have also obtained similar results [110, 135, 181]. Notably, the name “p53”, which was termed due to the molecular weight of the protein itself might be considered a misnaming in these days. Based on its migration in the sodium dodecyl sulphate (SDS)-polyacrylamide gel, the molecular weight of the protein is about 53 kDa. Later it was realized that this was an overestimation since the presence of a proline-rich region decreased the speed of migration of the protein in SDS-polyacrylamide gels. The correct molecular weight of human p53 protein is only 43.7 kDa while the correct molecular weight of mouse p53 is even lower [119].

1.1.2 p53 and cancers

A series of studies have shown that transfected p53 can work very effectively with many established oncogenes (most notably Harvey rat sarcoma viral oncogene homolog, H-Ras) to transform cultured primary cells and can promote immortalization of such cells [62, 95, 158]. In addition, it was demonstrated that the cloned p53 enhanced the transformation characteristics of the established cell line and enhanced the *in vivo* tumorigenic properties [61, 210]. In short, p53 was still considered an oncogene with unknown mechanisms in the 1980s [119].

Conversely, Rotter and colleagues showed that the *TP53* gene was extensively

rearranged in the human leukemia-derived cell line HL60, and its coding sequence was deleted, thereby excluding the production of p53 protein which suggested that p53 function is necessary to prevent cancer [211]. Moreover, with other *TP53* complementary deoxyribonucleic acid (cDNA) clones the transformation effect observed with the earlier clones was lost. When the researchers compared the DNA sequences of the various *TP53* clones used there and in other early studies, they did not detect two identical clones, indicating that at least some clones actually have mutations in the *TP53* coding region. Later the p53 wild-type (p53WT) (also called Full Length p53 or p53α in the following text) sequence derived from normal tissues and *Trp53* mutations were found in tumor-derived murine cell lines [60, 63, 81].

One study demonstrated that in human colorectal tumors, intact alleles encoding p53α were often lost due to mutations, deletions, or a combination of both, so tumor cells did not retain any p53α [14], which indicated a tumor suppressor gene. *TP53* mutations were also found to play a role in the progression to advanced, invasive, and metastatic disease in some cancers [15]. Therefore, previous studies demonstrating a carcinogenic activity of p53 used murine or human p53 mutants which are usually derived from cancer cell lines that overexpress theses p53 mutants. Such mutants can exert a carcinogenic effect through the dominant negative inactivation of endogenous p53α, often further strengthened by a carcinogenic gain of function [37].

For the tumor suppressor gene status to be proven, two additional criteria needed to be fulfilled. Firstly, people carrying germline mutations in the gene should show higher susceptibility to cancer. Secondly, its loss should trigger a cancer-prone phenotype in experimental animal models. p53 fully meets these two criteria with the facts that germline *TP53* mutations are the main cause of the hereditary Li-Fraumeni syndrome, which is characterized by early onset of various types of cancer [126, 186] and p53 knockout mice develop cancers (mainly lymphomas) with high penetrance [55]. In addition, p53-deficient heterozygous *Trp53+/-* mice present various tumors while the tumor spectrum of the *Trp53+/-* mice resembles to the Li–Fraumeni syndrome [54, 56].

1.1.3 p53 and its transcriptional activities

p53 is capable of sliding on DNA to search for the specific binding sites. This sliding ability is dependent on the non-sequence specific binding of p53 C-terminal domain (CTD) [85, 133]. Upon cell stress such as DNA damage, hypoxia, oncogene

activation, etc, p53 is activated to search the specific binding sites via the sequence specific DNA-binding domain (DBD) [18, 53, 65, 101] while sliding on DNA and acts as transcriptional factor through binding to p53 response elements (REs) [65].

Hence, p53 plays essential roles in cell cycle arrest by transactivating genes like *cyclin-dependent kinase inhibitor 1A (CDKN1A,* also called *p21)*, apoptosis by transactivating *Bcl-2 Associated X-protein* (*BAX*), *p53 Up-Regulated Modulator of Apoptosis (PUMA)*, *Phorbol-12-myristate-13-acetate-induced protein 1* (*NOXA)* or regulating p53 itself by transactivating *Mouse Double Minute 2 (MDM2)* which forms a negative-regulatory feedback loop with p53, etc [20, 148, 201].

On the other hand, p53 also represses various target genes though this repression mediated by p53 with several mechanisms have been described [20, 198]: (a) p53 transactivate a target protein and subsequently the target protein serves as repressor, which is an indirect repression, for example, p21, transactivated by p53, suppresses cyclin-dependent kinase (CDK)-dependent phosphorylation of the retinoblastoma protein [214] that keep E2F-regulated genes silence [52]; (b) p53 binds directly to REs and recruits cofactors that repress the target genes or compete with other transcriptional factors which interact with this site [89] .

1.1.4 p53 and DNA damage responses

Precise DNA replication is important for cell homeostasis and genome stability [131]. To protect the genome integrity and stability, the DNA damage response (DDR) network is utilized by cells to detect and repair DNA damage [47]. The loss of intact p53 is a major driving factor for cancer development because cells cannot be fully protected from mutations and genomic aberrations which are the consequence of the absence of this "genomic guardian" [113]. In fact, the best-known function of p53 is its ability to respond to DNA damage. With the emergence of metazoans, genome maintenance has become a special task with unique requirements in germ cells and somatic cell tissues [208].

When mammals are exposed to a series of genotoxic damage types, p53 is stabilized and activated by DNA damage checkpoint signals [177]. The target genes of p53 which might induce cell cycle arrest are diverse. p53 aids the maintenance of the genome stability by allowing DNA repair mechanisms which are used to remove lesions before resumption of cell proliferation. When the DNA damage occurred before entering the S phase, the G1 phase cell cycle can be stopped by p21 which is transcriptionally induced by p53 [59]. During cell cycle arrest, the

respective DNA repair mechanism will start to remove the damage. p53 is also known to be directly involved in the regulation of several DNA repair mechanisms in addition to its function in regulating the cell cycle or apoptosis induction. p53 plays important roles in DNA repair mechanisms including nucleotide excision repair (NER), base excision repair (BER), mismatch repair (MMR), nonhomologous end joining (NHEJ) and homologous recombination (HR) which that are able to repair the DNA lesions in cells [208]. Some of these mechanisms are dependent on p53 transcriptional activities while others are controversial or are independent [22, 71, 175].

1.1.5 p53 and DNA damage tolerance

Previously mentioned DDR are effective in resolving DNA damage. However, some DNA lesions escape from repair mechanisms and lead to the interruption of replication fork progression. As a consequence, cells have adopted DNA damage tolerance (DDT) pathways to bypass lesions encountered during replication which allow the repair of replication obstacles to decrease the frequency of replication fork stalling and the risk of fork collapse [118].

Two DDT pathways have been recognized: translesion synthesis (TLS) and homology-directed DDT including template switch (TS) and fork reversal [162]. Four Y-family polymerases (POLι, POLη, POLκ, Rev1), one B-family polymerase (POLζ, catalytic subunit REV3L) and two A-family polymerases (POLθ and POLν) are able to catalyze the TLS to bypass DNA damage [115, 118, 125, 170]. Due to their more flexible active site these specialized polymerases are enabled to incorporate nucleotides opposite to the damaged DNA template and replicate over the lesions [118, 164]. Therefore this bypass results in an error-prone rescue of the replication fork as it increases mutagenesis [220]. On the contrary, homology-directed DDT including TS and fork reversal is rather error free. Therefore, it is essential for cells to determine which DDT pathway to utilize as the results can be error-prone or error-free. nd this decision is made by Proliferating cell nuclear antigen (PCNA) [51, 88].

PCNA is a homotrimer that encircles DNA and serves as a sliding platform which can mediate the interaction of DNA and proteins including replication associated proteins and cell cycle related proteins [139, 205]. Of note, these functions of PCNA are mainly regulated by post-translational modifications at different lysine residues [88].

When DNA replication encounters the lesions, the replication forks stall and cause

the generation of replication protein A (RPA)-coated single-stranded DNA (ssDNA) [39, 123, 136, 204, 223]. The ssDNA coated by RPA results in the activation of two pathways. On the one hand, the Ataxia telangiectasia mutated and Rad3-related (ATR) protein activates a cell cycle checkpoint [222, 223]. On the other hand, it triggers a the DDT pathway which is mediated by the ubiquitination of PCNA [51, 88] which is graphically shown in Figure 1. RPA recruits the RAD6-RAD18 complex which causes PCNA mono-ubiquitination at Lysine (Lys) 164 of PCNA [86]. This results in the exchange of the replicative POLs by TLS-POLs [84, 187]. In yeast, once being mono-ubiquitinated, PCNA can be further modified at lysine 63 residue (K63) with poly-ubiquitin chains by another E2-E3 ubiquitin ligase Rad5/Ubc13/Mms2 [36, 88, 90, 187, 195]. In mammalians, this poly-ubiquitination is mediated by the Rad5 functional homologs helicase-like transcription factor (HLTF) and SNF2 histone linker PHD RING-helicase (SHPRH) (mammalian orthologs of yeast Rad5 ubiquitin ligase) [144, 197]. Mono-ubiquitination of PCNA leads to TLS while poly-ubiquitination of PCNA induces homology-directed DDT [162].

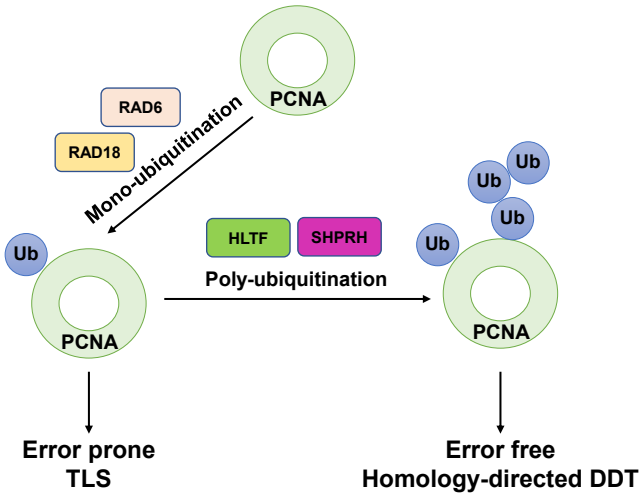

Figure 1 PCNA switchboard triggers DDT in human cells.

When DNA replication encounters the lesions, the DDT pathway which is mediated by the ubiquitination of PCNA can be initiated. PCNA mono-ubiquitination is induced in a RAD6-RAD18 dependent manner. Once being mono-ubiquitinated, PCNA can be further poly-ubiquitinated by the HLTF and SHPRH (mammalian orthologs of yeast Rad5 ubiquitin ligase). In the end, mono-ubiquitination of PCNA leads to TLS while poly-ubiquitination of PCNA leads to homology-directed DDT. (Figure based on [23]).

1.1.5.1 TLS and homology-directed DDT

As both are important pathways for my studies, here, I will briefly introduce the models of TLS and homology-directed DDT, which are also shown in Figure 2 in more detail. Classical studies in yeast have proven that DNA damage results in discontinuous DNA synthesis on both the leading and lagging strands, whereby uncoupling of DNA polymerase and DNA helicase or the restart of DNA synthesis at a distance from the lesion occur [35, 40, 183]. This restart triggers formation of a ssDNA gap behind the replication fork with the lesion located at the 3' end of the ssDNA gap (Figure 2A).

One branch of the DDT pathway is TLS shown in Figure 2H. The replicative DNA polymerase will be temporarily removed, and then a special TLS polymerase will be recruited to the site and replicate across DNA lesions [76]. TLS polymerases lack the proofreading activity, show less processivity in comparison to replicative polymerases and possess more flexible active sites that allow to bypass nucleotides with modifications which might cause conformational changes that stop the normal replicative polymerase. As they show less fidelity in comparison to replicative polymerases, they might incorporate wrong nucleotides during the synthesis. Hence, TLS is mutagenic and error prone and perhaps is one of the major sources of cellular mutation [23]. Recently, findings revealed that POLη messenger RNA (mRNA) and protein are greatly upregulated when cells were treated with Ultraviolet (UV) or cisplatin and promotes cell viability through more efficient bypass of lesions by POLη. This discovery is p53 dependent which suggest that p53 may play certain role in regulating TLS polymerases and involve in TLS process [117, 121].

The second DDT pathway is homology-directed DDT and involves the rearrangement of the replication fork [162]. Two models have been proposed: TS and fork reversal [43, 162]. The TS mechanism is the process when the stalled nascent DNA strand switches to the newly synthesized intact sister strand temporarily in order to replicate across the lesion (Figure 2B and C). The strand invasion process allows the pairing of two newly replicated DNA strands (Figure 2B). Then the structure: sister chromatid junction (SCJ) is formed after filling the ssDNA gap using newly replicated strand based on the undamaged sister strand (Figure 2C). The SCJ is then resolved to complete the damage tolerance process (Figure 2D) [23]. Fork reversal requires the formation of a chicken-foot structure (Figure 2E) followed by the tolerance of damaged DNA [162].

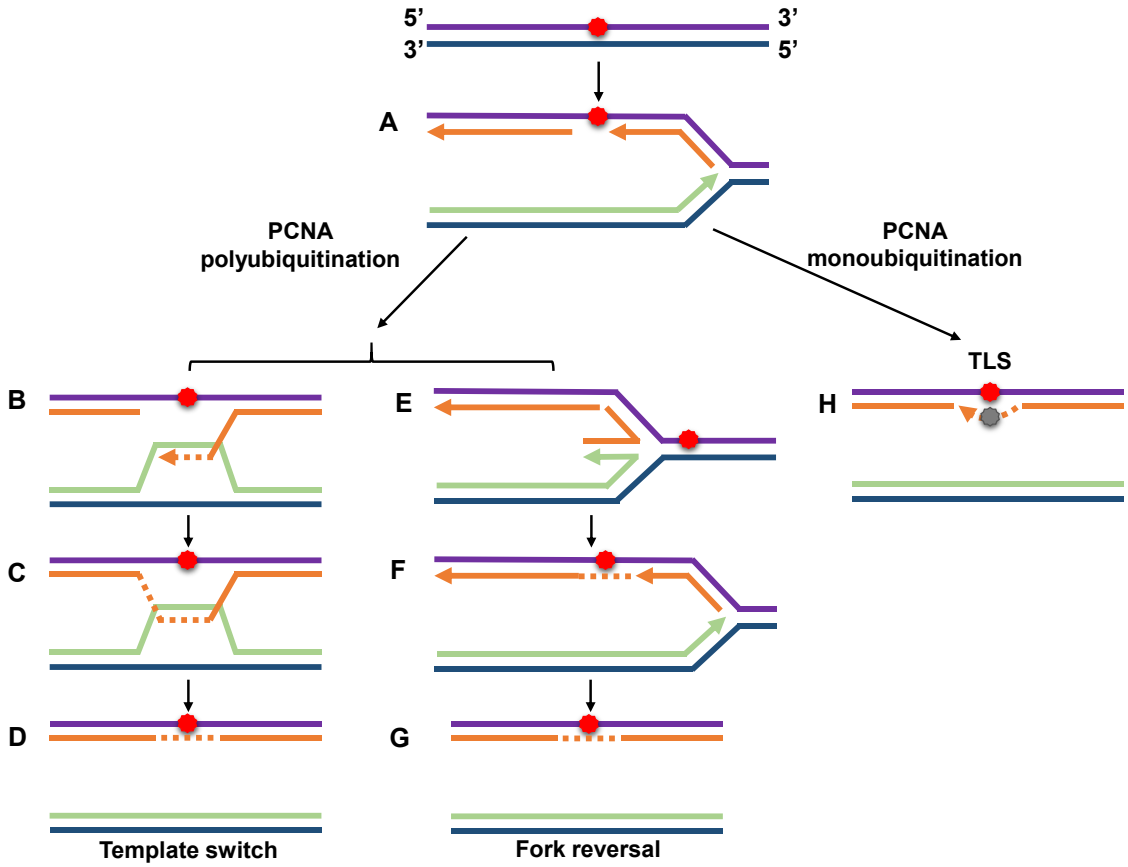

Figure 2 TLS and homology-directed DDT.

A: DNA replication stalls because of DNA damage (dot in red). Restart of DNA synthesis lead to a formation of ssDNA gap behind the replication fork with the lesion located at the 3' end of the ssDNA gap. The ssDNA gap in this figure is on the lagging strand.

B-D: PCNA poly-ubiquitination by HLTF/SHPRH induces TS. Strand invasion is firstly processed and a new DNA strand is synthesized according to the undamaged sister strand, followed by the formation of SCJ. Lastly, SCJ is resolved and generates two duplex DNA strands.

E-G: PCNA poly-ubiquitination induces fork reversal which requires the formation of a chicken foot-structure followed by the opportunity to replicate using the newly synthesized DNA strand of the sister chromatid as a template.

H: PCNA mono-ubiquitination by RAD18/RAD6 results in a switch from the replicative polymerase that will stop at the lesion to a TLS polymerase that will synthesize across the lesion which is error prone.

(Figure based on [23, 162])

1.1.5.2 p53-POLι dependent DDT pathway

Previously, two main DDT pathways were described. Now I would like to present a new p53-POLι dependent DDT pathway which was firstly reported in 2016 by our lab [83]. The model is shown in Figure 3. p53 was found to possess a 3` → 5`

exonuclease activity which suggests a potential role in DNA replication [146, 159]. And this p53-POLι dependent DDT pathway proved that p53α is involved in ensuring safe DNA replication, whereas an exonuclease-deficient mutant p53(H115N) was defective. p53 stimulates the spontaneous replication-associated recombination in a RAD51 independent manner and this stimulation was further found to be dependent on RAD18, TLS-POL POLι, HLTF and Zinc Finger Ran-Binding Domain-Containing Protein 3 (ZRANB3). Further evidence was provided showing that p53 acts together with POLι in so-called idling events when replication encounters the replication barrier. This process protects the replication fork from collapse and permits the DNA damage bypass mediated by HLTF and ZRANB3 or Meiotic Recombination 11 Homolog (MRE11) dependent DNA resection [83]. Idling events are defined such that the exonuclease activity removes the same base which was incorporated by the DNA polymerase [70]. In such a pathway, POLι is proposed to become recruited to the replication site and incorporate the base. While POLι lacks the 3′ → 5′ exonuclease activity [132], p53 forms a complex with POLι and provides the missing 3′ → 5′ exonuclease activity to remove the same base which is incorporated by POLι. During these continuous idling-events, the replication speed (which can be visualized by DNA fiber-spreading assay) slows down. This DDT pathway involving p53 provided new insight into the biological role of p53, moreover, served as the basis of my project.

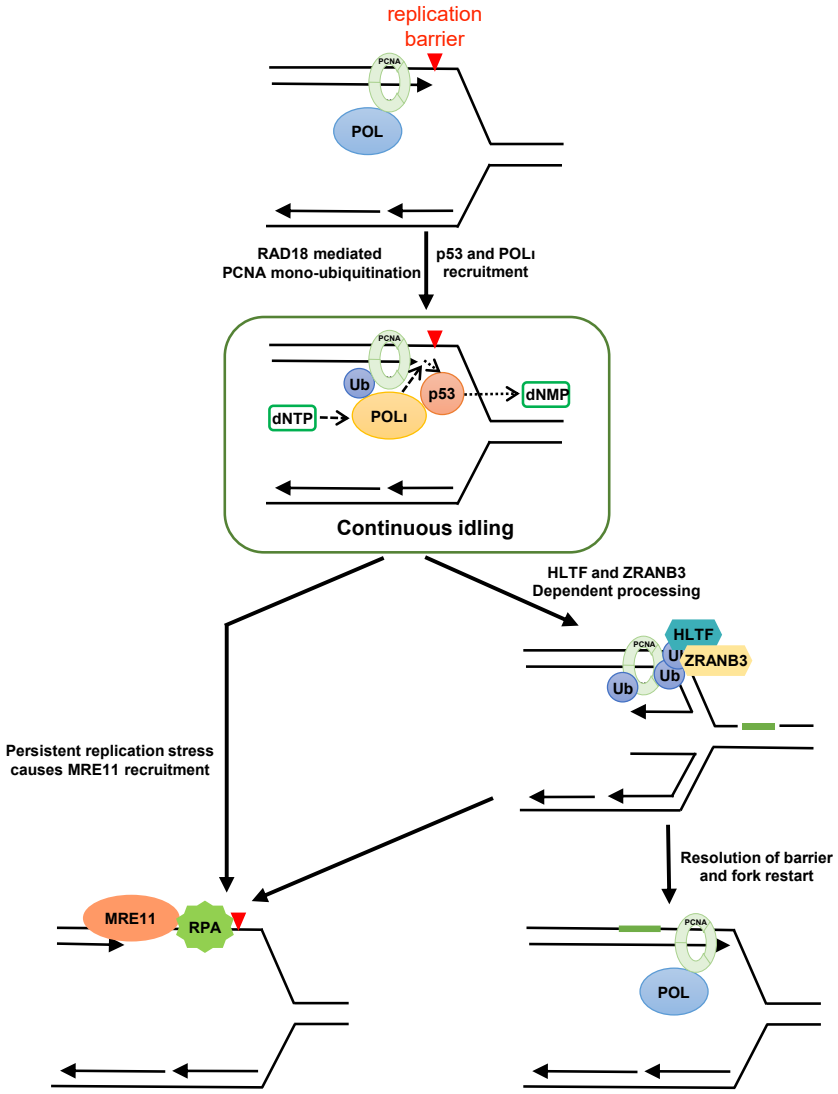

Figure 3 p53-POLι dependent DDT pathway.

When DNA replication encounters the replication barrier (red triangle), mono-ubiquitination (Ub) of PCNA by RAD18 occurs and POLι and p53 are recruited to the replication site. Then p53α and POLι interact and perform continuous idling events which results in the slowdown of replication speed. This allows PCNA-polyubiquitination and the resolution/bypass via HLTF and ZRANB3. A model of the ZRANB3-mediated DDT and repair suggests that ZRANB3 possesses a structure-specific endonuclease activity and could induce a DNA break at the double-stranded region ahead of the replication fork which is coordinated with the replication fork reversal. The free 3‘ - OH group created by ZRANB3 serves as a primer for the newly synthesized DNA sequence [161, 206] (green lines). Finally, the lesion blocking replication is replaced by a newly synthesized DNA sequence (green line) and allows restart of the replication fork. Alternatively, persistent replication stress causes MRE11-dependent ssDNA formation coated by RPA.

(Figure based on [83])

1.2 The identification and function of p53 isoforms

1.2.1 The generation of p53 isoforms

The first *TP53* splice variants were discovered in the 1980s [129, 209], but only after almost 20 years the *TP53* splice variants were found to exist in various species with their biological and clinical relevance being determined [5, 33]. By utilizing different promotors, alternative splicing and the internal ribosome entry site (IRES), 12 different isoforms of *TP53* can be generated while p53α is one of them [78, 102].

As shown in Figure 4A, canonical *TP53* transcription starts from the promoter P1. In human cells this transcript produces p53α, alternative splicing produces variants that contain intron 2 and intron 9. mRNA variants containing exons 9β or 9γ can be created by alternative splicing of intron 9, which produces β and γ subtypes respectively. Both Exon 9β and 9γ contain stop codons and hence exons 10 and 11 remain untranslated in *TP53* β and γ mRNA variants. The α isoform contains all the exons [5, 200].

All p53 isoforms containing the first 40 amino acids are transcribed from the P1 promoter with a spliced-out intron 2 and use the first start codon in Exon 2 for translation [5]. However, translation from the IRES in the 5′ untranslated region (UTR) using the start codon at amino acids 40 results in N-terminally truncated p53 isoforms which can be co-expressed with p53α [5]. The presence of intron 2 in the human *TP53* transcript results in translation-initiation at the start codon at amino acids 40 and results only in the expression (and no co-expression) of the N-terminally truncated Δ40p53 isoforms. Additionally, transcription of the *TP53* mRNA may also start from the internal promoter P2 which is located in intron 4. Then the *TP53* mRNA produced could be translated from start codon 133 and 160 and thereafter produce Δ133p53 and Δ160p53 isoforms separately [5]. Complementary splicing at intron 9 results in the respective β or γ isoforms with N-terminal truncations (Δ133β/γ and Δ160β/γ).

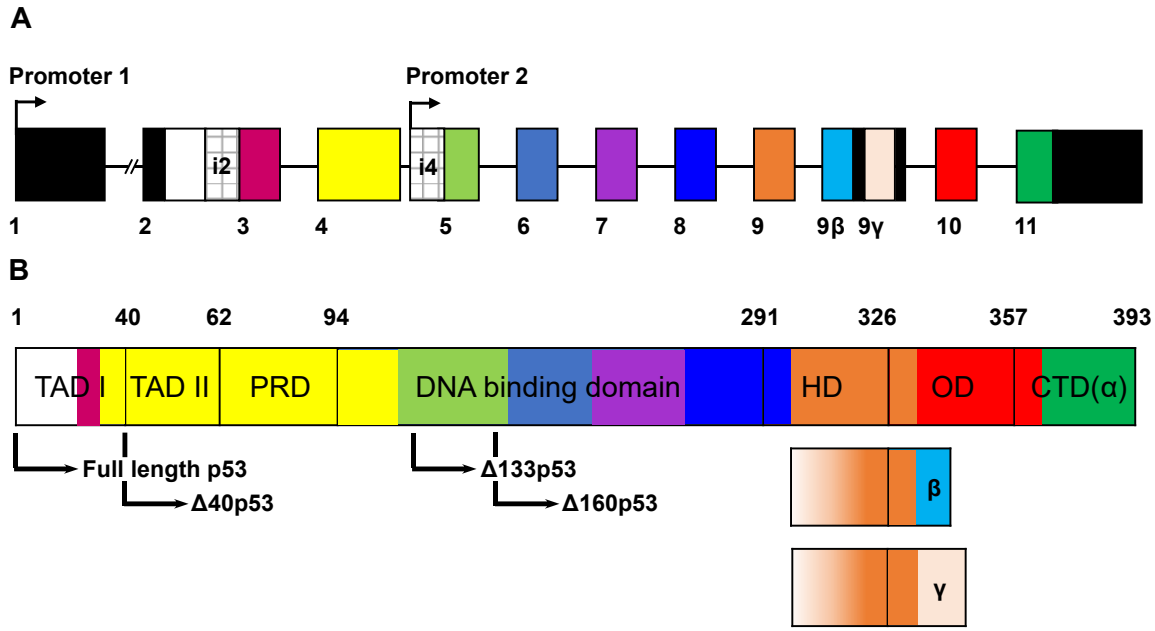

Figure 4 *TP53* gene and p53 domains.

A: The canonical exons (colored boxes) of the *TP53* gene. Different domains of p53 protein are coded by exons with different colors. On the one hand, transcription from promoter 1 results in a mRNA transcript which can be eventually translated into the full length p53 (FLp53) or Δ40p53 isoforms. Δ40p53 isoforms will only be translated with the existence of intron 2 in the mRNA transcript. On the other hand, transcription from promoter 2 could produce a mRNA transcript that codes Δ133p53 or Δ160p53 isoforms. C-terminally deviating isoforms of p53 (α, β and γ) is modulated by alternative splicing of the exon 9.

B: The different domains of the p53 protein and their connections with different *TP53* gene exons shown in A (Exon and its coding domains are in same color). The p53 protein has six different domains. The arrows located at the TAD or DBD indicate the initiating points of the specific isoforms. Colored boxes in the bottom right represent the two C-terminally altered isoforms: β and γ.

(Figure and legend based on [5, 200])

1.2.2 Different domains of p53 isoforms

The p53 protein is a tetramer which usually consists of four monomers and predominantly acts as a transcriptional factor [65]. These tetramers can also stack on each other and lead to DNA looping to enhance p53`s concentration at separated REs [188]. Each p53 monomer contains several domains (Figure 4B), and they are two transactivation domains I and II (TAD I and TAD II, residues 1–61), the proline-rich region (PRD, residues 62–93), the DNA-binding domain (DBD, also named core domain, residues 94–290), the hinge domain (HD, residues 291–324), the

oligomerization domain (OD, residues 325–356), and the C-terminal domain (CTD, residues 357–393) [5, 97].

The intrinsically disordered region (IDR) which is located within the N-terminal region of p53 plays a more and more important role in the signaling cascade [57]. IDR permits highly specific interactions with other proteins though with low affinity [212]. The TAD located within the IDR region has been found to interact with different proteins, which are important for the regulation of p53 protein functions. TAD could interact with factors involved in transcription mechanisms, MDM2, histone acetyltransferase p300-CREB-binding protein [165], DNA replication polymerases and proteins involved in the DDR [44, 58, 111, 140]. Functionally, TAD I plays a more important role than TAD II in p53-dependent transactivation and is required for the DNA damage-induced G1 cell cycle arrest and apoptosis but it is unnecessary for RAS-induced fibroblast senescence [34] while both TADs are able to mediate tumor suppressive signaling pathways of p53 [5, 96, 189]. Δ40p53 isoforms have lost the TAD I (Figure 4B). p53 and MDM2 are linked to each other via an autoregulatory negative feedback loop which could maintain low p53 levels in cells in the absence of stress. MDM2 also binds to the p53 TAD, which counteracts transcriptional transactivation by p53 [44, 111, 140].

The PRD 12 proline residues connects the TAD with the DBD [200]. This region contains five polyproline (PXXP) motifs which serve as the binding site for Src-Homology-3 domains [203] which are responsible for protein-protein interactions in signal transduction [217]. In addition, through proline isomerization, the PRD can change the 3 dimensional (3D) structure of the protein, thereby adjusting the direction and angle of functionally interacting domains [154]. The PRD is necessary for growth inhibition and apoptosis that are triggered by p53 [199] and is functional as a spacer or scaffold module necessary for tumor suppression by p53 [5, 17, 154, 192].

The DBD is the core domain of p53 and mediates the interaction of p53 with DNA. Therefore, a considerable number of highly conserved histidines and cysteines within the DBD facilitate the coordination with Zn^{2+} or Mg^{2+} and thereafter facilitate the p53 conformation and DNA binding ability [46, 160, 215]. Additionally, the interaction of the p53 DBD and its N-terminal help to promote the stability of p53 as tetramer [149]. Mutations in the DBD might cause conformational changes and/or changes of p53`s binding to target DNA sequences. The huge amount of oncogenic

mutations within this domain emphasizes the essential role of this domain in regulating tumor suppression [31]. As we can see in Figure 4B, the Δ40p53 isoforms possess the full-length DBD. the Δ133p53 and the Δ160p53 isoforms lack part of the DBD. While Δ133p53 only partially, Δ160p53 fully misses the first conserved cysteine box of the DBD. Despite the truncation of the DBD [5], Δ133p53β and Δ160p53β are able to adopt a stable 3D conformation [116].

The HD links the DBD and OD. HD provides structural flexibility for p53, which permits binding of p53 to the response elements [10]. Germline mutations of p53 in HD (p53R306P) have been described to be attributed to the loss of transcriptional activation of p53 target genes like *BAX* [108]. Moreover, p53 lacking the HD cannot recognize the consensus sequences, which may indicate that HD plays a role in the allosteric regulation of DNA binding [5, 108].

The OD is essential for the formation of p53 tetramers. In addition, it contains the nuclear export signal (NES) which is masked by p53 tetramerization and therefore keeps p53 in the nucleus where p53 can regulate the expression of target genes [167]. The OD can aid the deformation of the bound DNA and facilitate stable DBD-DNA binding [49]. It has been found that though lysine residues within the OD are unnecessary for p53's tetramerization ability, they can regulate p53-mediated apoptosis and cell cycle arrest [21].

The CTD is responsible for the control of the structure and function of the protein itself [77] and contains multiple post-translational modification sites that can modulate the protein degradation, tetramerization, transactivation and protein interactions [134]. The extreme CTD of p53 is enriched in positively charged amino acids, i.e. arginines, histidines and lysines. These properties allow p53 to nonspecifically bind to negatively charged nucleic acids such as RNA and DNA [172]. Many proteins bind to the CTD and this explains why so many p53 missense mutants still possess their biochemical and biological activities [5]. In addition, the nonspecific DNA binding capacity of the CTD allows p53 to diffuse along the DNA linearly or to transfer itself to another DNA molecule [133].

Different domains of p53 bind to different polymerases and proteins involved in the DDR and DDT. The N-terminal of p53 is required for its interaction with POLβ and POLι. A mutant p53 (L22Q/W23S) failed to interact with POLβ and lose the ability to stimulate BER [221] as well as POLι to generate idling events which is essential for the POLι dependent DDT [25].

RPA binds to p53. p53 D48H/D49H (48,49) and p53 W53S/F54S (53,54) proteins which are mutated at the N-terminal specifically disrupt RPA binding without significantly altering the transactivation activity. The region between amino acids 40–60 of p53 is most critical for RPA binding [1, 168]. The C-terminal of p53 (289 - 393 amino acids) also interacts with RPA [29, 58].

PCNA has as well been proven to bind to the p53 N-terminal and the binding site on p53 is mainly located at amino acids 1 – 50. Moreover, p53ΔN50 and p53ΔN100 which lack the first 50 and first 100 amino acids, respectively, still exert some binding to PCNA as deduced from Co-Immunoprecipitation [16].

The RAD51 binding sites on p53 have been mapped to amino acids 94 – 160 and 264 – 315 of p53 and may be essential for direct suppression of p53 on RAD51-mediated HR [38].

Topoisomerase 1 (topo-I) binds to p53 and it is found that GST-p53 (299 – 390) fusion protein binds to topo-I as efficiently as full-length GST-p53, which indicated that topo-I interacts with the p53 C-terminal [4]. Another group found that GST–p53 containing amino acids 1 – 362 could activate topo-I while GST–p53 containing amino acids 320 – 393 did not and further analysis mapped the topo-I binding site on p53 to amino acids 302 - 320 [73].

1.2.3 The biological roles of p53 isoforms

The biological functions of the p53 isoforms have been revealed gradually and include different aspects of both malignant and normal cells derived from different tissues [5]. Table 1 summarizes these functions.

Table 1 Classification of p53 isoforms according to their molecular functions in different cells/animals. Alterations in protein/gene expression/activity following p53 isoform modulation are presented. (Table based on [5], Updated by Yitian Guo)

Functions related to p53 isoforms	p53 isoforms studied	Cell lines/Models Studied	Altered Expression or Activity	References
Cell cycle regulation	Δ133p53 and p53β	MRC-5, WI-38	*microRNA-34a(miR-34a), Plasminogen activator inhibitor-1 (PAI-1), Insulin-like growth factor-binding protein 7(IGFBP7), matrix metalloproteinase-3 (MMP3), BUB1, cell division cycle protein 20 homolog (CDC20),* p21	[67]
	Δ133p53 and p53β	CD8+ T lymphocytes	L-selectin (CD62L), Programmed cell death protein 1 (PD-1), Lymphocyte-activation gene 3 (LAG-3), *Interleukin 6 (IL-6), IL-8, Serine/Arginine Rich Splicing Factor 3 (SRSF3), Cluster of Differentiation 28 (CD28), CD57*	[141]

	Δ133p53 and p53β	(Hutchinson-Gilford progeria syndrome) HGPS fibroblasts	STIP1 homology and U-Box containing protein 1 (STUB1), SRSF3, *p21, IL-6, IL-8*	[145]
	Δ40p53 (p44)	Transgenic mice	Insulin-like growth factor (IGF)-1R, IGF-1, GADD45, *Phosphatase and tensin homolog (PTEN), MDM2, p21, Insulin-like growth factor-binding protein 3 (IGFBP-3)*	[124]
	Δ40p53 (p44)	Transgenic mice	*p66Shc, G2-M genes*	[69]
	Δ122p53 (mouse ortholog of human Δ133p53)	Transgenic mice	*MDM2, p21*	[180]
	Δ133p53	Human Aortic Smooth Muscle Cells (HAMSCs)	Early growth response protein 1 (EGR1), SRSF1, Kruppel Like Factor 5 (KLF5), p21	[213]
	Δ133p53α	Human neonatal foreskin and normal prostate tissue	*p21, PUMA, NOXA, Human telomerase reverse transcriptase (hTERT)*	[142]
	Δ40p53	129/SvJ Embryonic stem cells (ESCs)	*p21, MDM2*	[196]
Apoptosis	p53β and p53γ	MCF7	p21, BAX	[128]
	Δ40p53	H1299	BAX, p21	[216]

	Δ40p53	A375 melanoma cells	*p21, p53-induced protein with a death domain (PIDD)*	[191]
	Δ113p53 (zebrafish ortholog of human Δ133p53)	Zebrafish model	*p21, MDM2, Bcl-2-like 1 (BCL2L)*	[155]
	Δ113p53	Zebrafish model	*p21, BAX, MDM2, BCL2L*	[45]
	p53β and Δ133p53β	H1299	*BAX*	[33]
	Δ133p53β	HCT116, SW480, LoVo, SW620, Colo205	Ras Homolog Family Member B (RhoB)	[9]
	∆122p53α	Transgenic mice	Annexin A5 (ANXA5), Translationally-controlled tumor protein (TPT1)	[173]
	Δ122p53	Transgenic mice	*Baculoviral inhibitor of apoptosis repeat-containing 5 (BIRC5), TNF receptor-associated factor 1 (TRAF1)*	[180]
	∆133p53α	Human neonatal foreskin and normal prostate tissue	*BAX*	[142]
DNA repair	Δ133p53 and p53β	HGPS fibroblasts	RAD51	[145]
	Δ133p53 or Δ113p53	QSG-7701, Zebrafish model	RAD51, DNA Ligase 4 (LIG4), RAD52	[75]
	∆122p53α	Transgenic mice model	Valosin-containing protein (VCP)	[173]

	∆133p53α	Saos 2, HCT116, H1299	p73, RAD51*, LIG4, RAD52*	[74]
Inflammatory response	Δ122p53 or ∆133p53	Transgenic mice, A549 cells	p21, IF-6, Interferon-gamma (IFN-g)	[179]
	Δ122p53	Transgenic mice	Alpha-enolase, Tumor necrosis factor (TNF)-alpha, Chaperonin containing TCP1 subunit 5 (CCT5), 14-3-3, Aldehyde Dehydrogenase 2 Family Member (ALDH2)	[173]
	Δ122p53	Transgenic mice	IL-6, IL-3, IL-5, TNF-alpha,IFN-g, *STAT1, Transcription factor jun-B (JUNB)*	[180]
Autophagy	Δ40p53	HCT116, H1299	Phospho protein kinase R (p-PKR), Damage-regulated autophagy modulator (DRAM)	[218]
Pluripotency	Δ133p53β	MCF7	*Sex determining region Y box 2 (SOX2), Octamer-binding transcription factor 3/4 (OCT3/4), NANOG*	[8]
	Δ40p53	129/SvJ ESCs	OCT4, GATA-4, NANOG*, IGF-1R*	[196]
Cellular invasion	Δ133p53β	MDA-MB-231, D3H2LN, MCF7, LoVo, SW480, SW620, Colo205, HCT116	E-cadherin, β1-integrin	[68]
	Δ122p53	Transgenic mice model	*Integrin Subunit Beta 7 (ITGB7), Vascular cell adhesion protein 1 (VCAM1)*	[180]

	Δ122p53 or ∆133p53	Transgenic mice model, HCT116	RhoA, Rho-associated protein kinase (ROCK), IL-6	[41]

1.2.4 p53 isoforms exert biological functions in various ways

p53 isoforms exert their cellular roles independently of p53α. For example, Δ40p53α still bind to p53 REs: Δ40p53α binds and activates genes including *MDM2*, *BAX* and *Growth Arrest And DNA-Damage-Inducible 45 Alpha* (*GADD45*) independently of p53α [216]. However, ∆40p53, possesses only TAD II, and therefore transactivates a different set of p53-responsive genes than p53α [176] such as several apoptosis related genes: *Nucleolysin TIAR (TIAL1)* and *Apoptosis-stimulating of p53 protein 2 (ASPP2)* which are not induced by p53α [153]. The ∆160p53 was thought to show similar molecular functions like p53 gain of function mutants due to the missing main part of the DBD which might contribute to oncogenesis [42]. It is described that the Δ160p53α isoform is commonly involved in the gain of function phenotype of mutant p53 proteins like p53(273H), p53(175H) or p53(248W). These authors show that stably and transiently expressed p53(273H) induces Δ160p53 expression as well as some endogenously mutant p53 expressing cell lines, whereas p53α failed to do so [42]. Moreover, they connected the gain of function activities of the p53 mutants with the expression of Δ160p53α and established differences between 2D and 3D cell cultures [42]. However, the exact target genes of Δ160p53α and how Δ160p53α affects the role of p53α remain unclear [5]. Hence, this isoform still requires more research to reveal its role.

In addition, the biological functions of certain p53 isoforms are altered by the existence of other p53 isoforms. For instance, stimulation of proliferation seen for Δ133p53α in p53α fibroblasts was missing in p53-negative MDAH041 fibroblasts [67]. In H1299 cells which are p53α null, the overexpression of Δ133p53α led to increasing DSB repair, whereby knock out of p73 also caused a reduction in DSB repair. However, the change of p73 expression level alone did not affect DSB repair, suggesting that the isoform Δ133p53α and p73 collaborate to upregulate the expression of DSB repair genes including *RAD51*, *RAD52* and *LIG4* when p53α is absent [74]. Therefore, p53 isoforms do not only possess independent functions themselves, but also can cooperate with other isoforms and p53 family members to play biological roles.

Even though lacking the typical OD partially, p53β still indirectly interacts with p53α at the *BAX* promoter and modulates p53 ´s *BAX* promoter activity [33]. On the other side, Δ40p53α and Δ133p53α isoforms, which retain the full OD for direct complex formation with p53α or other α isoforms indeed form particular heterologous

oligomeric complexes, which affect the binding of interacting proteins such as MDM2 and murine double minute X (MDMX) and/or biological activities such as transcriptional activity [5, 80, 216]. The Δ40p53α/p53α complex mediates the transition from pluripotency to differentiation by regulating the transcriptional activity of the *Insulin-like growth factor 1 (IGF1) receptor* as well as *Nanog* [196].

Research has also shown that Δ133p53α exerts a dominant negative effect on apoptosis induction by p53α through direct hetero-oligomerization, which is beneficial to p53 dependent cell cycle modulation and DNA damage repair [67]. Von Muhlinen and colleagues indeed co-immunoprecipitated p53α with FLAG-labeled Δ133p53α and this hetero-oligomerization led to down regulation of p21 mRNA and miR-34a levels, which further proved a dominant negative effect of Δ133p53α also on p53α mediated cell senescence [145]. Induction of Δ133p53α by p53α via the internal *TP53* promoter in the presence of doxorubicin inhibits p53α-dependent apoptosis and G1 cell cycle arrest without affecting the p53α dependent G2 cell cycle arrest in U2OS cells [7]. However, in zebrafish the observed modulation of promoter binding activities of p53 by Δ113p53α (zebrafish ortholog of human Δ133p53α) did not follow a simple dominant negative pattern [50]. Altogether, Δ133p53α differentially affects transcription by p53α in human cells.

Of note, the p53 isoforms hetero-oligomerization influence the biological activities in a dose-dependent manner which is due to the relative expression levels of different isoforms. For instance, lower levels of Δ40p53α enhance the transactivation ability of p53α while higher levels of Δ40p53α inhibit the anti-proliferative effect of p53α [80]. However, the roles of hybrid oligomers containing three or more kinds of p53 isoforms are still unknown [5].

1.2.5 p53 isoforms in cancers

There is accumulating evidence indicating that dysregulation of p53 isoform co-expression in cells may change p53 responses, thereby driving oncogenesis while conferring sensitivity to certain cancer treatments [5]. Table 2 summarizes the roles of p53 isoforms in cancers.

Table 2 The expression of p53 isoforms and their association with clinicopathologic outcomes in human cancers. (Table based on [5, 200], Updated by Yitian Guo)

Isoforms	Key results	References	Tumor type
p53β	• mRNA expression correlated with better disease-free survival (DFS) in breast cancer patients particularly in presence of mutant p53	[11]	Breast
	● mRNA expression is related to estrogen receptor expression in breast cancer. *TP53* mutation status is related to cancer recurrence in the p53β-positive cohort	[32]	Breast
	● mRNA overexpressed in colon adenoma versus non-adenoma/normal colon tissue	[67]	Colon
	● elevated mRNA in renal cell carcinoma (RCC) samples correlating with tumor stage. Unknown p53 mutant status	[184]	RCC
	● mRNA expression correlated with improved DFS and overall survival (OS) in p53 mutant RCC	[219]	RCC
	● high protein expression associated with marker (mutated *Nucleophosmin* (*NPM1)*) of improved OS in p53WT acute myeloid leukemia (AML)	[6]	AML
	● mRNA detected in squamous cell carcinoma of the head and neck (SCCHN)	[30]	SCCHN
	● mRNA and protein detected in melanoma cell lines but not melanocytes	[12]	Melanoma

	● decreased p53β and Nucleoside diphosphate kinase A (NME1) mRNA level in melanoma associated with poorer OS in the presence of p53WT	[157]	Melanoma
p53γ	● mRNA expression in mutant p53 expressing breast tumors improves DFS	[32]	Breast
	● increase mRNA in uterine serous carcinoma (USC) associated with poorer DFS. 2 samples out of 27 samples harbor *TP53* somatic mutations	[27]	USC
	● high protein expression associated with marker (mutated *NPM1*) of improved OS in p53WT AML	[6]	AML
	● mRNA detected in SCCHN, tumor adjacent tissues and normal tissues	[30]	SCCHN
Δ40p53α	● increased mRNA in breast tumor and associated with triple negative subtype	[11]	Breast
	● decreased Δ40p53α:p53 (mRNA) ratio is associated with increased DFS in breast cancer	[143]	Breast
	● mRNA expression correlated with better recurrence-free survival (RFS) in patients with p53WT mucinous/serous ovarian cancer	[92, 91]	Ovarian
	● mRNA highly expressed in melanoma cell lines but low in melanocytes	[12]	Melanoma
	● protein detected glioblastoma tissues not in non-tumor cerebral cortex	[190]	Glioblastoma
Δ40p53β/γ	● mRNA expression reduced in melanoma versus normal tissues	[157]	Melanoma

Δ133p53(α)	● high mRNA expression correlated with improved RFS and OS in patients with mutant p53 expressing serous ovarian cancer	[92]	Ovarian
	● reduced mRNA expression in endometroid ovarian cancer compared to mucinous and serous ovarian cancer	[91]	Ovarian
	● elevated mRNA expression in high-grade serous ovarian cancer associated with improved OS and progression-free survival (PFS)	[26]	Ovarian
	● reduced mRNA expression in colon adenoma compared to non-adenoma/normal colon tissue	[67]	Colon
	● elevated mRNA expression correlated with poorer DFS in colon cancer	[41]	Colon
	● increased expression and Δ133p53/p53 (mRNA) ratio in Cholangiocarcinoma associated with poorer OS	[152]	Cholangiocarcinoma
	● lower mRNA expression in p53WT RCC versus normal adjacent tissue	[106]	RCC
	● mRNA detected in SCCHN	[30]b	SCCHN
	● elevated mRNA level in lung cancer versus adjacent non-cancer tissue	[66]	Lung
	● elevated protein level in melanoma versus normal tissue	[157]	Melanoma
	● elevated mRNA expression and Δ133p53/p53α (mRNA) ratio in esophageal squamous cell carcinoma (ESCC) versus adjacent normal tissue; correlated with poor OS and PFS	[194]	ESCC
	● increased protein expression in invasive versus non-invasive breast cancer	[137]	Breast

Δ133p53β /γ	● mRNA expression decreased in HER2+ breast tumors and associated with poorer DFS and OS	[68]	Breast
	● increased mRNA expression in *TP53* WT glioblastoma	[99]	Glioblastoma
	● mRNA detected in SCCHN	[30]	SCCHN
	● increased mRNA level indicates poorer OS in *TP53* WT melanoma	[157]	Melanoma
	● elevated mRNA level in subsets of prostate cancer and correlated with shorter PFS	[100]	Prostate
Δ160p53α	● elevated protein level in melanoma compared to normal tissue	[157]	Melanoma
	● pro-oncogenic ability inducing p53 mutant-like phenotype, possibly involved in p53 mutant gain of function	[42]	

Increased expression of p53β was found to correlate with better DFS and/or OS in breast cancer, clear cell RCC, AML and melanoma [6, 11, 157, 219] and was detected in several other tumor types [30, 67]. Overexpression of p53β in cancer cell lines and normal fibroblasts that co-express endogenously p53 isoforms induce apoptosis and cell senescence via up-regulation of genes including *BAX*, *p21* and *miR-34* in a p53α dependent manner [67]. In p53 mutant expressing breast cancer patients, p53ß and p53γ may compensate the function of p53α and result in low cancer recurrence and an OS as good as that of breast cancer expressing p53α [11, 32]. Other researches have reported that the relative higher expression of p53γ isoforms among all isoforms is related to reducing the risk of cancer progression in uterine serous carcinoma [27].

Δ40p53α expression level in glioblastoma and breast cancer is higher than that in corresponding normal tissues [11, 190]. It is also found to be associated with more malignant triple-negative breast cancer [11]. Along this line, lower Δ40p53α/p53α ratio indicates decreasing progression of breast cancer [143]. However, the expression of Δ40p53α in mucinous ovarian cancer is associated with improved recurrence-free survival [91]. In summary, Δ40p53α is highly relevant to cancers, but whether it is oncogenic or tumor suppressor is unknown since the activity of Δ40p53α is dependent on the cell context and on the co-expressed oncogenes.

Δ133p53α has been proven to be overexpressed in tumor tissues of cholangiocarcinoma, lung cancer, colon cancer and ovarian cancer [66, 67, 92, 152]. Δ133p53α overexpression was reported to be accompanied by reduced p21 expression in lung cancer tissues though this relationship was not statistically significant due to the small sample size [66]. Increased expression of the Δ133p53α isoform relative to p53α correlated with poor DFS in colorectal cancer patients. The mechanism was found to be tumor invasion promoted by the Δ133p53α activated Janus kinase (JAK) - signal transducer and activator of transcription 3 (STAT3) and Ras Homolog Family Member A (RhoA) - Rho-associated protein kinase (ROCK) pathway [41]. However, Δ133p53α expression is related to better DFS and OS in advanced serous ovarian cancer tissues with mutated *TP53*, which may indicate that mutated *TP53* modifies the prognosis of patients associated with p53 isoforms [5].

One type of p53 isoform was never expressed alone as the only p53 protein in cancer or normal cells, it is of more interest to learn the functions of co-expression of p53 isoforms [5]. Taken together, the expression levels and roles of p53 isoforms in cancers

varied. Evidence above demonstrate that most tumors listed in Table 2 present high expression level of ΔN-isoforms and is correlated with poorer prognosis while the C-terminally altered isoforms show diverse effects.

1.3 Aim of study

p53 isoforms exert specific biological roles in DNA damage repair, aging, senescence, etc. Interestingly, they also feature aberrant expression patterns in different types of cancers leading to altered biological functions through mutual interference within differently composed isoforms. Therefore, p53 isoforms have increasingly attracted attention among researchers. Precise knowledge of their roles in cells, especially cancer cells, and how the expression of single isoforms or co-expression of several isoforms influences the activity of these cells will provide new insights in cancer development and responsiveness to cancer treatment.

Moreover, the novel role of p53α in the p53-POLι dependent DDT pathway could facilitate the DNA lesion bypass in cancer cells, which may indicate that p53α could enhance the cellular resistance to DNA lesions and promote the survival of cancer cells under stress such as during cancer therapy. It will be appealing to understand whether the isoforms of p53 including C-terminally modified isoforms and N-terminally truncated (ΔN)-isoforms are also involved in the p53-POLι dependent DDT pathway. Even more fascinating is the perspective to investigate how p53 isoforms affect the role of p53α in the p53-POLι dependent DDT pathway by co-expression of p53α and its isoforms as this is the situation happening in a lot of cancer and normal cells. The project of this thesis is to elucidate the role of the p53 isoforms in the p53-POLi dependent DDT and by doing so to gain deeper knowledge of the p53 isoforms in the development of cancer.

2 Material and Methods

2.1 Materials

2.1.1 Chemicals and solutions

2-Mercaptoethanol	Sigma-Aldrich, St. Louis, USA
Acetic acid	Sigma-Aldrich, St. Louis, USA
Acrylamide/Bisacrylamide (30%)	National Diagnostics, Atlanta, USA
Agarose, SeaKem LE	Lonza, Köln, Germany
Ammoniumpersulfate (APS)	BioRad, Hercules, USA
Ampicillin sodium salt	Sigma-Aldrich, St. Louis, USA
Aqua ad iniectabilia	B.Braun, Melsungen, Germany
Bacto Agar	BD Biosciences, Franklin Lakes, USA
Bacto Tryptone	BD Biosciences, Franklin Lakes, USA
Bacto Yeast extract	BD Biosciences, Franklin Lakes, USA
Bromophenol blue	BioRad, Hercules, USA
1,4-Diazabicyclo[2.2.2]octane (DABCO)	Sigma-Aldrich, St. Louis, USA
Dimethylsulfoxide (DMSO)	Merck, Darmstadt, Germany
dNTP-Mix (10 mM)	NEB, Frankfurt, Germany
Dithiothreitol (DTT)	Sigma-Aldrich, St. Louis, USA
Deoxycholic Acid sodium	Sigma-Aldrich, St. Louis, USA
Ethidium bromide	Sigma-Aldrich, St. Louis, USA
Ethylene-diamine-tetraacetic acid (EDTA)	Roth, Karlsruhe, Germany
Ethylene-glycol-bis(2-aminoethylether)-N,N,N',N' (EGTA)	Roth, Karlsruhe, Germany
FACS Clean	BD Biosciences, Franklin Lakes, USA
FACS Flow	BD Biosciences, Franklin Lakes, USA
FACS Rinse	BD Biosciences, Franklin Lakes, USA

Fetal Bovine Serum (FBS) superior	Biochrom, Berlin, Germany
FluoDNA Gel Stain (Fluorescin)	Promokine, Heidelberg, Germany
Formaldehyde 37% ChemSolute	Sigma-Aldrich, St. Louis, USA
Formaldehyde 16%(w/v) methanol free	Thermo Scientific, Waltham, USA
100x L-Glutamine (200 mM)	Gibco, Waltham, USA
Glycerol	Sigma-Aldrich, St. Louis, USA
Glycine	Sigma-Aldrich, St. Louis, USA
Glycerol phosphate Disodium	Sigma-Aldrich, St. Louis, USA
Goat serum	Sigma-Aldrich, St. Louis, USA
HCl (1M)	Sigma-Aldrich, St. Louis, USA
HEPES (1M)	Gibco, Waltham, USA
Isopropanol	Sigma-Aldrich, St. Louis, USA
Mccoy's 5a medium modified	Gibco, Waltham, USA
$MgCl_2$	Sigma-Aldrich, St. Louis, USA
Milk powder	Roth, Karlsruhe, Germany
Mitomycin C (MMC)	Sigma-Aldrich, St. Louis, USA
NaCl	Sigma-Aldrich, St. Louis, USA
Nonidet P40 (NP40)	Sigma-Aldrich, St. Louis, USA
PCR-Buffer S (10x)	Peqlab, Erlangen, Germany
100x Penicillin-Streptomycin-Glutamine	Gibco, Waltham, USA
Poly-L-Lysine	Sigma-Aldrich, St. Louis, USA
Ponceau S solution	Sigma-Aldrich, St. Louis, USA
phenylmethylsulfonyl fluoride (PMSF)	Roche, Mannheim, Germany
Proteinase Inhibitor Cocktail tablets	Roche, Mannheim, Germany
Proteinase K	Sigma-Aldrich, St. Louis, USA
Rotiophorese 10x SDS-PAGE buffer	Roth, Karlsruhe, Germany

RPMI 1640	Gibco, Waltham, USA
Sodium Dodecyl sulphate (SDS)	Merck, Darmstadt, Germany
Sodium fluoride	Merck, Darmstadt, Germany A
Sodium metavanadate ($NaVO_3$)	Sigma-Aldrich, St. Louis, USA
Sucrose	Sigma-Aldrich, St. Louis, USA
Synth-a-Freeze	Gibco, Waltham, USA
Taq-DNA-Polymerase	Peqlab, Erlangen, Germany
N,N,N',N'-Tetramethylethylendiamide (TEMED)	Roth, Karlsruhe, Germany
Tris pure Ph.Eur., USP	AppliChem, Darmstadt, Germany
Tris-HCl	Sigma-Aldrich, St. Louis, USA
Triton X-100	Sigma-Aldrich, St. Louis, USA
Trypan Blue Stain 0.4%	Gibco, Waltham, USA
Trypsin	PAN biotech, Aidenbach, Germany
Tween 20	Merck, Darmstadt, Germany
Vectashield moutning medium	Vectorlab, Burlingame, USA

2.1.2 Experimental Kits and other materials

Amaxa transfection solution Kit V	Lonza, Basel, Switzerland
BCA Protein Assay Kit	Thermo Scientific, Waltham, USA
Cell-Scrapers	Sarstedt, Nümbrecht, Germany
Ceramic plates (size: 8 x 10 x 0.075 cm)	Amersham Biosciences, GE Healthcare, München, Germany
Clarity Western ECL Substrate	BioRad, Hercules, USA
Combs	Amersham Biosciences, GE Healthcare, München, Germany

Cover Slides (24x40/60 mm)	Menzel-Gläser, Braunschweig, Germany
Cover Slips (24x40/60 mm)	Menzel-Gläser, Braunschweig, Germany
Cryotubes	Greiner-Bio-One, Frickenhausen, Germany
Cell Line Nucleofector Kit V	Lonza, Basel, Switzerland
dNTPs (5 mM stock)	Peqlab, Erlangen, Germany
Electroporation cuvettes (0.4 mm)	BioRad, Hercules, USA
FACS tubes (5 ml)	BD Biosciences, Franklin Lakes, USA
Filter Paper Whatmann 3MM	Schleicher and Schüll, München, Germany
FCM tube	Sarstedt, Nümbrecht, Germany
Gel caster SE215	Hoefer Pharmacia Biotech, CA, USA
Glass plates (size: 8 x 10 x 0.075 cm)	Amersham Biosciences, GE Healthcare, München, Germany
Hybond-C-Extra Nitrocellulose	Amersham Biosciences, GE Healthcare, München, Germany
Immobilon-P Membrane (PVDF)	Amersham Biosciences, GE Healthcare, München, Germany
PowerPrep-HP Plasmid Maxi-Prep kit	OriGene, Rockville, USA
Protein G Sepharose 4 Fast Flow	GE healthcare, München, Germany
Markers	
6x DNA loading dye	MBI Fermentas, St. Leon-Rot, Germany

PageRuler Prestained Protein Ladder	Thermo Scientific, Waltham, USA
Menzel-Gläser superfrost ultra (plus)	Menzel-Gläser, Braunschweig, Germany
Mircrotube (1.5ml)	Sarstedt, Nümbrecht, Germany
Mircrotube (2ml)	Sarstedt, Nümbrecht, Germany
Mircrotube (0.5ml)	Sarstedt, Nümbrecht, Germany

Mycoplasma primer — Thermo Scientific, Waltham, USA

5’ primers (Myco-5’)

CGC CTG AGT AGT ACG TWC GC

TGC CTG RGT AGT ACA TTC GC

CGC CTG AGT AGT ATG CTC GC

CGC CTG GGT AGT ACA TTC GC

3’ primers (Myco-3’)

GCG GTG TGT ACA ARA CCC GA

GCG GTG TGT ACA AAC CCC GA

(R = mixture of G and A; W = mixture of T and A)

10x PCR buffer (including 5 mM $MgCl_2$)	Peqlab, Erlangen, Germany
Restore™ Western Blot Stripping Buffer	Thermo Scientific, Waltham, USA
Rotiphorese 10x SDS-PAGE buffer	Roth, Karlsruhe, Germany
Surgical Disponsable Scalpels	B.Braun, Melsungen, Germany
SONOREX SUPER RK 31	Bandelin, Berlin, Germany
Taq-DNA-Polymerase (5U/µl)	Peqlab, Erlangen, Germany

TE-Buffer	OriGene, Rockville, USA	

2.1.3 Buffers and solutions

Cell lysis buffer for protein extraction	50 mM	Tris-Base, pH 7.4
	150 mM	NaCl
	2 mM	EGTA
	2 mM	EDTA
	25 mM	Sodium fluoride
	25 mM	β-Glycerol phosphate
	0.1 mM	$NaVO_3$
	0.2 %	Triton X-100
	0.3 %	Nonidet P40
	1 Protease inhibitor cocktail tablet in 10 ml	
IP lysis buffer	50 mM	Tris-HCl, (pH 8)
	150 mM	NaCl
	1 %	NP40
	1 Protease inhibitor cocktail tablet in 10 ml	
CSK buffer	250 mM	Sucrose
	25 mM	KCl
	10 mM	HEPES
	1 mM	EGTA
	1 mM	$MgCl_2$
RIPA buffer without inhibitors	10 mM	Tris-HCl (pH 7,4)
	25 mM	NaF
	20 mM	NaCl
	1 %	NP40
	1 mM	Deoxycholic Acid sodium

	1 %	SDS
RIPA buffer with inhibitors	10 mM	Tris-HCl (pH 7,4)
	25 mM	NaF
	20 mM	NaCl
	1 %	NP40
	1 %(w/v)	Deoxycholic Acid sodium
	1 %	SDS
	10 mM	PMSF
	10 mM	Na_3VO_4
	1 mM	DTT
	1 Protease inhibitor cocktail tablet in 10 ml	
4x SDS Stacking gel buffer	0.5 M	Tris/HCl, pH 6.8
	0.4 %	SDS
4x SDS Separating gel buffer	1.5 M	Tris/HCl, pH 8.8
	0.4 %	SDS
6x SDS loading buffer	350 mM	Tris/HCl, pH 6.8
	9.3 % (w/v)	DTT
	10 % (w/v)	SDS
	36 % (v/v)	Glycerol
	0.6 % (w/v)	Bromophenol blue
	10 %	Mercaptoethanol
	(freshly added)	
10x High-molecular-weight (HMW) buffer	495 mM	Tris-Base
	400 mM	Glycine
10 x LB-medium	100 g	Bacto™Tryptone
(Luria-Bertani, Sambrook *et al.,* 2001)	100 g	NaCl

	50 g	Bacto™Yeast extract
	fill to1 L with ddH_2O and autoclaved	
1 x LB-medium	100 ml	10 x LB-medium
	900 ml	ddH_2O
	Autoclaved	
1 x PBS-EDTA	0.2%	EDTA in 1 x PBS
1 x PBST	0.1 %	Tween 20 in 1x PBS
Pre-extraction buffer for	20 mM	HEPES, pH 7.4
immunofluorescence	50 mM	NaCl
	1 mM	EDTA
	3 mM	$MgCl_2$
	300 mM	Sucrose
	0.5 %	Triton X-100
50x TAE-buffer	2 M	Tris-Base
	1 M	Acetic acid
	0.1 mM	EDTA
	pH	8.3
TBST	20 mM	Tris/HCl, pH 7.6
	137 mM	NaCl
	0.1 %	Tween 20
LB-Agar	15 g	Bacto-Agar in 1l 1xLB-medium
	(autoclaved, warm and apply antibiotics before use)	
Lysis mix for Mycoplasma test	0.45 %	Tween20
	0.45 %	NP40

	1 % Proteinase K (stock: 1mg/ml)
	98.1 % ddH_2O
Lysis buffer for DNA fiber-spreading assay	0.5 % SDS
	200 mM Tris–HCl, pH 7.4
	50 mM EDTA

2.1.4 Cell culture medium

Culture medium for suspension cells (K562 cells and K562 (*HR-EGFP / 3'EGFP*) cells)

RPMI 1640 medium (Gibco, Waltham, USA)

13 % fetal bovine serum (Biochrom, Merck Millipore, Darmstadt, Germany)

1.3 % 100 x Penicillin-Streptomycin-Glutamine (Gibco, Waltham, USA)

For culture medium for suspension cells (-antibiotics), 1.3 % 100 x L-Glutamine (Gibco, Waltham, USA) was absent

For electroporation, RPMI 1640 Medium (no phenol red) (Gibco, Waltham, USA) was used.

Culture medium for adherent cells (Saos 2 cells)

McCoy's 5A (Modified) Medium (Gibco, Waltham, USA)

10 % fetal bovine serum (Biochrom, Merck Millipore, Darmstadt, Germany)

1 % 100 x Penicillin-Streptomycin-Glutamine (Gibco, Waltham, USA)

For culture medium for adherent cells (-antibiotics), 1 % 100 x L-Glutamine (Gibco, Waltham, USA) was absent.

2.1.5 Equipment

Agarose gel-electrophoresis chamber:

RunOne™ Electrophoresis Cell	EmbiTec, San Diego, USA
PerfectBlue MiniM	Peqlab, Erlangen

Analysis Balances:

P1200	Mettler Toledo, Gießen, Germany
Sartorius BP61	Sartorius, Göttingen, Germany

Autoclave, Varioklav 75S	H+P, Oberschleißheim, Germany

Centrifuges:

Biofuge 13	Heraeus-Sepatech, Osterode, Germany
Biofuge pico	Kendro, Osterode, Germany
Multifuge 1$_{S-R}$	Kendro, Osterode, Germany
Multifuge 3$_{S-R}$	Kendro, Osterode, Germany
Rotanta 96R	Hettich, Tuttlingen, Germany
Cytospin3 Centrifuge	Shandon, Bohemia, USA
FACSCalibur™	BD Biosciences, Franklin Lakes, USA
ChemiDoc MP Imaging System	BioRad, Hercules, USA
Gene Pulser Xcell Electroporation System	BioRad, Hercules, USA
Incubators:	
Incubator B6760	Heraeus, Hanau, Germany
Incubator 311	Thermo Scientific, Waltham, USA
Incubator 3862	Forma Scientific, Marietta, USA
Lamina Flow:	
Clean Air DLF/REC6	Clean Air Techniek, Woerden, Netherlands
Clean Air DLF/BSS6	Clean Air Techniek, Woerden, Netherlands
NanoDrop 2000 Spectrometer	Thermo Scientific, Waltham, USA
Nucleofector 2b Device	Lonza, Basel, Switzerland
Microscopes:	
Axiovert 25	Zeiss, Jena, Germany
Olympus IX50-S8F	Olympus, Tokyo, Japan
Olympus BX51	Olympus, Tokyo, Japan
Keyence BZ-9000	Keyence Germany, Neu-Isenburg

pH-Meter Seven Multi	Mettler Toledo, Gießen, Germany
Tecan Sunrise Photometer	Tecan, Crailsheim, Germany
Microwave intellowave	LG, Seoul, South Korea
Polyacrylamide-Gel electrophoresis system:	
Mighty Small II Mini SE250	Hoefer, San Francisco, USA
Mighty Small TE22	Hoefer, San Francisco, USA
Power Supply:	
EPS 1000	Amersham Biosciences, GE Healthcare, München, Germany
EPS 1001	Amersham Biosciences, GE Healthcare, München, Germany
Shakers:	
CertomatR	B.Braun, Melsungen, Germany
Rotamax 120	Heidolph, Schwabach, Germany
Variospeed	Biotech-Fischer, Reiskirchen, Germany
EasiaShaker	Medgenix, Ratingen, Germany
PCR FlexCycler	Analytic Jena, Jena, Germany
Tissue Culture Flask	Sarsted, Nümbrecht, Germany
($25cm^2$, $75cm^2$, $175cm^2$)	
Tissue Culture Dish	Sarsted, Nümbrecht, Germany
(100x20mm, 150x20mm)	
Tissue Culture Plate	Sarsted, Nümbrecht, Germany
(6 well, 12 well, 24 well, 96 well)	
Tube PP	Sarsted, Nümbrecht, Germany
(15ml, 50ml)	

VortexGenie 2	Bender und Hobein, Zürich, Switzerland

2.1.6 Software

BZ-II Viewer	KEYENCE Germany, Neu-Isenburg
BZ-II Analyzer	KEYENCE Germany, Neu-Isenburg
BD Cell Quest Pro 5.2.1	BD Biosciences, Franklin Lakes, USA
Image Lab Software 5.1	BioRad, Hercules, USA
GraphPad Prism 8.4	GraphPad Software, CA, USA
Magellan3	Tecan, Crailsheim, Germany
Microsoft office 365	Microsoft, Redmond, USA

2.1.7 Plasmids

The following plasmids were used in this study:

Table 3: List of used plasmids

Name	Description
pcDNA3.1	Empty vector control for protein expression; Invitrogen Karlsruhe
pBS	Empty vector control for protein expression; Invitrogen Karlsruhe
pcDNA3.1p53α	Expression plasmid of p53α from Jean-Christophe Bourdon, University of Dundee
pcDNA3.1p53β	Expression plasmid of p53β from Jean-Christophe Bourdon, University of Dundee
pcDNA3.1p53γ	Expression plasmid of p53γ from Jean-Christophe Bourdon, University of Dundee
pcDNA3.1Δ40p53α	Expression plasmid of p53Δ40α from Jean-Christophe Bourdon, University of Dundee
pcDNA3.1Δ133p53α	Expression plasmid of p53Δ133α from Jean-Christophe Bourdon, University of Dundee
pcDNA3.1Δ160p53α	Expression plasmid of p53Δ160α from Jean-Christophe Bourdon, University of Dundee

2.1.8 Cell Lines and Bacterial Strains

Table 4: List of used cell lines and bacterial stains

Name	Description
E.coli DH5α	DH5α competent *E. coli* (High Efficiency), NEB, Frankfurt/M，Germany
K562	Human myeloid leukaemia (ATCC® CCL-243). p53 null [138, 150, 156]
K562(HR-*EGFP*/3`*EGFP*)	Derived from human myeloid leukemia cell line K562 and was stably with integrated recombination substrate *HR-EGFP/3`EGFP* [3] .
Saos 2	Human osteosarcoma cell line (ATCC® HTB-85), p53/p63/p73 null [87, 98]

2.1.9 Antibodies

2.1.9.1 Primary Antibodies

Table 5: List of primary antibodies

Name	Description	Company
Anti-Bromodeoxyuridine	Rat monoclonal antibody, ab6326	Abcam, Cambridge, UK
Anti-Bromodeoxyuridine	Mouse monoclonal antibody, clone B44, 347580	BD Biosciences, Franklin Lakes, USA
Anti-MDM2	Mouse Monoclonal Antibody, clone 2A10, MABE281	Millipore, Burlington, USA
Anti-p21	Mouse monoclonal antibody 556430	BD Biosciences, Franklin Lakes, USA
Anti-p53 DO 1	Mouse monoclonal antibody DO-1, 554293	BD Biosciences, Franklin Lakes, USA
Anti-p53 DO-11	Mouse monoclonal antibody, MCA1704	BioRad, Hercules, USA
Anti-p53 DO-11	Mouse monoclonal antibody, GTX75258	Genetex, Irvine,USA
Anti-p53 Pab 421	Mouse monoclonal antibody, OP03	Millipore, Burlington, USA
Anti-p53 Pab1801	Mouse monoclonal antibody, OP09	Millipore, Burlington, USA
Anti-PCNA	Mouse monoclonal antibody, ab29	Abcam, Cambridge, UK
Anti-Polymerase ι	Rabbit polyclonal antibody, PA5-29442	Invitrogen, Waltham, USA
Anti-Polymerase ι	Rabbit polyclonal antibody, A301-303A	Bethyl Laboratories, Montgomery, USA
Anti-Ubiquityl-PCNA	Rabbit monoclonal antibody, 134395	Cell Signaling, Danvers, USA
Anti-β Actin	Mouse monoclonal antibody, sc-47778	Santa Cruz, Dallas, USA

2.1.9.2 Secondary Antibodies

Table 6: List of secondary antibodies

Name	Description	Company
Alexa Fluor 555	Goat anti-mouse, A21424	Invitrogen, Waltham, USA
Alexa Fluor 555	Goat anti-rabbit, A21428	Invitrogen, Waltham, USA
Alexa Fluor 488	Goat anti-mouse, A11001	Invitrogen, Waltham, USA
Alexa Fluor 488	Donkey anti-rat, A21208	Invitrogen, Waltham, USA
Goat anti Mouse Immunoglobulin G (IgG), light chain specific	Peroxidase Conjugated, 115-035-174	Jackson Immuno, Cambridgeshire, UK
Mouse anti Rabbit IgG, light chain specific	Peroxidase Conjugated, 211-032-171	Jackson Immuno, Cambridgeshire, UK
Goat anti Rabbit IgG (H&L) Antibody	Peroxidase Conjugated, 611-1322	Rockland, Philadelphia, USA
Donkey anti Goat IgG (H&L) Antibody	Peroxidase Conjugated, 605-703-002	Rockland, Philadelphia, USA
Goat anti Mouse IgG (H&L) Antibody	Peroxidase Conjugated, 610-1319	Rockland, Philadelphia, USA

2.2 Methods

2.2.1 Molecular Biology

2.2.1.1 Plasmid Preparation

2.2.1.1.1 Transformation of *E.coli DH5α*

The method previously described in [94] was modified as described in the following. To amplify the target plasmid, 50 microliters (µl) of competent *E. coli* DH5α was thawed on ice, mixed with 100 - 500 ng plasmid and incubated on ice for at least 30 min. Afterwards the bacterial-plasmid mixture was heat-shocked at 42 °C for 90 seconds (s) and then incubated on ice for 2 min. After adding 500 µl of 1 x LB medium, the mixture was incubated at 37 °C for 1 hour (h) on a shaker. Later, the transformed bacteria were

distributed on 1 x LB agar plates with respective selective antibiotics and incubated at 37 °C overnight. On the second day, a single colony was picked and transferred into a culture tube containing 1 x LB medium (with freshly added selective antibiotics). Then incubated on a shaker for 5 - 7 h at 37 °C, the bacterial suspension in culture tube was transferred to a culture flask containing 1 x LB medium (with selective antibiotics) and incubated overnight at 37 °C on a shaker. On the third day, 900 µl bacterial suspension was mixed with 100 µl DMSO (final concentration of 10 %) to prepare a bacterial stock solution which was stored at - 80 °C.

2.2.1.1.2 Amplification and Extraction of Plasmid from *E.coli*

For amplification, a sterile pipette tip was used to take a small amount of bacterial solution from the stock solution and put into a culture tube containing 1 x LB medium (with freshly added respective selective antibiotics). Subsequently, this solution was incubated at 37 °C on a shaker for 5-7h, then the suspension was aspirated and transferred to a culture flask containing 1 x LB medium (with freshly added selective antibiotics). This was incubated overnight on a shaker at 37 °C.

On the second day, the bacterial suspension was centrifuged (4500 g, 5 min) and the plasmid preparation was performed according to the instructions of OriGene (PowerPrep-HP Plasmid Maxi-Prep System; OriGene, Rockville, USA). After drying the plasmid overnight at room temperature (RT), the pellet was dissolved in TE buffer. In the end, the plasmid concentration was determined with NanoDrop2000 and the plasmid concentration adjusted to 1 microgram / microliter (µg / µl). Finally, the plasmids were stored at - 20 °C.

2.2.1.1.3 Restriction Digestion

To analyze if the correct plasmid has been amplified a restriction digest was performed. The digestion (with the addition of restriction enzymes) and non-digestion (without the addition of restriction enzymes) samples was prepared according to Table 7. Then samples were incubated at 37 °C for 5 h and separated via agarose gel electrophoresis.

Table 7 Restriction digestion system

	Digestion (µl)	Non digestion (µl)
Enzyme I	0.5	0
Enzyme II	0.5	0
Buffer	2	2
Bovine serum albumin (BSA) (10 x)	2	2
Double distilled H_2O (ddH_2O)	13.5	14.5
Plasmid(1:10)	1.5	1.5
Total	20	20

2.2.1.1.4 Agarose gel electrophoresis of DNA

First of all, a 1% agarose gel containing 0.01% FluoDNA Gel Stain (Fluorescin; Promokine, Heidelberg, Germany), 1 x TAE-buffer and DNA (diluted 1:10 with TE buffer) was prepared. Subsequently, this agarose gel was placed in the running chamber. To verify the size of the DNA the RTU ladder IIK (Promokine, Heidelberg, Germany) was used. For this, 10 µl of RTU DNA ladder IIK were mixed with 2 µl 6 x DNA loading dye (MBI Fermentas, St.Leon-Rot, Germany) in one well of a 96 well plate and 10 µl transferred to one well of gel. After loading all samples (mixed with loading dye), the voltage of running chamber was set to 100 V and run for 30 - 60 min. Then bands were detected with ChemiDoc MP Imaging System (BioRad, Hercules, USA).

2.2.2 Cell Culture

2.2.2.1 Culture of suspension cells

K562 and K562 *(HR-EGFP/3`EGFP)* were cultured with culture medium for suspension cells and grown at 5 % CO_2, 37 °C. Cells were split 1:2 to 1:40 for proliferation. One day prior the transfection, cells were split 1:2 to maximize the transfection efficiency.

2.2.2.2 Culture of adherent cells

Saos 2 cells were cultured with culture medium for adherent cells and grown at 5 % CO_2 and 37 °C. To harvest cells were washed with 1 x Phosphate-buffered saline (PBS) for 2 times prior adding trypsin. To detach cells, they were incubated at 37 °C for 3 - 5 min. To stop the reaction culture medium for adherent cells was added and centrifuged 240 g for 5 min to remove the supernatant. To amplify cells, resuspend the harvested cells with culture medium for adherent cells and split 1:2 to 1:5. Afterwards, transfer to either plates or flasks. One day before the transfection, split cells 1:2.

2.2.2.3 Mycoplasma test to exclude contamination of the cells

To exclude a possible Mycoplasma-contamination in cells, 0.25 x 10^5 cells were harvested. Then, the pellet was resuspended with 50 µl sterile ddH_2O. Afterwards, 250 µl lysis mix was added and then incubated for 60 min at 56°C followed by 10 min at 95 °C. Store the lysate at -20 °C. Cell lysate from Mycoplasma positive cells is considered as control.

Perform the PCR according to instruction below:

2.5 µl lysate (use as template)

1 µl mycoplasma primer mix (including Myco-5' and Myco-3', 5 µM stock)

1 µl dNTPs (5 mM stock)

2.5 µl 10 x PCR buffer

0.5 µl Taq-DNA-Polymerase (5 U/µl)

17.5 µl dH_2O

PCR program:

1. Denaturation	95 °C 5 min	
2. Denaturation	94 °C 30 sec	35 cycles
3. Annealing	60 °C, 30 sec	
4. Elongation	72 °C,30 sec	
5. Final Elongation	72 °C,15 min	
6. Final hold	4 °C	

Samples stored at 4 °C.

2.2.2.4 Drug treatment

Mitomycin C (MMC) medium: culture medium for suspension/adherent cells (without [w.o.] antibiotics) + MMC (stock solution concentration: 5mM, final concentration: 3 µM)
Mock medium: culture medium for suspension/adherent cells (w.o. antibiotics) + ddH2O (volume = volume of MMC stock solution added into MMC medium)
K562 cells or Saos 2 with MMC were harvested 48 hours or 24 hours after transfection and incubated with respective amount of MMC-supplemented medium for 45 min at 37 °C. In parallel, cells were incubated with Mock medium. Then, the cells were washed and incubated with fresh culture medium for suspension/adherent cells for another 3h at 37 °C.

2.2.2.5 Transfection technologies

2.2.2.5.1 Electroporation transfection

K562 and K562 (HR-EGFP/3`EGFP) cells were transfected via electroporation. One day prior to the transfection, cells were split to 1:2 to maximize the transfection efficiency. First, cells were harvested and resuspended in ice-old RPMI 1640 Medium (w.o. phenol red) to a final concentration of 107 cells / ml. Afterwards, cells were mixed with calculated amount of the DNA, 400 µl cells were transferred into a cuvette (0.4 mm, BioRad, Hercules, USA). The cuvette was electroporated with Gene Pulser Xcell Electroporation System (BioRad, Hercules, USA) using a voltage of 200 Volts (V). After electroporation, cell suspension was split into two wells of one 6-well plate, pre-filled with 2 ml of culture medium for suspension cells (w.o. antibiotics).
To study the recombination frequencies of K562 (HR-EGFP/3`EGFP) cells and perform corresponding western blot experiments, the cells were transfected with empty vector or expression plasmids and culture transfected cells for 72 hours.
To perform IF, PLA, Co-IP and DNA fiber-spreading assay and their corresponding western blots, K562 cells were transfected and incubated for 48 hours prior to the start of experiments.

2.2.2.5.2 Cell transfection via Amaxa nucleofector

Amaxa nucleofection was used to transfect adherently growing Saos-2 cells. For one transfection, the respective amount of plasmid was transferred into one well of a 96 well plate. Then Saos 2 cells were harvested and resuspended with Amaxa transfection solution V (Lonza, Basel, Switzerland) to a final cell concentration of 1.5 x 10^6 cells / ml. For each transfection, 100 µl cell suspension was transferred into the

well pre-filled with the plasmid. This Mix was transferred to the one cuvette (Lonza, Basel, Switzerland) and the transfection Performed with program D-24 using Nucleofector 2b Device (Lonza, Basel, Switzerland). Afterwards, cell suspension of one cuvette was split into two wells of a 6 well plate, prefilled with 2 ml of medium without antibiotics.

2.2.3 Flow Cytometry

Recombination frequencies were determined via Flow Cytometry (FCM) (FACSCalibur™, BD Biosciences). During the measurements, the cells were exposed to a specific wavelength laser beam (argon laser: 488 nm) and different readouts were obtained. First, cell size and particle size were detected by the scattering of light. Second, the light emitted by fluorescent molecules (such as EGFP) is measured by using different detectors controlled by filters. To measure the size of the cells, a forward scattering channel (FSC) is used, which collects light scattered forward. The side-scattering channel (SSC) indicates the cell granularity.

2.2.3.1 Measurement of replication-associated recombination frequency

To measure the spontaneous replication-associated recombination frequencies, K562 *(HR-EGFP/3`EGFP)* with stably integrated *HR-EGFP/3`EGFP* substrate [3] were used. The principle of this experiment is the recovery of a functional EGFP from two mutant *EGFP* variants.

The cells were cultured for 72 hours after transfection. Then cells were harvested and resuspended in 150 µl – 300 µl 1 x PBS / 0.2 % EDTA. Next, the cell suspension was transferred to FCM tubes (Sarstedt, Nümbrecht, Germany). The frequencies of spontaneous replication-associated recombination were determined via the measurement of green fluorescence cells within 1 million living cells (SSC / FSC gate) using the diagonal gating method in the FL1/FL2 dot blot. Here, FL1 shows a green fluorescence signal (530/30nm), and FL2 shows orange (585/42nm) cell autofluorescence.

2.2.4 Biochemistry and Immunodetection

2.2.4.1 Western Blot technology

2.2.4.1.1 Prepare cell lysates

Suspension cells were collected and centrifuged with 240 g for 5 min to obtain the pellet. Adherent cells were collected into a 1.5 ml microtube by the use of cell-scrapers after washing with ice-cold PBS.

Cells were washed with ice-cold PBS once and centrifuged to remove PBS (16000 g, 5 min, 4 °C). Afterwards, Cells were resuspended with cell lysis buffer for protein extraction and incubated on ice for 30 min followed by centrifugation (16000 g, 15 min, 4 °C). Finally, the supernatant (lysate) was transferred to new 1.5 ml microtube and stored at -80°C.

2.2.4.1.2 Determination of protein concentration by Bicinchoninic acid (BCA) assay

The BCA protein assay kit (Thermo Scientific, Waltham, USA) was used to determine the protein concentration. The principle of this method is based on two reactions [93]. Reaction I is a biuret reaction, and the peptide bond of the protein reduces the copper ion (Cu2+) of copper sulfate to copper ion (Cu+). In Reaction II, Cu+ ions react with BCA and form a dark blue or purple complex.

To perform the BCA assay, the cell lysates 1:10 were diluted in cell lysis buffer for protein extraction. Afterwards, a series of 0.125 mg/ml to 2 mg/ml gradient BSA standard samples was prepared, 10ul of diluted cell lysates and BSA standard samples were transferred to a 96-well plate with addition of 200 µl of reagent A+B (50:1) mixture in each well. After incubation at 37 °C for 30 min, optical densities of each well detected by Tecan Sunrise photometer at 570 nm using spectrophotometry. The BCA calibration curve is then used to calculate the protein concentration. Finally, the final concentrations were adjusted to 6 µg / µl with lysis buffer and 6 x SDS loading buffer containing 15 % mercaptoethanol. For denaturation, samples were incubated at 95 °C for 10 min, and then the samples were stored at - 80 °C.

2.2.4.1.3 SDS-polyacrylamid-gel-electrophoresis (SDS-PAGE)

The method was previously described in [112]. Ethanol was used to clean combs, glass plates and ceramic plates (size: 8 x 10 x 0.075 centimeters (cm); Amersham Pharmacia Biotech, Freiburg, Germany) before the preparation of the gels. According to different requirements, different concentrations of separation gels for SDS-PAGE were prepared (Table 8).

Table 8: Solution for separation gels

Size of the protein [kDa]	100-200	40-100	30-90	12-45
Separating Gel [%]	8	10	12	15
Acrylamide 30 %, 0.8 Bisacrylamide	12 ml	15 ml	18 ml	21 ml
4x SDS/Tris pH 8.8	11.25 ml	11.25 ml	11.25 ml	11.25 ml
H_2O	21.75 ml	18.75 ml	15.7 5ml	11.75 ml
10 % APS	150 µl	150 µl	150 µl	150 µl
TEMED	30 µl	30 µl	30 µl	30 µl

The solution for separation gels was filled into the Gel caster SE215 (Hoefer Pharmacia Biotech, CA, USA) with about 2 cm distance left to the top. Isopropanol was added to equalize the separation gels before polymerization. Once the separation gel was polymerized, isopropanol was removed and the solution for collecting gels was added (Table 9). In the end, one comb was placed between one glass and one ceramic plate to obtain the pocket for loading samples.

Table 9: Solution for collecting gels

Loading Gel [%]	
Acrylamide 30 %, 0.8 Bisacrylamide	3.9 ml
4x SDS/Tris pH 6.8	7.5 ml
H_2O	18.3 ml
10 % APS	150 µl
TEMED	30 µl

Once gels were polymerized, they were placed in the gel electrophoresis chamber filling with 1x Rotiphorese SDS-PAGE buffer. 10 µl protein molecular mass marker and 10-60 µg samples were added into the pocket running with a current of 25 milliampere (mA) per gel.

2.2.4.1.4 Blotting of proteins

The method was described in [193]. After electrophoresis, the separated proteins were transferred to PVDF membrane (Amersham Biosciences, GE Healthcare, München,Germany) or nitrocellulose membrane (Amersham Biosciences, GE

Healthcare, München,Germany). The PVDF membrane was activated in methanol for 30 seconds and then equilibrated with 1 x high molecular weight (HMW) buffer. The nitrocellulose membrane needs to be soaked in 1 x HMW buffer. Depending on the size of the protein of interest, the duration of transfer varied from 30 to 60 min with a voltage of 100 V on ice.

2.2.4.1.5 Immunodetection on blots [28]

The membrane was blocked with 5 % milk powder (Roth, Karlsruhe, Germany) in Tris-buffered saline (TBS) buffer for 45 - 60 min at RT on a shaker. Then the membrane was incubated with primary antibody diluted in 1 % milk powder / TBS solution overnight at 4 °C. On the next day, the membrane was washed 3 times for 5 min with 1 x TBST buffer and incubated with secondary antibody diluted in 1 % milk / TBS solution for 45 - 60 min. After washed again for 3 times with 1x TBST. Clarity Western Enhanced Chemiluminescence (ECL) Substrate (BioRad, Hercules, USA) was applied to the membrane for detecting the bands by ChemiDoc MP Imaging System (BioRad, Hercules, USA). Image Lab 5.2.1 (BioRad, Hercules, USA) was applied for densitometry analysis.

To strip the membrane, Restore Western Blot Stripping Buffer (Thermo Scientific, Waltham, USA) was added on the membrane and shake for 5 - 15 min at RT. Then wash the membrane 3 times for 5min in 1 x TBST followed by blocking with 5 % milk in TBS for 45 – 60 min at RT with shaking. Re-incubate the membrane with the primary antibodies.

Following primary antibodies were used for detecting protein bands of interest on western blots (including detection of bands from immunoprecipitation samples): anti-MDM2 (mouse, MABE281, Millipore), anti-p21 (mouse, 556430, BD Biosciences), anti-p53 (DO-1, mouse, 554293, BD Biosciences), anti-p53 (DO-11, mouse, GTX75258, Genetex), anti-PCNA (mouse, ab29, Abcam), anti-POLı (rabbit, A301-303A, Bethyl), anti-Ubiquityl-PCNA (rabbit, 134395, Cell Signaling). Anti-β actin antibody served as loading control (mouse, sc-47778, Santa Cruz).

2.2.4.2 Co-Immunoprecipitation (Co-IP)

Cell lysates were prepared as described in 1.2.4.1.1 except that 250 µl IP lysis buffer was used for cell lysis instead of cell lysis buffer for protein extraction.

During cell lysis, 400 µl Protein G Sepharose 4 Fast Flow beads (GE healthcare, München, Germany) were prepared. For each cell lysate, five groups were set

according the following Table 10. To remove the storage solution, Ethanol, from the beads, the beads were washed three times with 1 x PBS and to equilibrate the beads to the lysis buffer, they were washed three times with IP lysis buffer. Afterwards the beads were diluted to an end-concentration of 10 % sediment with IP lysis buffer.

Table 10 Prepare microtubes for one Co-IP reaction

Each cell lysate	A, 1.5 ml Eppendorf tube	0µl beads	50 µl lysate
	B, 1.5 ml Eppendorf tube	100 µl beads	100 µl lysate
	C, 1.5 ml Eppendorf tube	100 µl beads	Primary antibody
	D, 1.5 ml Eppendorf tube	100 µl beads	100 µl lysate
	E, 1.5 ml Eppendorf tube	100 µl beads	IgG antibody

Four tubes containing beads were incubated overnight at 4 °C on a rotator. For C and E, the incubation allows the specific antibody or IgG to bind the beads. For B and D, the incubation allows all components in the lysates that unspecifically bind to beads being removed to avoid disturbance of Co-IP. On the second day, B and D were centrifuged at 16000 g for 5 min at 4 °C and then the supernatant was transferred to C and E respectively followed by incubating C and E on the rotator at 4° C for 3 h to 24 h. C and E were centrifuge again at 16000 g for 5 min at 4 °C to precipitate the beads that had already bind to the antibody and its interaction components. Beads were washed for 4 times with IP lysis buffer. In the end, beads were resuspended with 30 µl 6 x SDS buffer containing 15 % Mercapthoethanol and heated for 10 min at 97 °C for denaturation. Finally, samples were stored at -80 °C. Following antibodies were used for Co-IP: anti-p53 (DO-11, MCA1704, BioRad) and anti-p53 (PAb421, Merck, OP03) were used to precipitate p53. Anti-POLı (A301-304A, Bethyl) or anti-PCNA (ab29. abcam) antibody were used to precipitate either POLı or PCNA. Anti-Mouse IgG antibody (sc-2025, Santa Cruz), Anti-Rabbit IgG antibody (12-370, Merck) or Anti-Rabbit IgG antibody (sc-2027, Santa Cruz) served as control.

2.2.4.3 Chromatin crosslinking IP

Cell lysates preparation was previously described in [24, 127]. Cells were collected by centrifuge 240 g for 5 min Then cells were resuspended with 4.5 ml Cytoskeletal (CSK)

buffer in a 50 ml centrifuge tube and incubated for 12 min at 4 °C while shaking. Afterwards, cells were centrifuged 240 g for 5 min at 4 °C and supernatant was discarded followed by resuspending the cell pellet with 4.5 ml freshly prepared 1% formaldehyde (methanol free) / PBS and incubated for 10 min at RT while shaking. After 10 min, cells were added with 0.5 ml 1 M glycine and incubated at 4 °C for 5 min while shaking. Then, cells were centrifuged to remove the supernatant and washed once with ice-cold 1 x PBS. Finally, cells were resuspended with ice-cold RIPA buffer with inhibitors, transferred to a 1.5 ml microtube and incubated for 15 min on ice while being mixed every 5 min.

Next, the sonication in SONOREX machine filled by ice cold water with an ultrasonic frequency of 35 Kilohertz (kHz) was performed. The sonication was performed with 30 s on and 30 s off for 7.5 min, repeated for another 2 times. In the end, the cell sample were centrifuged 16000 g for 15 min at 4 °C and the supernatant was collected. BCA assay was Performed with RIPA buffer without inhibitors. The Following steps are the same as during normal Co-IP. In the end, beads were washed with RIPA buffer without inhibitors and resuspended with 30 µl 6 x SDS buffer containing 15 % Mercapthoethanol, heat beads for 30 min at 97 °C with shaking. Samples were Stored at -80 °C.

2.2.4.4 Immunofluorescence (IF)

2.2.4.4.1 Prepare Poly-L-Lysine cover slides

Poly-L-Lysine was diluted 1:10 in dH_2O. Cover slides were incubated in this solution for 5 min at RT and dried.

2.2.4.4.2 IF Staining

Suspension cells were collected in 1.5 ml microtubes after corresponding treatment. Then cells were resuspended with 200 µl 1 x PBS and spun onto the glass slides covered with Poly-L-Lysine. Soak glass slides in pre-extraction (20 mM HEPES, pH 7.4, 50 mM NaCl,1 mM EDTA,3 mM $MgCl_2$,300 mM Sucrose, 0.5 % Triton X-100) buffer for 1 min. Then cells were fixed with 3.7 % Formaldehyde / PBS for 10 min. Afterwards, the samples were washed 3 times for 5 min with 1 x PBS. Next permeabilization was performed using 0.5 % TritonX-100 (Sigma-Aldrich) / PBS and an incubation time of 12 min which was followed by 3 washing steps for 5min in 1 x PBS. Samples were blocked with 5 % goat serum / PBS for 1 h at RT. Samples were

incubated with the primary antibodies (anti-PCNA [mouse, ab29, Abcam], anti-POLι [rabbit, PA5-29442, Invitrogen]) for 1 h at 37°C and washed (3 x 5 min in 1 x PBS). Then samples were incubated with AlexaFluor555 (Goat anti-rabbit, A21428, Invitrogen) and AlexaFluor488 (Goat anti-mouse, A11001) for secondary antibody staining which is done at 37 °C for 45 min, followed by another washing step for 3 times for 5 min with 1 x 0.1 % PBST. In the end, samples were mounted with Vectashield mounting medium with DAPI and cover the slides with coverslips.

2.2.4.4.3 IF microscopy and analysis

Images captured with Keyence BZ-9000 microscope (Keyence). The foci and co-localization foci quantified with BZ-II Analyzer software. The brightness threshold and foci size threshold were consistent within one experiment. Foci and co-localization foci that have perimeters less than 0,1 µm were neglected during analysis.

2.2.4.5 DNA fiber-spreading assay

Figure 5 a brief overview of the DNA fiber-spreading assay. Method was described in [83, 185]. The sequential incorporation of labelled nucleotides into synthesized DNA permits the visualization of the newly synthesized DNA via fluorescence microscopy. By sequentially incorporating two different halogenated nucleotides 5 -Chloro- 20-deoxyuridine (CldU) and 5-Iodo- 20-deoxyuridine (IdU) into the nascent DNA strands the replication of DNA can be measured directly.

First, suspension cells are labelled with nucleotide analogue CldU. Cells were cultured with culture medium for suspension/adherent cells (w.o.antibiotics) supplemented with 20 µM CldU for 20 min at 37 °C. Then the CldU-medium was removed and cells were labelled with the second label IdU (For adherent cells, wash with 1 x PBS twice before labelling IdU). Cells were cultured with culture medium for suspension/adherent cells (w.o. antibiotics) containing 200 µM IdU for another 20 min at 37 °C. After double labelling, cells were washed with ice-cold PBS and centrifuged to remove the PBS. Cells were resuspended with ice-cold PBS and the final cell concentration was adjusted to 1250 cells/µl. 2 µl cell suspension was pipetted at the top of the glass slide and 6 µl lysis buffer (0.5 % SDS, 200 mM Tris–HCl, pH 7.4, 50 mM EDTA) for DNA fiber-spreading assay was mixed with cells on the slide for 6 times. Then the mixture was gently stirred with a tip and incubated for 6 min at RT to lyse cells. Afterwards, the top of slides where the lysate is located were moved upward and tilt to around 20 ° to 30 °

to make the lysate drop down from the top to the bottom via gravity which allows the spread of the DNA fibers along the long axis of the slides. Then the slide was lied horizontally flat and air dried for 6 min, fibers were fixed by soaking slides in fixation solution (3:1, methanol: acetic acid, freshly prepared) and dried for 7 min. Then the slides were either stored in 70 % ethanol at 4 °C overnight or directly proceeded to denaturation with 2.5N HCl for 1 h at RT.

Prior to staining, samples on the slide were blocked with 5 % BSA / PBS for 45 min at 37 °C. Samples were stained with primary antibodies: anti-BrdU (mouse, mAb, 347580, BD Bioscience) for IdU and anti-BrdU (rat, ab6326, abcam or rat, OBT0030, BioRad) for CldU detection diluted in 0.5% BSA/PBS. Next, Samples were stained with AlexaFluor555 (Goat anti-mouse, A21424, Invitrogen) and AlexaFluor488 (Donkey anti-rat, A21208, Invitrogen) diluted in 0.5 % BSA / PBS for 1 h at RT. Finally, samples were mounted with VectaShield mounting medium and were covered with coverslips. Images of fibers captured with Keyence BZ-9000 microscope (Keyence). Use Fiji software [174] or BZ-II Analyzer software to measure fiber track length.

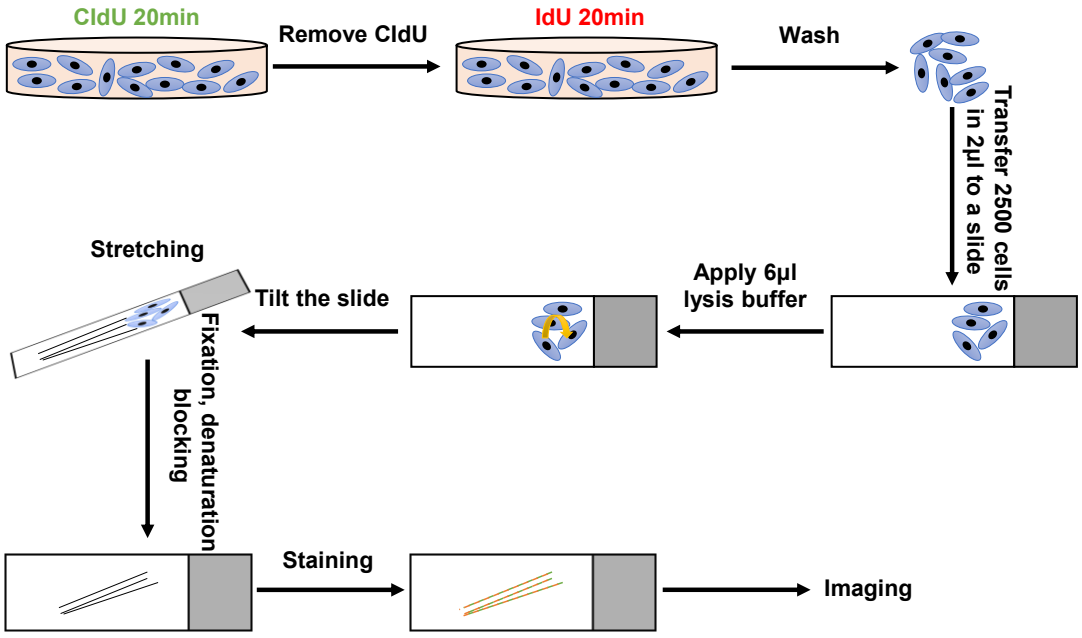

Figure 5: Brief flow of DNA fiber spreading assay

Incorporate different nucleotides analogues in the cells, then wash the cells and transfer 2500 cells on the slide. Apply lysis buffer, then tilt the glass slide to stretch DNA fibers. Staining is performed after fixation, denaturation and blocking described above.

2.2.5 Statistics

Graphic presentation of data was performed using GraphPadPrism 8.4 software (La Jolla, CA). Error bars indicating either mean+/-SD or mean+/-SEM were calculated with GraphPadPrism 8.4. Statistically significant differences in recombination measurements were calculated with Kruskal-Wallis test followed by Mann-Whitney two-tailed test. For calculating the statistically significant differences of DNA fiber-spreading analysis and IF analysis, Dunns-multiple comparison test was used. To calculate the statistically significant differences among western blot quantification, Friedman test followed by Wilcoxon matched-pairs signed rank test were used. Statistical analysis was performed by GraphPadPrism 8.4.

* represents a statistically significant difference between the linked two groups. # represent a statistically significant difference between marked group and ctrl group within either mock or MMC-treatment. *(#) $P < 0.05$, **(# #) $P < 0.01$, ***(# # #) $P < 0.001$, ****(# # # #) $P < 0.0001$.

3 Results

3.1 Roles of p53 isoforms in the transactivation activity and replication-associated recombination

Six p53 isoforms included in this study are shown in Figure 6A. K562 leukemia cells carrying chromosomally integrated EGFP-based recombination substrate: K562 (*HR-EGFP/3`EGFP*) (Figure 6B), K562 cells and Saos 2 osteosarcoma cells were utilized in this part. In the beginning, the transactivation activities of p53 isoforms were investigated. Therefore, Saos 2 osteosarcoma cells were transfected with empty vector (EV: pcDNA3.1) or expression plasmids for p53 isoforms. Saos 2 cells are p53 (p63, p73) negative and hence cells transfected with EV are p53 negative and are considered as control (ctrl). After being transfected by Amaxa nucleofector, proteins were harvested 24 hours post transfection (hpt). As shown in Figure 6C, D, western blots indicate that only p53α but not any of the other isoforms induce MDM2 or p21 expression in Saos 2 cells.

Then EV was introduced or p53 isoforms were expressed in p53-negative K562 leukemia cells by electroporation and proteins were harvested 48 or 72 hpt followed by the western blot analysis which is shown in Figure 6E, F. Thus, p53α and C-terminally altered isoforms induced the expression of MDM2, which means that a change at p53´s C-terminal did not alter the expression of MDM2. However, when p53α and ΔN-isoforms were expressed, only p53α, p53Δ40α and Δ133p53α showed on average increases in MDM2 expression while Δ160p53α showed a minor change compared to ctrl. Surprisingly, p21 expression can only be induced by p53α (Figure 6E, F).

As already mentioned in the introduction, p53α stimulates DSB-independent but replication-associated recombination, which can be detected as increase of EGFP-positive cells by FACS analysis among cells expressing exogenous p53α compared to ctrl cells. To examine the role of other p53 isoforms in replication-associated recombination, K562 (*HR-EGFP/3`EGFP*) cells (Figure 6B) were transiently transfected with EV plasmid or expression plasmids for p53 isoforms via

electroporation and incubated with fresh medium without antibiotics. Cells were harvested 72 hpt and then EGFP-positive cells among 1 x 10^6 living cells were measured via FACS. p53α induced a recombination frequency of 3.7 X 10^{-5} which represented a 3.7-fold increase compared to ctrl while p53β and p53γ caused no significant difference compared to ctrl (Figure 6E). As mentioned above, in Figure 6E, a representative western blot of ctrl, p53α, p53β and p53γ expressing cells is shown. Similar to the p53 C-terminally altered isoforms, the ΔN-isoforms Δ40p53α, Δ133p53α and Δ160p53α caused no significant effect on recombination frequencies compared to ctrl while p53α showed the expected recombination frequency increase up to 3.9 X 10^{-5}, i.e. a 3.7-fold increase compared to ctrl (Figure 6F). As mentioned above, in Figure 6F a representative western blot of ctrl, p53α, Δ40p53α, Δ133p53α and Δ160p53α expressing cells is presented.

Therefore, only p53α induces MDM2 and p21 protein expression in both Saos 2 and K562 cells while MDM2 protein expression patterns induced by other p53 isoforms in Saos 2 and K562 cells are different, which may indicate a cell line-dependence. Furthermore, it can be concluded that only p53α possesses the ability to facilitate replication-associated recombination while the other five isoforms mentioned above are defective when these proteins were similarly expressed at comparable protein levels in K562 (*HR-EGFP/3`EGFP*).

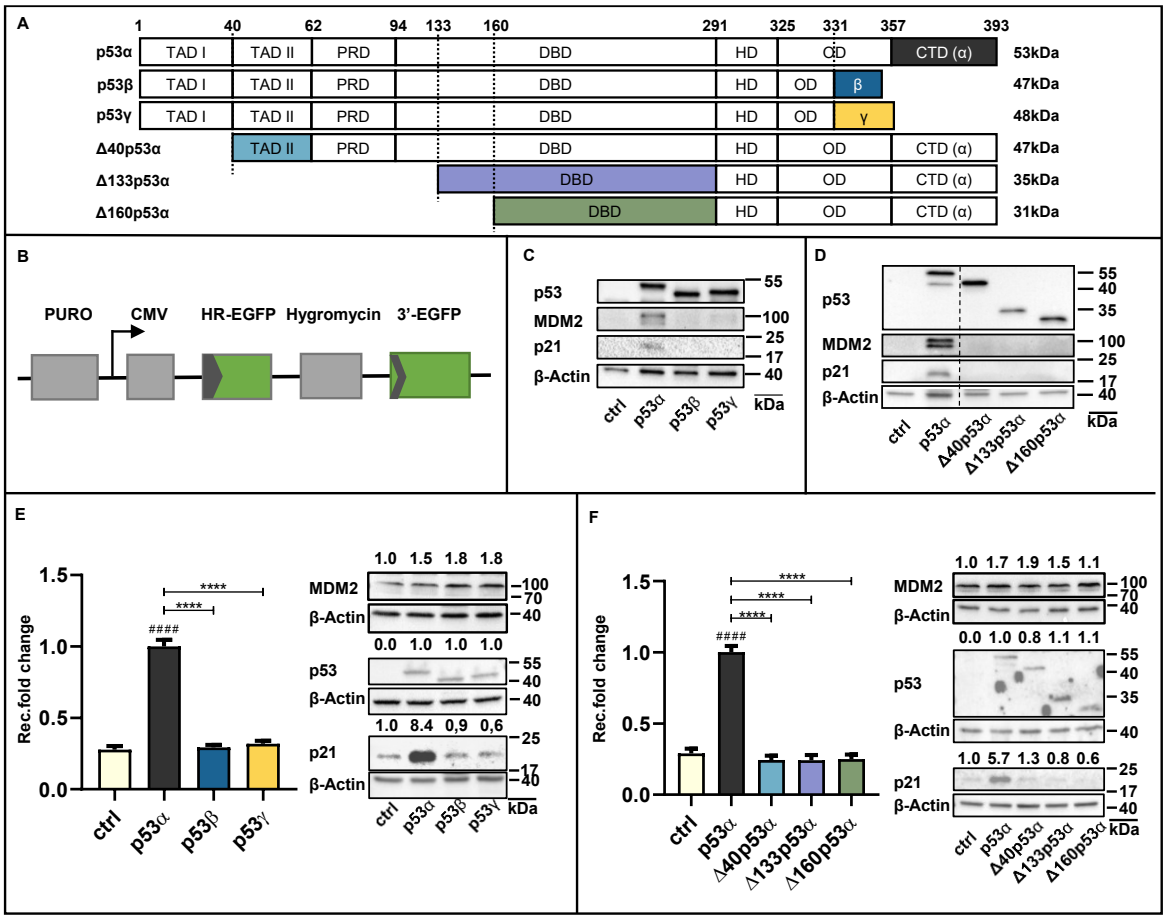

Figure 6 Transactivation activities of p53 isoforms and regulation of replication-associated recombination.

A: Schematic overview of different domains of p53 isoforms. p53α is the full length p53. **B**: Scheme of the recombination substrate *HR-EGFP/3'EGFP* which is chromosomally integrated in K562 cells and therefore generated the K562 (*HR-EGFP/3'EGFP*) cells. **C**, **D**: Transactivation activities of p53α, p53β and p53γ (C) or p53α, Δ40p53α, Δ133p53α and Δ160p53α (D) in Saos 2 cells. Protein harvested 24 hpt, Images in (D) separated by stippled line were derived from the same image of the same blot but were cropped to remove unrelated samples. **E**, **F**: K562 *(HR-EGFP/3`-EGFP)* cells were transfected with EV or expression plasmids for p53α, p53β, p53γ (E) or Δ40p53α, Δ133p53α, Δ160p53α (F). FACS analysis performed 72 hpt. EGFP-positive cells versus living cells ratio were calculated in each group and values from each group were corrected to the mean values of p53α-expressing samples that was set to 1 (absolute mean frequency in E: 3.7 X 10^{-5}, F: 3.9 X 10^{-5}). Data collected from 24 (E) or 18 (F) measurements. Error bars indicate standard error of mean (SEM). For western blots, K562 or K562 *(HR-EGFP/3`-EGFP)* cells were transfected with EV or expression plasmids of p53α, p53β, p53γ (E) or p53α, Δ40p53α, Δ133p53α, Δ160p53α (F). Protein harvested 48 or 72 hpt. Quantifications of MDM2 and p21 protein levels were normalized to β-Actin and mean values from at least 3 independent experiments were shown. Quantification of p53 protein levels were normalized to β-Actin and the values corresponding to the representative blot were indicated.
(Contents of this figure were published in [79])

3.2 p53 isoforms regulate DNA replication speed differently under mock or MMC-treatment

Since p53 isoforms except p53α fail to induce replication-associated recombination, their roles in decelerating DNA elongation, which is the characteristic phenotype of the p53-POLι DDT pathway, were investigated as well. To this end, DNA fiber-spreading assay in K562 cells was done to see if these isoforms could affect the DNA track length or not. Sequential incorporation / labeling with CldU firstly and IdU secondly is shown in schemes (Figure 7A, B, C, D), but for clarity only graphs displaying IdU track lengths are presented. In unperturbed cells (Figure 7A), p53α (average IdU track length: 4.140 μm), p53β (4.324 μm) and p53γ (4.981 μm) shortened the track lengths of DNA fibers compared to ctrl (5.458 μm) though the reduction by p53β or p53γ was less than that by p53α. However when cells were subjected to MMC-treatment, only p53α (3.702 μm) still decreased the DNA track length while p53β and p53γ no longer did (Figure 7B).

To study p53 ΔN-isoforms, corresponding expression plasmids or EV plasmid were transfected. In Figure 7C, p53α (3.481 μm) as well as ΔN-isoforms including Δ40p53α (3.764 μm), Δ133p53α (3.658 μm) and Δ160p53α (3.733 μm) reduced DNA track lengths compared to ctrl (4.691 μm) while the reduction by ΔN-isoforms was diminished compared to that by p53α under mock-treatment. But when cells underwent MMC-treatment (Figure 7D), only p53α (2.824 μm) was effective in DNA track length reduction while others were completely ineffective compared to ctrl (3.545 μm). Of note, POLι protein levels in K562 cells were not markedly affected (Figure 7E, F).

Then, DNA fiber-spreading assay was performed with Saos 2 cells. Consequently, similar results were observed in Saos 2 cells (Figure 8). Additionally, less efficient replication track shortening compared to p53α was observed in ΔN-isoforms expressing cells, which only reached statistical significance in Δ40p53α expressing Saos 2 cells (Figure 8C)

Taken together, p53α and other five isoforms decrease the track length of DNA fiber and slow down the replication speed under mock-treatment, but only p53α still possesses this ability when cells undergo MMC-treatment.

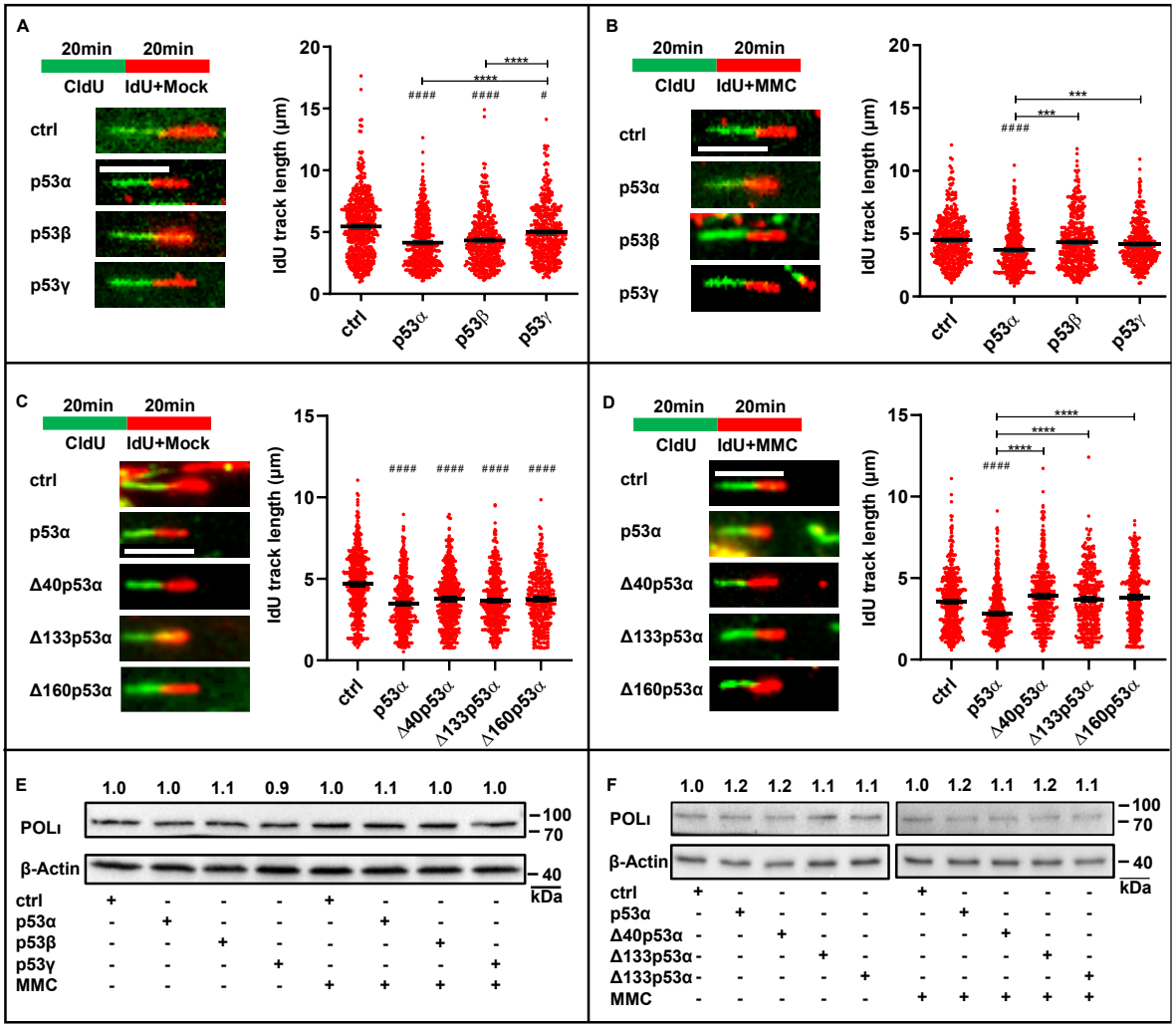

Figure 7 p53 isoforms regulate DNA replication in K562 cells.

DNA fiber-spreading assay was performed in cells transfected with EV or expression plasmids for p53 isoforms 48 hpt. A schematic overview is shown on top of each panel and representative fiber images below. Cells were sequentially incubated with CldU (20 μM) for 20 min and then IdU (200 μM) 48 hpt. During IdU-labeling cells were either mock- or MMC-treated (3μM). Error bars indicate SEM. For clarity, only IdU track lengths originating from a CldU track are shown graphically. Total numbers of fibers analyzed were ≥361 in each group out of 2 independent experiments. Scale bar: 5 μm. **A**, **B**: IdU track length of cells transfected with EV or expression plasmids for p53α or C-terminally altered isoforms p53β, p53γ either treated with mock (A) or MMC (B). **C**, **D**: IdU track length of cells transfected with EV or expression plasmids for p53α or ΔN-isoforms Δ40p53α, Δ133p53α, Δ160p53α either treated with mock (C) or MMC (D). **E**, **F**: POLι expression level in K562 cells. Cells were transfected with expression plasmids for p53α and C-terminally altered isoforms p53β, p53γ (E) or p53α and ΔN-isoforms Δ40p53α, Δ133p53α, Δ160p53α or EV. 48 hpt, cells were either mock- or MMC-treated (3 μM, 45 min, 3 h release) and lysis was performed with either lysis buffer for protein extraction or IP lysis buffer. Quantifications of POLι levels by normalizing to β-Actin levels done in at least 3 independent experiments and mean values are shown above the representative western blot images.
(Contents of this figure were published in [79])

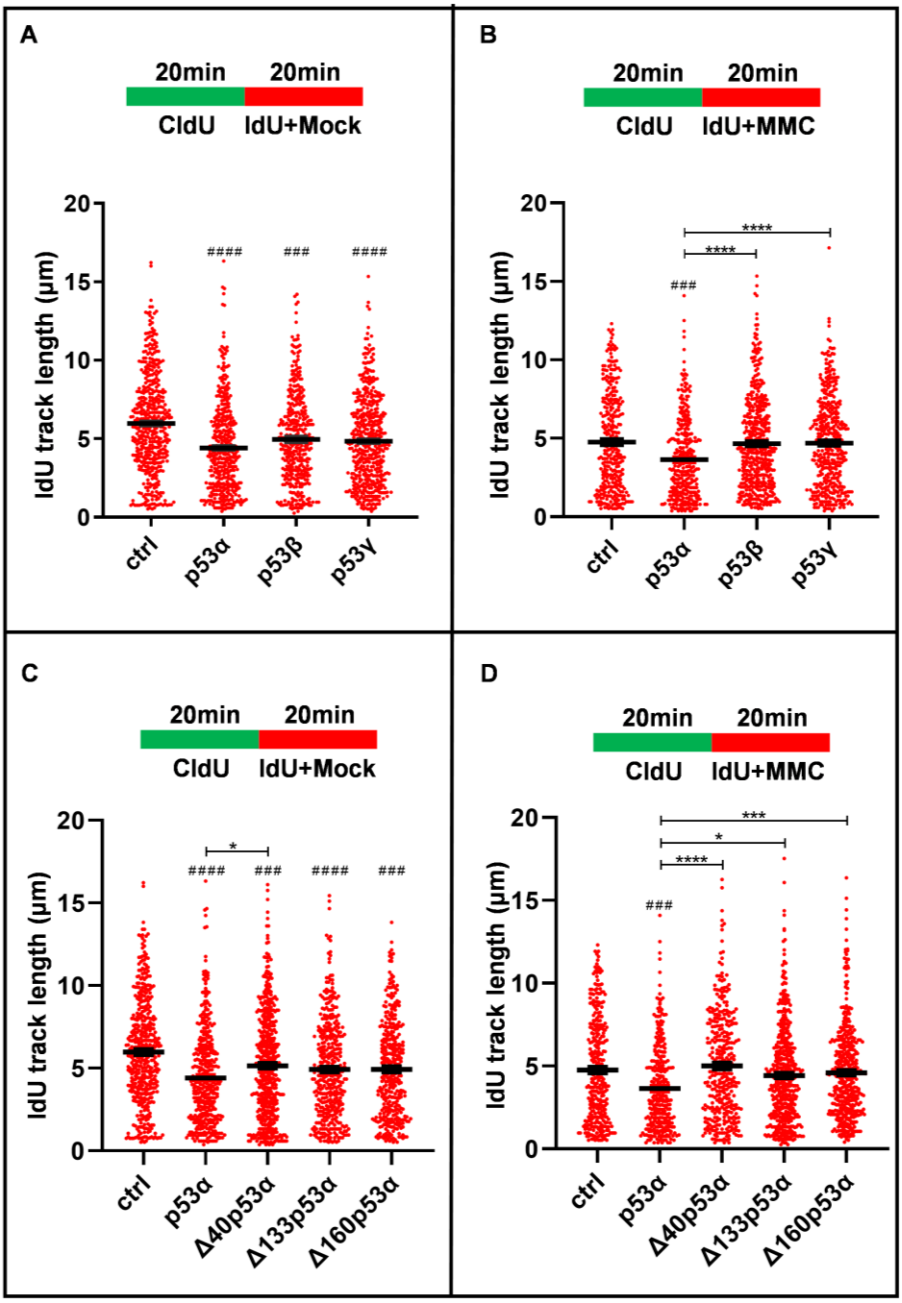

Figure 8 p53 isoforms regulate DNA replication in Saos 2 cells.

DNA fiber-spreading assay was performed in cells transfected with EV or expression plasmids for p53 isoforms 24 hpt. A schematic overview is shown on top of each panel and representative fiber images below. Cells were sequentially incubated with CldU (20 µM) for 20 min and then IdU (200 µM) 24 hpt. During IdU-labeling cells were either mock- or MMC-treated (3µM). Error bars indicate SEM. For clarity, only IdU track lengths originating from a CldU track are shown graphically. Total numbers of fibers analyzed were ≥325 in each group out of 2 independent experiments. **A**, **B**: IdU track length of cells transfected with EV or expression plasmids for p53α or C-terminally altered isoforms p53β, p53γ either treated with mock (A) or MMC (B). **C**, **D**: IdU track length of cells transfected with EV or expression plasmids for p53α or ΔN-isoforms Δ40p53α, Δ133p53α, Δ160p53α either treated with mock (C) or MMC (D).
(Contents of this figure were published in [79])

3.3 p53 isoforms cause the accumulation of POLι-PCNA colocalizing foci within the nucleus whereby MMC-treatment abolishes this feature of p53 isoforms other than p53α

My data above showed that p53 isoforms regulate DNA fiber length differently. To examine whether POLι, which participates in the p53-POLι idling complex that leads to deceleration of the DNA replication, is involved or not, immunofluorescence microscopy (IF) of POLι and the core DNA replication factor PCNA was performed in K562 cells (Figure 9, Figure 10, Figure 11).

First of all, cells were transfected with EV, expression plasmids for p53α or C-terminally altered isoforms and underwent mock-treatment. Thereupon a notable accumulation of POLι foci and POLι-PCNA colocalizing foci was observed in p53 expressing cells compared to ctrl (Figure 9A, C). On the one hand, p53α, p53β and p53γ expression led to increases of 32%, 45% and 52% in POLι foci numbers compared to ctrl, respectively. On the other hand, p53α, p53β and p53γ induced increases of 248%, 330% and 336% in POLι-PCNA colocalizing foci compared to ctrl respectively. Moreover, p53β and p53γ expressing cells showed significant increases of 17% and 41% in PCNA foci numbers compared to ctrl (Figure 9B).

Reminiscent of the fiber analysis in Figure 7B, D, when cells underwent MMC-treatment, the notable increases of POLι foci, PCNA foci as well as the POLι-PCNA colocalizing foci were diminished in p53β and p53γ expressing cells compared to ctrl (Figure 9A, B, C). Figure 11 shows the representative images of cells subjected to MMC-treatment. These results demonstrate that p53α and C-terminally altered isoforms trigger the accumulation of POLι foci as well as POLι-PCNA colocalization within the nucleus under mock but not MMC-treatment.

Subsequently, p53α and ΔN-isoforms were included in this investigation. When transfected cells underwent mock-treatment, an upregulation of POLι foci and POLι-PCNA colocalization in p53 expressing cells compared to ctrl was noticeable (Figure 10A, C). Thus, p53α, Δ40p53α, Δ133p53α and Δ160p53α caused increases of 32%,

26%, 34% and 17% in POLι foci, respectively, compared to ctrl. Furthermore, p53α, Δ40p53α, Δ133p53α and Δ160p53α expressing cells showed increases of 248%, 318%, 202% and 95%, respectively, in POLι-PCNA colocalizing foci compared to ctrl. Moreover, significant upregulation of 23% and 17% in PCNA foci was detected in Δ133p53α or Δ160p53α expressing cells, respectively, compared to ctrl (Figure 10B). Nevertheless, similar to IF results of C-terminally isoforms expressing cells, when ΔN-isoforms expressing cells underwent MMC-treatment, the significant accumulation of POLι foci, POLι-PCNA colocalizing foci were lost compared to ctrl (Figure 10A, C). Figure 11 exhibits the typical images of cells undergoing MMC-treatment.

In the end, these results indicate that all p53 isoforms lead to accumulation of POLι foci and POLι-PCNA colocalizing foci within the nucleus while isoforms other than p53α cannot do so under MMC-treatment.

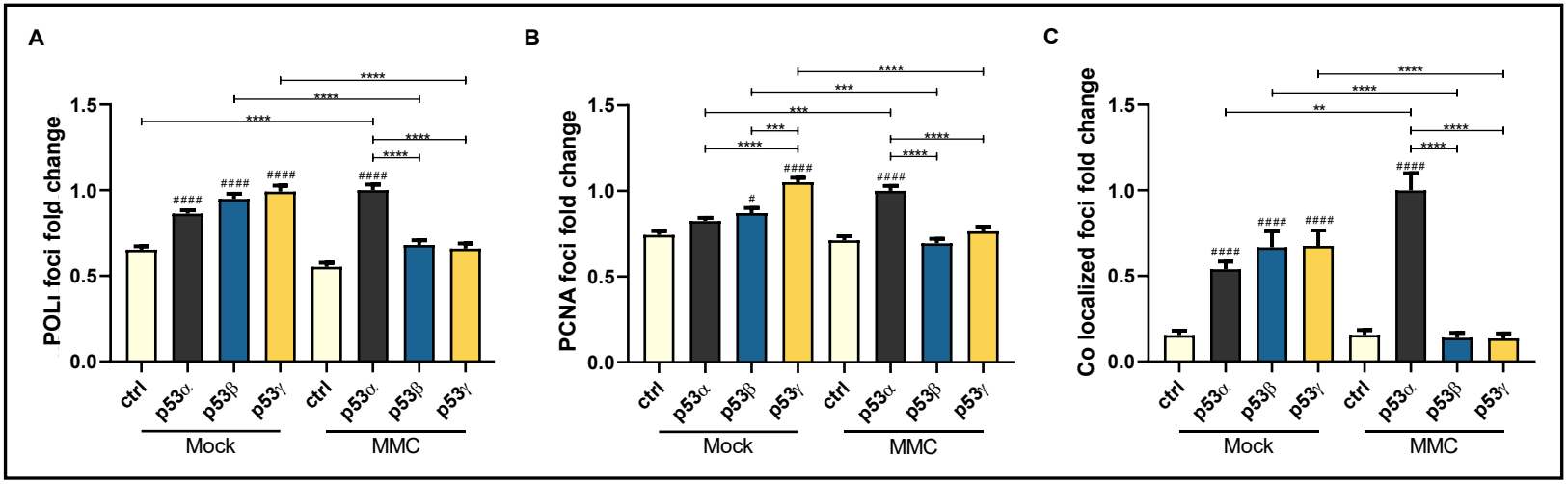

Figure 9 IF of POLι and PCNA in K562 cells transfected with empty vector or expression plasmids of p53α or C-terminally altered isoforms.

IF was performed in cells transfected with EV or expression plasmids for p53 isoforms 48 hpt. Cells were either mock- or MMC-treated (3 μM, 45 min, 3 h release) 48 hpt and IF of cells transfected with EV, expression plasmids for p53α or C-terminally altered isoforms was performed. Foci with perimeter ≤ 0.1μm was neglected during analysis and ≥100 nuclei per group were quantified out of at least two independent experiments. All values were normalized to the mean value for p53α expressing and MMC treated cells that was set to 1 in each experiment. Error bars indicate SEM. Statistical significance between groups was calculated using Dunn's multiple comparisons test. The absolute mean value of p53α expressing MMC-treatment samples was 100 POLι foci (A), 130 PCNA foci (B) and 14 POLι-PCNA colocalizing foci (C) per nucleus.

A, **B**, **C**: Cells transfected with EV, expression plasmid for p53α or C-terminally altered isoforms. POLι foci (A), PCNA foci (B), POLι-PCNA colocalizing foci (C) fold changes in K562 cells.

(Contents of this figure were published in [79])

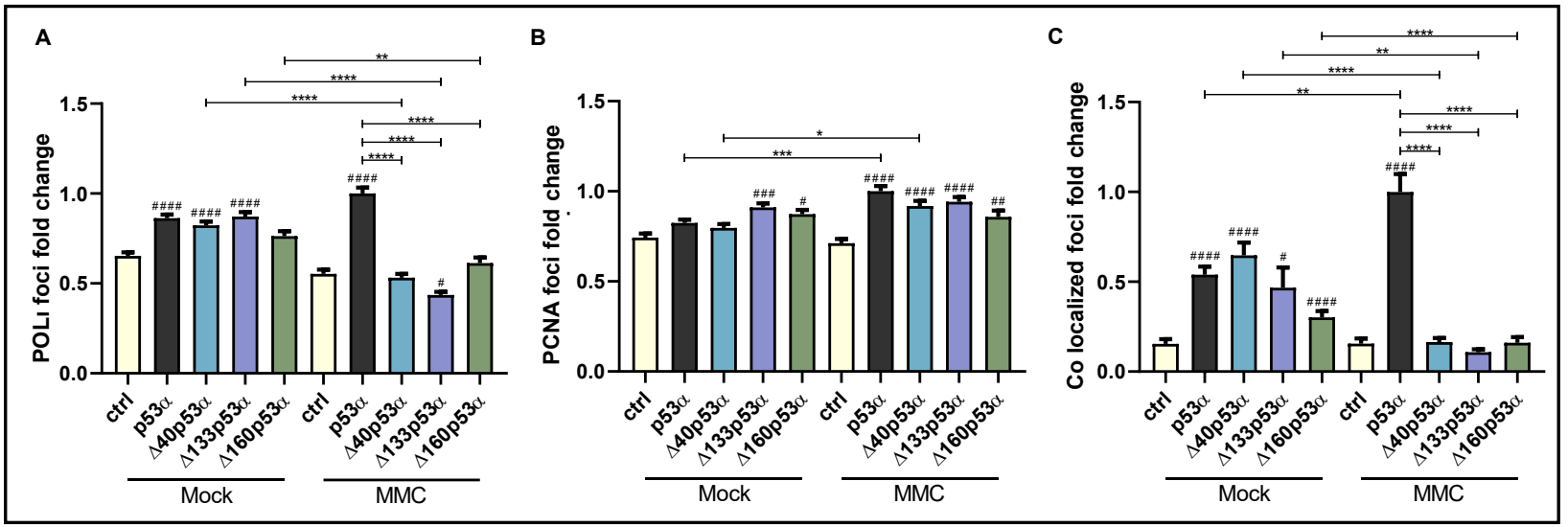

Figure 10 IF of POLι and PCNA in K562 cells transfected with empty vector or expression plasmids of p53α or ΔN-isoforms isoforms.

IF was performed in cells transfected with EV or expression plasmids for p53 isoforms 48 hpt. Cells were either mock- or MMC-treated (3 μM, 45 min, 3 h release) 48 hpt and IF was performed. Data of ctrl and p53α groups are identical to that in Figure 9 because transfection and IF analysis was performed together with transfection and IF analysis in Figure 9, but for clarity they were split into different parts. Foci with perimeter ≤ 0.1μm was neglected during analysis and ≥100 nuclei per group were quantified out of at least two independent experiments. All values were normalized to the mean value for p53α expressing and MMC treated cells that was set to 1 in each experiment. Error bars indicate SEM. Statistical significance between groups was calculated using Dunn's multiple comparisons test. The absolute mean value of p53α expressing MMC-treatment samples was 100 POLι foci (A), 130 PCNA foci (B) and 14 POLι-PCNA colocalizing foci (C) per nucleus.

A, **B**, **C**: Cells transfected with EV, expression plasmid for p53α or ΔN-isoforms. POLι foci (A), PCNA foci (B), POLι-PCNA colocalizing foci (C) fold changes in K562 cells.

(Contents of this figure were published in [79])

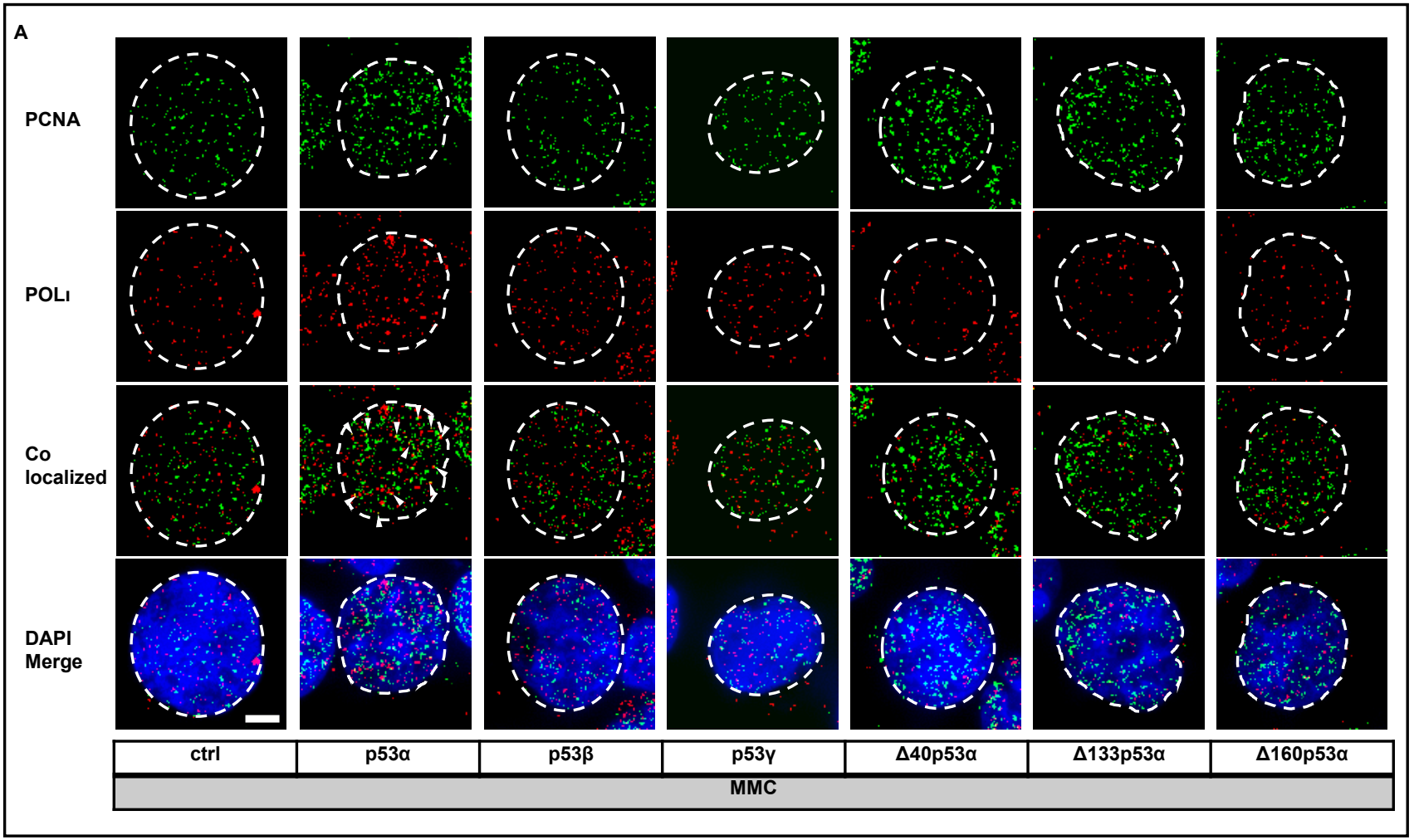

Figure 11 Representative images of IF with cells transfected with EV or expression plasmids for p53 isoforms that underwent MMC-treatment (quantified in Figure 9 and Figure 10). Scale bar: 5 μm. (Contents of this figure were published in [79])

3.4 The different p53 isoforms differ in forming complexes with POLι and PCNA

To further delineate whether p53 isoforms are involved in POLι-PCNA complex or not, Co-IP and chromatin crosslinking IP were performed in K562 cells (Figure 12). In the beginning, p53α and C-terminally altered isoforms were expressed in K562 cells for chromatin crosslinking IP (Figure 12A, B). When I pull down p53α and C-terminally altered isoforms with anti-p53 (DO-1) antibody, PCNA and POLι can be barely detected. So, either PCNA with anti-PCNA antibody or POLι with anti-POLι antibody were immunoprecipitated and western blots were done to detect p53 with anti-p53 (DO-1) antibody. The results showed that p53α and C-terminally altered isoforms interact with PCNA (Figure 12A) and POLι (Figure 12B) and results for the input are shown in Figure 12E.

Subsequently, when pulling down PCNA or POLι to detect p53α and ΔN-isoforms with anti-p53 (DO-11) antibody, p53 isoforms cannot be detected. Therefore, IP in K562 cells to pull down p53α and ΔN-isoforms with anti-p53 antibodies was done (Figure 12C, D). Figure 12C exhibits the blot from Co-IP which presented that p53α and all three ΔN-isoforms interact with PCNA (Figure 12C, input shown in Figure 12F). When I perform chromatin crosslinking IP to pull down p53 isoforms and do the POLι detection, only p53α and Δ40p53α are able to interact with POLι (Figure 12D shows the blot from chromatin crosslinking IP, input shown in Figure 12G). However, when pulling down p53α and Δ40p53α with Co-IP protocol but not chromatin crosslinking IP protocol (Figure 12H), only p53α interacts with POLι but Δ40p53α cannot.

All-in-all, p53α and C-terminally altered isoforms are able to interact with PCNA and POLι with results from chromatin crosslinking IP. Moreover, all three ΔN-isoforms are shown to interact with PCNA via Co-IP protocol. Interestingly, both p53α and Δ40p53α can interact with POLι when chromatin crosslinking IP was performed whereas Δ40p53α loses the interaction with POLι in Co-IP. Though Δ133p53α and

Δ160p53α interact with PCNA in Co-IP, they failed to interact with POLι with the result from chromatin crosslinking IP.

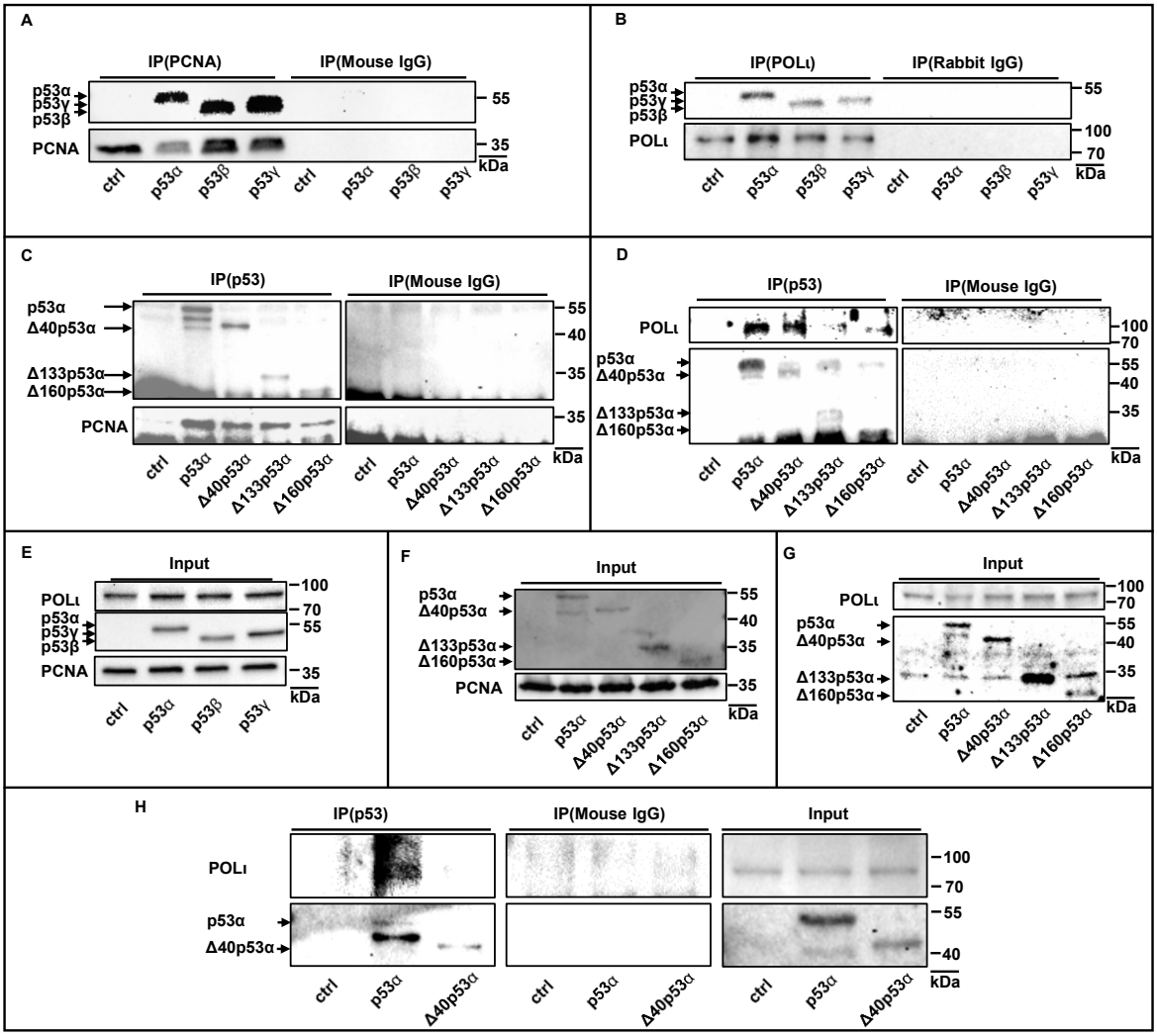

Figure 12 Investigating interactions between p53 isoforms and PCNA or POLι in K562 cells.

Cells transfected with EV or p53 isoforms expression plasmids were mock-treated and harvested for IP 48 hpt. Mouse IgG or Rabbit IgG were applied to cell lysates as control.

A, **B**: PCNA (A) or POLι (B) was pulled down from lysates of cells transfected with EV, p53α or C-terminally altered isoforms with anti-PCNA or anti-POLι antibody following chromatin crosslinking IP protocol. p53 were detected with anti-p53 (DO-1).

C, **D**: p53 isoforms were pulled down from lysates of cells transfected with EV, p53α or ΔN-isoforms with anti-p53 antibodies following Co-IP (C) or chromatin crosslinking IP (D) protocol. PCNA (C) or POLι (D) was detected with anti-PCNA or anti-POLι antibody.

E: Input of IP samples from (A) and (B).

F: Input of IP samples from (C).

G: Input of IP samples from (D).

H: Cells transfected with EV or p53 isoforms expression plasmids were MMC-treated. p53 isoforms were pulled down from lysates with anti-p53 antibodies following Co-IP protocol.

(Part of contents in this figure were published in [79])

3.5 p53 isoforms differentially affect PCNA ubiquitination

POLι is one of the TLS-POLs and recruited by PCNA mono-ubiquitination. Hence, I hypothesized that p53 isoforms could affect the PCNA ubiquitination, which in turn could affect the recruitment of POLι. Western blot analysis quantified in Figure 13 was done to analyze mono-ubiquitinated PCNA and poly-ubiquitinated PCNA protein expression levels in K562 cells expressing corresponding plasmids. Typical western blot images are shown in Figure 14.

First of all, Figure 13A show that p53α, p53β and p53γ significantly increased the level of mono-ubiquitinated PCNA compared to ctrl under mock-treatment. p53α, p53β and p53γ lead to 80%, 60% and 60% increases in mono-ubiquitinated PCNA compared to ctrl, respectively. MMC-treatment enhanced PCNA mono-ubiquitination in ctrl and p53α expressing cells to a similar extent. However, after MMC-treatment induction of mono-ubiquitinated PCNA was reduced in p53β and p53γ compared to p53α expressing samples (Figure 13A).

p53α, p53β and p53γ expression led to increases of 40%, 90% and 50% in poly-ubiquitinated PCNA, respectively, compared to ctrl under mock-treatment whereby statistical significance was not reached. When cells underwent MMC-treatment, the increases in poly-ubiquitinated PCNA were less pronounced or even lost in p53β and p53γ compared with p53α expressing cells (Figure 13B).

Subsequently, PCNA ubiquitination in cells transfected with EV, p53α or ΔN-isoforms' expression plasmids were investigated (Figure 13C, D). p53α and ΔN-isoforms including Δ40p53α, Δ133p53α and Δ160p53α led to elevated mono-ubiquitinated PCNA compared to ctrl under mock-treatment with increases of 70%, 50%, 60% and 60%, respectively (Figure 13C). Elevated induction of mono-ubiquitinated PCNA in p53 ΔN-isoforms´ expressing cells was lost when cells were subjected to MMC-treatment, however, in this set of experiments it was also less pronounced after expression of p53α (Figure 13C).

p53α, Δ40p53α, Δ133p53α and Δ160p53α expression resulted in enhanced poly-ubiquitination of PCNA compared to ctrl under mock-treatment with increases of

50%, 20%, 40% and 40%, respectively, whereby a significant difference was only detected between p53α and ctrl values (Figure 13D). When p53 ΔN-isoforms expressing cells underwent MMC-treatment, upregulation of poly-ubiquitinated PCNA compared to ctrl was gone and p53α only led to 30% increase (Figure 13D). Altogether, p53 isoforms upregulate PCNA mono-ubiquitination under mock-treatment while only p53α sustains this upregulation after MMC-treatment. Regarding PCNA poly-ubiquitination the results show similar trends; however, the results are much less clear. But still, p53α showed consistent results that it promotes the PCNA poly-ubiquitination in all sets of experiments.

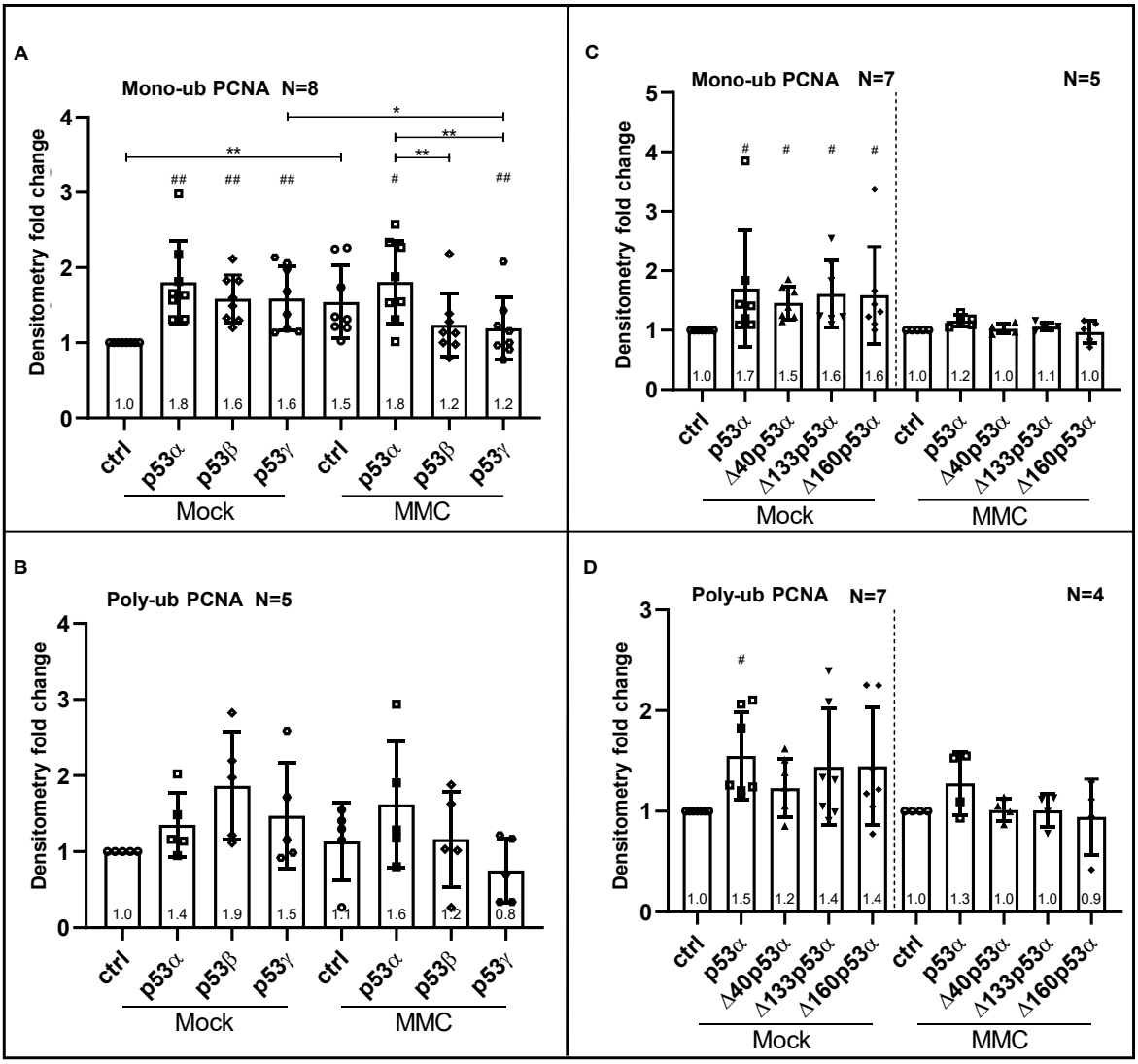

Figure 13 p53 isoforms affect the PCNA ubiquitination in K562 cells.

Cells transfected with EV or p53 isoforms underwent either mock or MMC-treatment 48 hpt. Protein extracted with cell lysis buffer for western blot or IP lysis buffer were used for western blot analysis. Ubiquitinated PCNA levels were normalized to the PCNA level on the same blot. On each blot, normalization to ctrl was done and ctrl was set to 1. “N” indicates the number of independent experiments used for quantification.

A, **B**: Cells transfected with EV, p53α and C-terminally altered isoforms´ expressing plasmids underwent mock or MMC-treatment. Eight protein samples were loaded on the same blot each.

C, **D**: Cells transfected with EV, p53α and ΔN-isoforms´ expressing plasmids underwent mock or MMC-treatment. Five mock samples were loaded on one blot while the other five MMC-treated samples were loaded on another blot as indicated by the stippled line in the graph.

(Data used to generate this figure were published in [79])

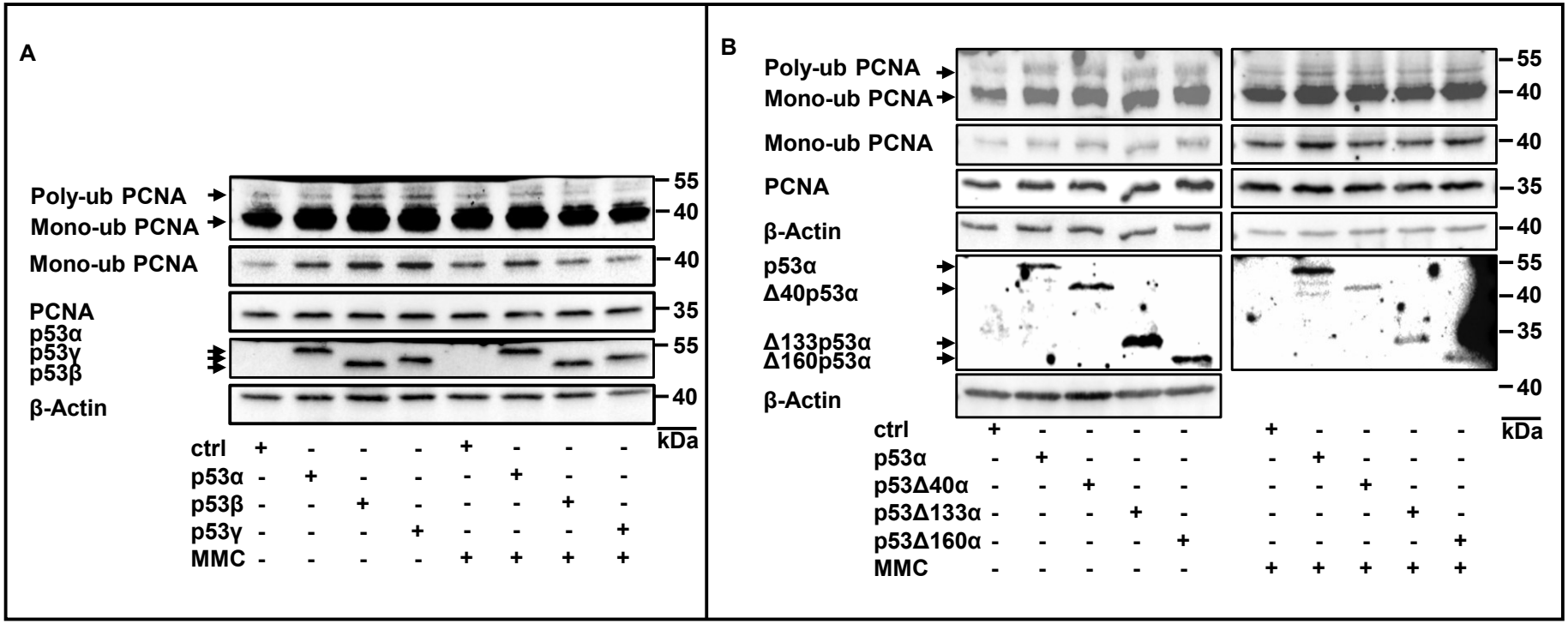

Figure 14 Representative images of PCNA ubiquitination by p53 isoforms in K562 cells (quantified in Figure 13, “ub” indicates ubiquitination)**.**

A: Proteins from cells transfected with EV, expression plasmids for p53α and C-terminally altered isoforms either underwent mock or MMC-treatment. Eight protein samples were loaded on the same blot.

B: Proteins from cells transfected with EV, expression plasmids for p53α and ΔN-isoforms either underwent mock or MMC-treatment. Five mock-treatment protein samples were loaded on one blot while the other five MMC-treatment protein samples were loaded on the other blot.

(Contents of this figure were published in [79])

3.6 The impact of p53 isoform co-expression on the p53α-POLı dependent DDT pathway

Up to now individually expressed p53 isoforms were explored in the POLı dependent DDT pathway and their differences compared to p53α. Then, I focused on investigating how the p53α-POLı dependent DDT pathway is affected in human cancer cells when p53 isoforms are co-expressed. Hence, the co-expression of p53α and the other five isoforms in K562 cells and Saos 2 cells was done for the subsequent experiments. For the samples labeled “p53α” in future figures, I used 10µg of p53α expression plasmid while for “p53α 50%” samples, only 5µg of p53α expression plasmid was used and filled up to a total amount of 10µg with EV. When co-expressing p53α and the other five isoforms, 5µg of p53α expression plasmid was used plus 5µg, i.e. half of the amount of isoforms´ expression plasmids that was used for individual isoform expression experiments.

First of all, DNA fiber-spreading assays in K562 cells (Figure 15) and Saos 2 cells (Figure 16) were carried out to check the elongation of DNA fibers in the co-expression setting.

Figure 15A displays the fiber analysis results from K562 cells that underwent mock-treatment. Both p53α 50% and p53α samples showed remarkably decreased track lengths compared to ctrl but p53α 50% showed an intermediate reduction. When p53α was co-expressed with one of the other five isoforms, none of them led to a significant reduction in fiber track length compared to ctrl. Interestingly, after co-expression of p53α&p53β, p53α&Δ133p53α and p53α&Δ160p53α the fiber length was significantly increased compared to p53α 50%.

In addition, Figure 15B exhibits the results from K562 cells subjected to MMC-treatment, whereby p53α resulted in a significant reduction of fiber track lengths compared to ctrl similar to mock-treatment while p53α 50% led to an intermediate decrease. Different from the untreated samples, here the co-expression of p53α&p53β led to a significant decrease of track length compared to ctrl which was

similar to that of p53α 50%. p53α&Δ40p53α, p53α&Δ133p53α and p53α&Δ160p53α co-expressions all caused a significant increase in fiber track lengths in comparison to p53α 50%. Then I did the fork asymmetry analysis by calculating the ratio of long track/short track of every individual fiber included in the track length analysis of K562 cells and result is shown in Figure 17A. MMC-treatment led to increases in fork asymmetry in all samples. Fork asymmetry was not altered significantly among samples treated with either mock or MMC, which indicates that the track length reduction by p53α is due to the existence of idling events.

Further experiments were done in Saos 2 cells (Figure 16) and similar results were obtained in the p53α co-expressing samples either under mock or MMC-treatment. While the co-expression of p53α and one of the other five isoforms had no significant influence on fiber track lengths in comparison to ctrl regardless of treatment, co-expression of p53α&Δ133p53α consistently showed an increase of the fiber track lengths compared to p53α 50% samples. Fork asymmetry analysis of Saos 2 cells in Figure 17B showed that MMC-treatment caused increases in fork asymmetry in most samples. p53α 50% expressing cells presented increasing fork asymmetry compared to ctrl after mock-treatment while this increase was lost after MMC-treatment. p53α expressing cells being MMC-treated showed increase in fork asymmetry compared to ctrl but this increase was not detected when cells were mock-treated.

Altogether, p53α caused the reduction in DNA track length which is due to the existence of idling events regardless of treatment in a dose-dependent manner at least in K562 cells. However, the co-expression of p53α with one of any other isoforms results in increases in DNA track length to different extent in comparison to p53α 50%.

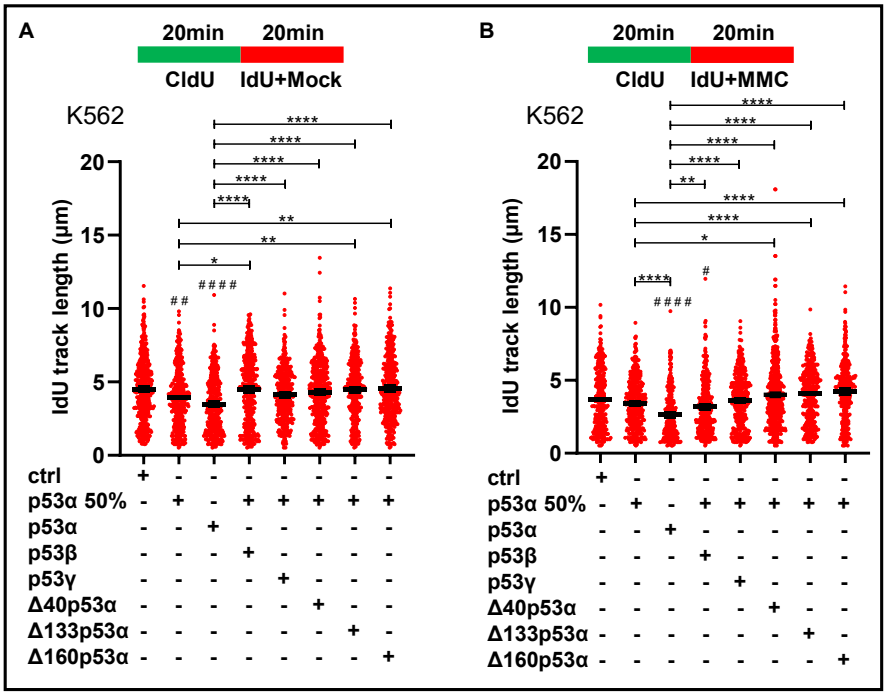

Figure 15 DNA fiber-spreading assay of cells with co-expression of p53α and one of the five isoforms in K562.

DNA fiber-spreading assay was performed in K562 cells transfected with EV, expression plasmid for p53α or co-transfected with expression plasmid for p53α and other five isoforms 48 hpt. Schematic overview is shown on top of each panel. Cells were sequentially incubated with CldU (20 µM) for 20 min and then IdU (200 µM) for 20 min 48 hpt. During IdU-labeling cells were either mock- or MMC-treated (3µM). Error bars indicate SEM. For clarity, only IdU track length originating from a CldU track are shown graphically. Total numbers of fibers analyzed ≥271 in each group out of 2 independent experiments. “p53α 50%” (5 µg) indicates the amount of p53α plasmid used is 50% of the amount of p53α plasmid in “p53α” (10 µg) which was filled up to 10 µg with 5 µg EV. When co-expressing p53α and one of the other five isoforms, I used 5µg of p53α expression plasmid plus 5µg of isoforms´ expression plasmid for transfection, i.e. half the amount of isoforms´ expression plasmids that was used for single isoforms´ expression experiments. Stars represent significant differences within p53 isoforms co-expression groups were not labelled.

A, **B**: IdU track length of K562 cells transfected with EV, expression plasmid for p53α and the same amount of expression plasmid for p53α or one of the other five isoforms. Cells were either treated with mock (A) or MMC (B) 48 hpt.

(Contents of this figure were published in [79])

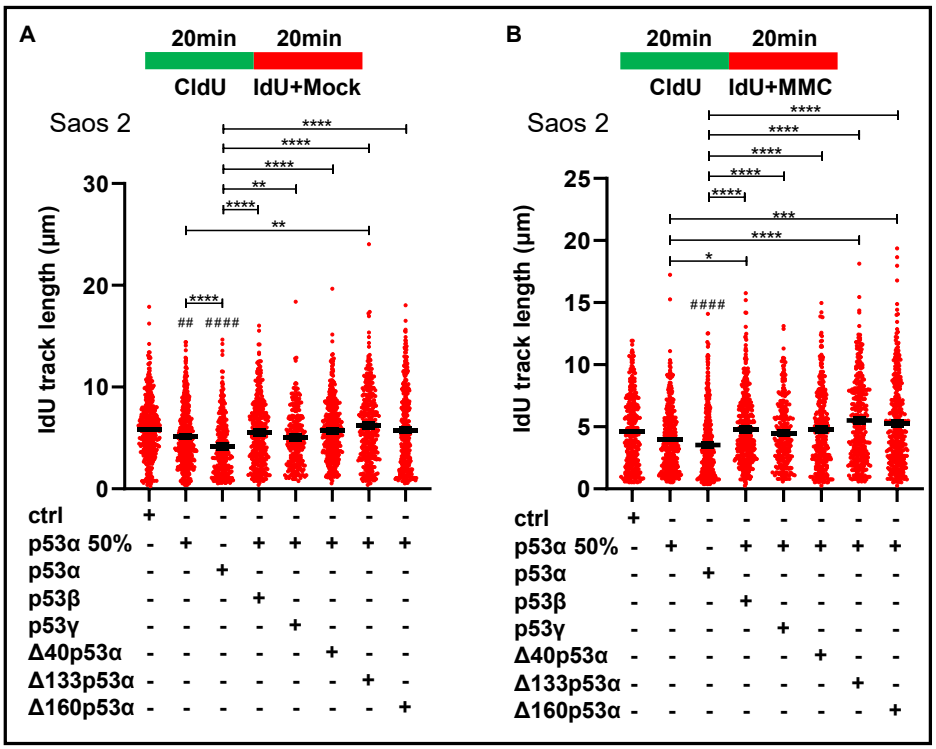

Figure 16 DNA fiber-spreading assay of cells with co-expression of p53α and one of the five isoforms in Saos 2.

DNA fiber-spreading assay was performed in Saos 2 cells transfected with EV, expression plasmid for p53α or co-transfected with expression plasmid for p53α and other five isoforms 24 hpt. Schematic overview is shown on top of each panel. Cells were sequentially incubated with CldU (20 µM) for 20 min and then IdU (200 µM) for 20 min 24 hpt. During IdU-labeling cells were either mock- or MMC-treated (3µM). Error bars indicate SEM. For clarity, only IdU track length originating from a CldU track are shown graphically. Total numbers of fibers analyzed ≥271 in each group out of 2 independent experiments. “p53α 50%” (5 µg) indicates the amount of p53α plasmid used is 50% of the amount of p53α plasmid in “p53α” (10 µg) which was filled up to 10 µg with 5 µg EV. When co-expressing p53α and one of the other five isoforms, I used 5µg of p53α expression plasmid plus 5µg of isoforms´ expression plasmid for transfection, i.e. half the amount of isoforms´ expression plasmids that was used for single isoforms´ expression experiments. Stars represent significant differences within p53 isoforms co-expression groups were not labelled.

A, **B**: IdU track length of Saos 2 cells transfected with EV, expression plasmid for p53α and the same amount of expression plasmid for p53α or one of the other five isoforms. Cells were either treated with mock (A) or MMC (B) 24 hpt.

(Contents of this figure were published in [79])

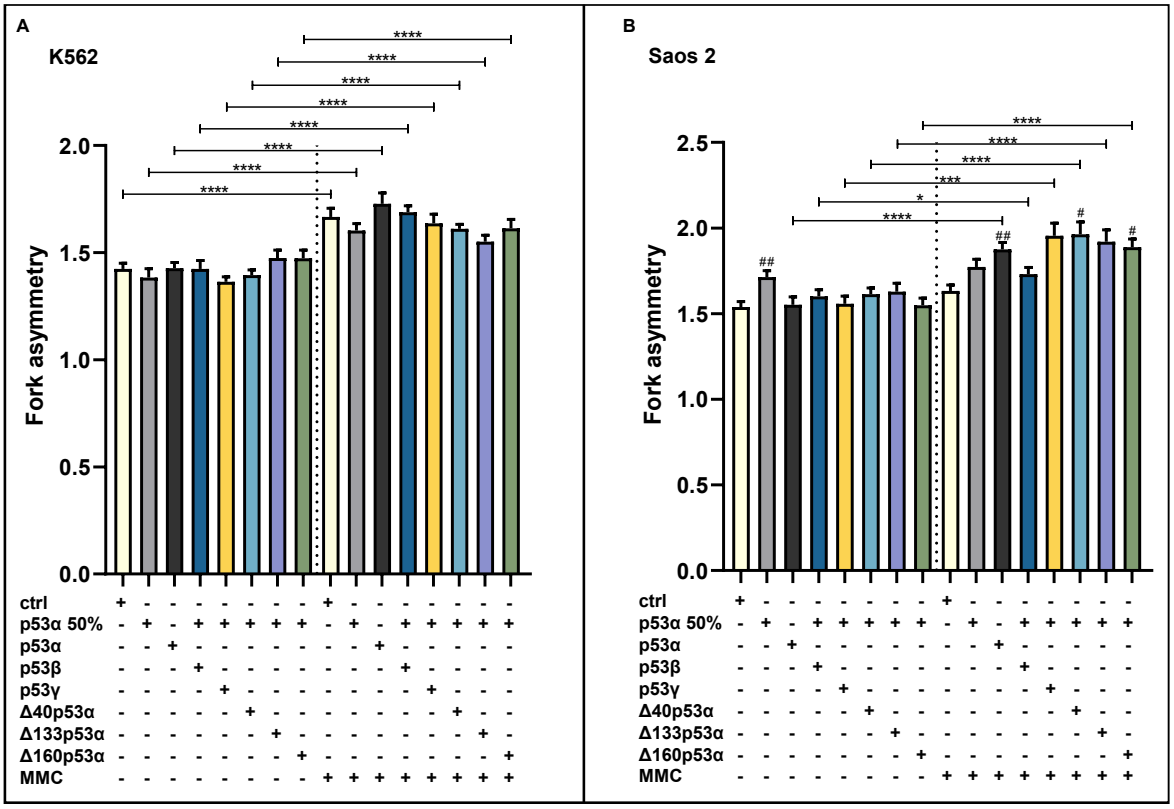

Figure 17 Fork asymmetry analysis of DNA fibers from K562 cells (A) and Saos 2 cells (B) quantified in Figure 15 and Figure 16.

For the analysis of replication fork stalling the fork asymmetry was evaluated. To this end, the ratio of longer vs. shorter tracks was calculated from the DNA fiber spreading assay shown in Figure 15 and Figure 16. Increased ratios of either CldU/IdU or IdU/CldU indicates replication fork stalling.

Next, IF of POLι and PCNA in K562 cells was done to investigate foci accumulation within the nucleus (Figure 18 and Figure 19, representative images shown in Figure 20). Both p53α 50% and p53α samples showed induction of a significant accumulation of POLι foci compared to ctrl either under mock or MMC-treatment (Figure 18A) while the co-expression of p53α and any one of the other five isoforms failed to upregulate POLι foci compared to ctrl under both treatment (Figure 18A).

Regarding PCNA foci differences were seen only when cells underwent MMC-treatment. Here expression of p53α induced PCNA foci significantly compared to ctrl while only samples with the following co-expressions: p53α&p53β and p53α&Δ160αp53, showed notable increases in PCNA foci numbers compared to ctrl in K562 cells (Figure 18B).

Regarding POLι-PCNA foci colocalization (Figure 19A), both p53α 50% and p53α samples showed enhanced co-localization of POLι-PCNA foci compared to ctrl regardless of treatment whereby p53α 50% samples showed an intermediate increase which was less than that for the p53α samples (Figure 19A). Remarkably, with none of the other samples co-expressing p53 isoforms we saw foci numbers above the control except for cells co-expressing p53α&p53β subjected to MMC-treatment, where an increase in the POLι-PCNA colocalization foci numbers compared to ctrl was observed (Figure 19A).

Figure 19B depicts the representative images of western blots from co-expression experiments. Taken together, accumulation of POLι foci at PCNA foci was induced by p53α in a dose-dependent manner. When p53α was co-expressed with isoforms other than p53β, this POLι foci formation was abrogated.

Taken together, the existence of p53 isoforms other than p53α alter the p53α-POLι dependent DDT pathway severely and show a dominant negative effect on p53α in cells co-expressing the different isoforms.

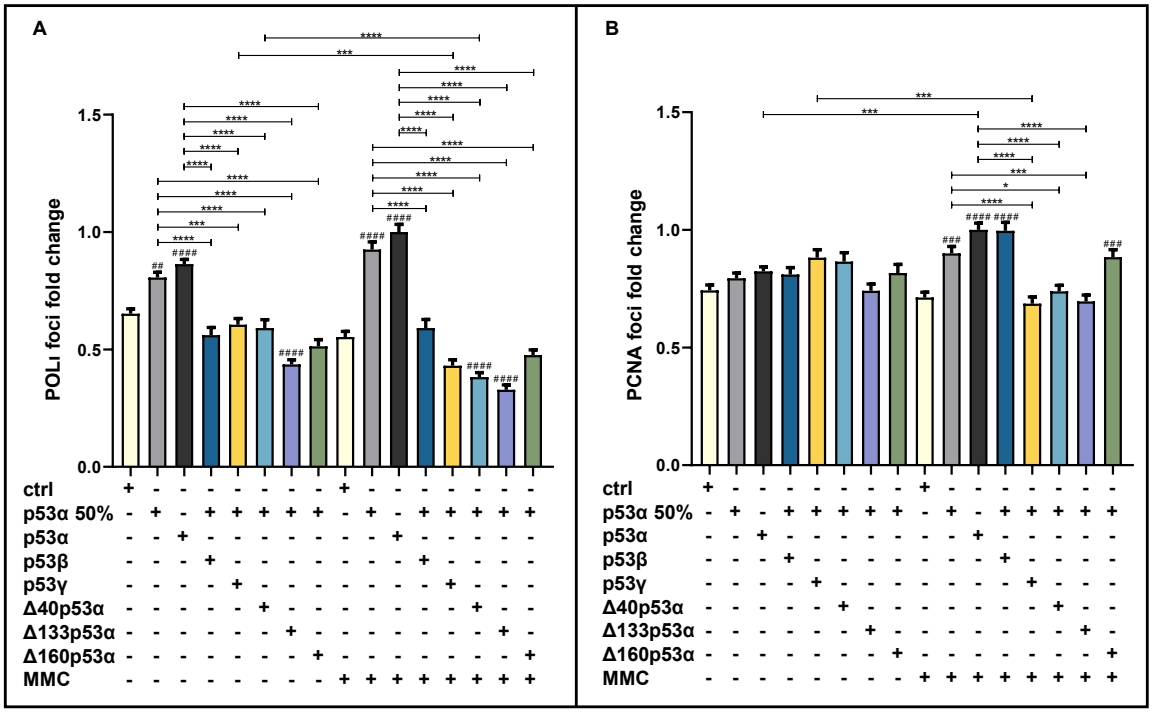

Figure 18 IF of POLı and PCNA in K562 cells with co-expression of p53α and five other isoforms.

Experiment and analysis conditions were the same as in Figure 15. ≥96 nuclei were analyzed in each group out of two independent experiments. Experiments were done together with experiments in Figure 9 and Figure 10 so that data of ctrl and p53α are identical to data of these two groups in Figure 9 and Figure 10. Absolute mean values of p53α expressing MMC-treatment samples were 100 POLı foci (A), 130 PCNA foci (B) per nucleus. Error bars indicate SEM. Statistical significances between groups were calculated using Dunn's multiple comparisons test. Stars represent significant differences and were not calculated for differences between p53 isoforms´ co-expressing groups.

A, **B**: IF of POLı foci (A), PCNA foci (B) fold changes to p53α (MMC) in K562 cells.

(Contents of this figure were published in [79])

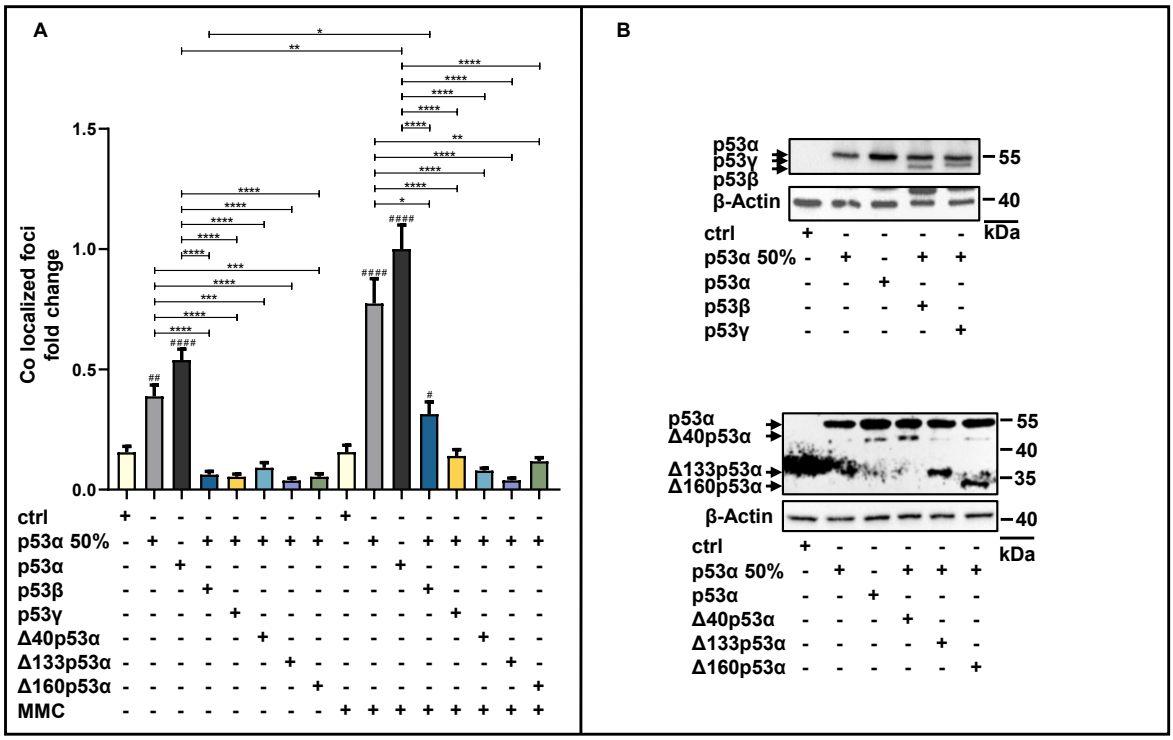

Figure 19 IF analysis of POLι-PCNA colocalization in K562 cells with co-expression of p53α and five other isoforms.

A: POLι-PCNA colocalization analysis of data in shown in Figure 18. Absolute mean values of p53α expressing MMC-treatment samples were 14 POLι-PCNA colocalized foci (A) per nucleus. Error bars indicate SEM. Statistical significances between groups were calculated using Dunn's multiple comparisons test. Stars represent significant differences and were not calculated for differences between p53 isoforms´ co-expressing groups.

B: Proteins extracted with cell lysis buffer for western blotting from K562 cells transfected as in Figure 15 and Figure 18. Protein samples from cells expressing p53α and co-expressing p53α and C-terminally altered isoforms: p53β or p53γ were detected with anti-p53 (DO-1) antibody. Protein samples from cells expressing p53α and co-expressing p53α and ΔN-isoforms: Δ40p53α, Δ133p53α or Δ160p53α were detected with anti-p53 (DO-11) antibody.

(Contents of this figure were published in [79])

.

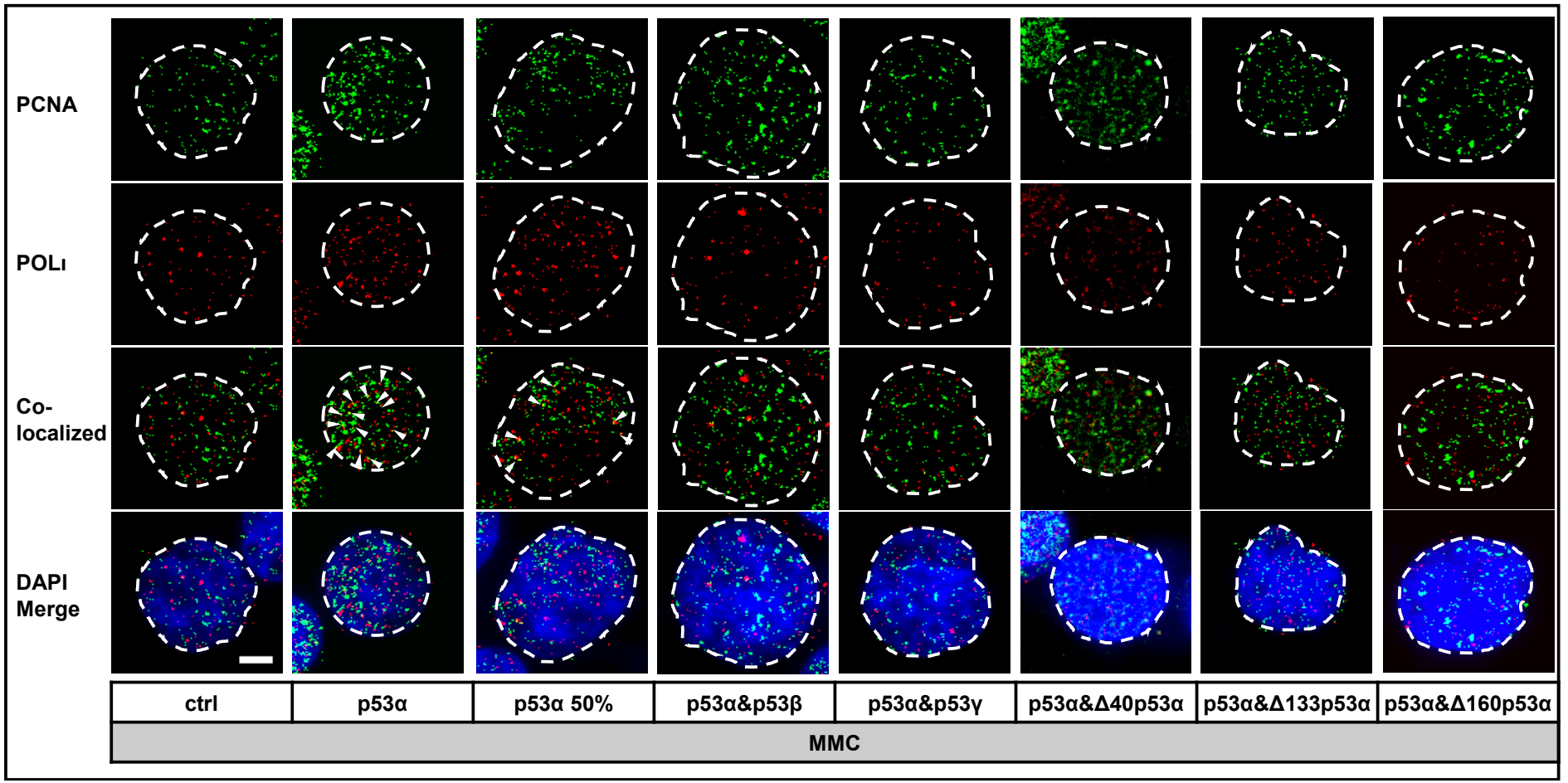

Figure 20 Representative IF images performed on cells transfected with EV, p53α or p53α plus one of the other five isoforms following MMC-treatment (quantified in Figure 18 and Figure 19). Scale bar: 5 μm.

4 Discussion

4.1 The transactivation activities of p53 isoforms

As a transcriptional factor, p53α modulates more than 3000 genes [65] and the transactivation activity is closely related to the function of p53α. Hence, it is interesting to understand the differences in transactivation activities between the p53 isoforms. First of all, p53 C-terminally altered isoforms were tested. In Saos 2 cells, p53β and p53γ were defective in inducing both MDM2 and p21 (Figure 6C). However, in K562 cells, I saw that p53α and C-terminally altered isoforms p53β and p53γ induced MDM2 protein expression while p53β and p53γ were defective in the induction of p21 protein (Figure 6E). Loss in the induction of p21 by p53β and p53γ differs from previous results showing p53β and p53γ lead to increased p21 protein expression in H1299 cells [178] and p53β binds more to *p21* and *BAX* promoters but not to *MDM2* promoter through chromatin immunoprecipitation [107] . But it was also proven that p53β and p53γ are incapable of activating genes including *DDI2, ARG2, p21, E2F7, SERPINE1, TP53INP1* or *TP73* through promoter reporter assay in H1299 cells [178]. Hence, p53β and p53γ may indeed be defective in transcriptionally inducing p21 expression. In support of this notion, another study investigating the p53 C-terminally truncated mutant p53Δ24 has shown that the mutant affects less the MDM2 than the p21 protein levels and that the p53 CTD is necessary for binding of p53 to the p21 promoter but not to the MDM2 promoter in H1299 cells [82]. Hence, p53β and p53γ are still somewhat effective in inducing MDM2 as seen in K562 cells. Importantly, the transactivation activities of p53β and p53γ are cell line dependent whereas p53α is always functional.

Next the transactivation activities of p53 ΔN-isoforms were investigated. Previous studies have shown that Δ40p53α shows much less binding to *Mdm2* and *p21* promoter compared to p53α in Balb/c 10.1 fibroblasts [48] and mediates no measurable protein induction of p21 in H1299 and Saos 2 cells [80]. However, it was also reported that the p53 N-terminal inhibits p53 binding to DNA, whereby increasing loss of N-terminal fragments strengthens this binding. Thus, p53 lacking

the first 40 amino acid fragment binds to the *CDKN1A* and *MDM2* promoter similarly compared to p53α while p53 (70-393) or p53 (90-393) fragments show 10 or 20 fold increases in *p21* and *MDM2* promoter binding compared to p53α in H1299 cells [85]. These studies indicate transactivation activity of ΔN-isoforms through measuring the binding affinities to promoters of target genes, but little was known regarding the target protein levels. Here, I found that only p53α is able to induce MDM2 and p21 in Saos 2 cells (Figure 6D). In K562 cells, p53α, Δ40p53α and Δ133p53α induced MDM2 expression while Δ160p53α did not (Figure 6F). p21 protein is only induced by p53α but not by other ΔN-isoforms (Figure 6F).

I also found that K562 cells express residual p21 and MDM2 even without p53α being expressed while Saos 2 cells do not. K562 cells express p73 [163] but Saos 2 cells are p53/63/73 null [87, 98]. Study has found that p73 binds to *p21* promoter in luciferase reporter assay and p73 induces p21 expression in IF [98]. In addition, p73 was also proven to bind the *MDM2* gene promoter [169]. Therefore, residual p21 and MDM2 expression may attribute to the fact that K562 cells express p73. Δ133p53α forms complex with p73 and act synergistically in transcriptional activation of certain genes [74], which probably explain the expression of Δ133p53α in K562 cells cause increase in MDM2 expression compared to ctrl.

Thus, truncations of p53α at its N-terminal show less effect on its transactivation activity towards *MDM2* in K562 cells while all ΔN-isoforms are generally transactivation defective in Saos 2 cells. However, other p53 isoforms possess abilities of transcription of other target genes instead of *MDM2* and *p21.* As shown in Table 1, p53 isoforms play important roles in many biological procedures such as cell cycle regulation, apoptosis and DNA damage repair by regulating many target genes including *CDC20, BUB1, BAX, PUMA, NOXA, RAD51, LIG4, RAD52*. All these target genes of different p53 isoforms explained their multiple functions in different cells (i.e. cancer cells, stem cells). In the future, more consideration should be paid to p53 isoforms due to their diverse transcriptional activities which made them have the potential of being new therapeutic targets of diseases especially

cancer.

4.2 The role of C-terminally altered isoforms of p53 in the POLι dependent DDT pathway

A previously in the introduction mentioned paper from the lab of my MD supervisor Prof. Dr. Wiesmüller has provided evidence for p53α collaborating with POLι in idling events when the DNA replication fork encounters a replication barrier. This idling process keeps the replication forks from being collapsed and permits the DNA damage bypass mediated by HLTF and ZRANB3 [83].

My thesis showed that two C-terminally altered p53 isoforms, p53β and p53γ, are involved in regulating the POLι dependent DDT pathway in the absence of p53α. These two isoforms were defective in stimulating recombination (Figure 6E) and still caused shortening of the DNA fiber track length, namely p53β in K562 and Saos 2 cells and p53γ at least in Saos 2 cells (Figure 7A, Figure 8A).

Further IF in K562 cells investigated the association of POLι and PCNA, which represents an initial step in the p53α and POLι dependent DDT pathway. The analysis revealed enhanced subnuclear distribution of POLι and PCNA in focal structures in the nucleus and accumulation of POLι-PCNA colocalizing foci when cells express p53β or p53γ at least as seen for p53α (Figure 9A, C). Then by chromatin crosslinking IP in K562 cells (Figure 12A, B), it is shown that both p53β and p53γ are capable of binding to PCNA and POLι like p53α under unperturbed condition. Therefore, p53β and p53γ are able to interact with PCNA and POLι which is a prerequisite for the idling events in which p53α is known to participate. Since POLι is one of the TLS-POLs which can be recruited by mono-ubiquitinated PCNA, I asked whether these p53 isoforms influence PCNA ubiquitination. Western blot quantification in Figure 13A showed that the expression of p53α, p53β and p53γ in cells led to significant increases in mono-ubiquitinated PCNA in comparison to ctrl. Analysis of poly-ubiquitinated PCNA levels showed that the expression of p53α, p53β and p53γ also induced PCNA poly-ubiquitination, though without statistical significance. Lack of statistical significance might be due to lower numbers of

independent experiments compared to the ones accomplished for PCNA mono-ubiquitination (Figure 13A, B). These findings were consistent with the preceding results from DNA fiber and IF analyses. Altogether they did lend support to the concept that under unperturbed conditions the DDT pathway is initiated in the presence of p53α as well as p53β and to a lesser extent also p53γ. However, compared to p53α, the C-terminally altered isoforms p53β and p53γ were defective in mediating full execution of replication-associated recombination downstream of complex formation with POLι (Figure 6E). These at first sight contradictory findings suggest that p53β or p53γ can participate in POLι complex formation and in idling processes at replication forks and therefore replication slow-down, however, these intermediate complexes cannot be resolved by homology-directed DDT, possibly due to failure to recruit HLTF, ZRANB3 or other factors known to execute fork reversal and/or fork regression.

Because the C-terminal of p53β and p53γ are truncated and replaced by another sequence, the alteration in CTD and OD may cause the defect in stimulate the replication-associated recombination. It is tempting to speculate that due to alternative sequences at the C- terminal, other proteins are recruited which bypass the lesion differently than the HLTF-ZRANB3 dependent homology directed DDT.

The p53α CTD contains a binding site that is essential for polymeric adenosine diphosphate ribose (PAR) binding which is mapped to amino acids 363 - 382. This binding site was mutated in the previously described p53α PBM4 mutant, abrogating PAR binding and PARylation, whereby oligomerization of the p53α PBM4 mutant remained unaffected. When expressing this mutant in K562 cells, the replication-associated recombination frequency was significantly reduced compared to p53α [64]. Moreover, cells expressing p53α and treated with poly ADP-ribose polymerase inhibitor (PARPi) featured a severe loss of the capacity to stimulate replication-associated recombination [64]. However, recent data from Biber et al showed that mutant p53ΔC (p53α missing amino acids 370 - 393) still retains the ability to stimulate replication-associated recombination [25] which therefore excludes the

possibility that deficiencies in PAR binding and PARylation cause the loss in stimulation of replication-associated recombination.

The OD of p53α, mapping to amino acids 325 – 356, mediates the formation of tetramers (Figure 4). p53β and p53γ still possess the OD from amino acids 325 to amino acids 331 partially, ending in p53β and p53γ at amino acids 331 within the OD sequence of p53α (Figure 6A). Biber et al found that mutant p53ΔO (p53α missing amino acids 327-346) failed to stimulate replication-associated recombination and to decrease the DNA track length compared to p53α [25].

Therefore, partial deletion of the OD in p53β and p53γ may cause the failure in facilitating replication-associated recombination, even though the necessary interactions with POLι, RPA and PCNA [25] via N-terminal regions and topoisomerase-I via the HD [73, 166, 168] are intact. On the other hand, researchers have also found that p53β is still capable of forming a stable and dimeric 3D conformation when bound to DNA [116], though lacking a large part of the OD. Thus, the residual OD fragment in p53β and p53γ may be sufficient for weak DNA binding to support idling events during DNA replication. However, we cannot exclude that due to the addition of alternative sequences at the C-terminal, other proteins are recruited which still cause fork slowing but help to bypass the lesion differently than via HLTF and ZRANB3 dependent homology-directed DDT. Regarding the moderate differences in replication phenotypes between p53β and p53γ, namely track shortening in the presence of p53β regardless of the cell type but in Saos 2 cells exclusively after p53γ expression, we again can only speculate about potential differences caused by the p53γ-specific C-terminal peptide and potentially new or specifically altered interactions. Interestingly also, MDM2 has been reported to enhance DNA replication speed independently of p53α [104, 105], and notably I did observe constitutive MDM2 expression in K562 cells as compared to Saos 2 cells without (Figure 6C-F).

In conclusion, subtle differences between p53β and p53γ in the capability to affect replication elongation might be amplified by differential expression of cooperating

proteins in the particular cellular background. Moreover, fork asymmetry analysis of cells expressing p53 C-terminally altered isoforms will be done to see if fork stalling is involved in the declaration of replication or not.

When cells were treated with MMC which introduces intra- and inter-strand crosslinks, p53β and p53γ both showed a defect in shortening of DNA track lengths (Figure 7B, Figure 8B), POLι recruitment (Figure 9A), POLι-PCNA complex formation (Figure 9C) and PCNA mono/poly-ubiquitination (Figure 13A, B) compared with p53α. Consequently, POLι can neither efficiently execute translesion synthesis nor homology-directed DDT in the presence of p53β and p53γ, as POLι-PCNA complex formation is a prerequisite for both DDT pathways [25]. Hence, the DNA lesions induced by MMC are unable to be processed by p53β and p53γ.

With all the information obtained by the recent work by Biber et al. 2020 [25] and my thesis work, it is concluded that the integrity of the complete OD is a prerequisite for initiating p53-POLι dependent idling and resolving the DNA lesions through homology-directed DDT.

4.3 The role of p53 ΔN-isoforms in the POLι dependent DDT pathway

p53 ΔN-isoforms failed to facilitate replication-associated recombination when compared to p53α (Figure 6F). Nevertheless, IF analysis of POLι and PCNA in K562 cells demonstrated that p53α, Δ40p53α, Δ133p53α and Δ160p53α still possess the capacity to stimulate the subnuclear accumulation of POLι-PCNA colocalizing foci (Figure 10C)

Consistently, PCNA mono-ubiquitination, a prerequisite for TLS-POL and PCNA interactions [84, 187], was unaffected by these N-terminal truncations (Figure 13C). Importantly however, poly-ubiquitination of PCNA was significantly increased only in the presence of p53α, but not of Δ40p53α, Δ133p53α or Δ160p53α (Figure 13D). Poly-ubiquitination is necessary for DDT pathways engaging fork reversal, which also explains failure of these isoforms to induce homology-directed DDT. Hence, p53 ΔN-isoforms affected ubiquitination of PCNA at a later stage compared with C-

terminally altered ones. As previous data from the Wiesmüller team had suggested that p53-POLι idling gives time for PCNA poly-ubiquitination [25, 83], these results suggested an idling defect.

In mock-treated cells expressing the N-terminally truncated isoforms I did notice less efficient replication track shortening compared to p53α, which however reached statistical significance only with Δ40p53α expressing Saos 2 cells (Figure 7C, Figure 8C). When I examined the physical interactions of the p53 isoforms in more detail by IP experiments, I noticed that p53α, Δ40p53α, Δ133p53α and Δ160p53α are all bound to PCNA without chromatin crosslinking (Figure 12C), but only p53α and Δ40p53α showed a clear pull-down of POLι with anti-p53 antibodies after chromatin crosslinking (Figure 12D). This finding was surprising, because p53α has been reported to bind POLι at around amino acids 22 and 23 [25]. Therefore, I also performed IP experiments from whole cell lysates without chromatin crosslinking, which revealed that the loss of the N-terminal amino acids 1-39 caused a loss of POLι binding to Δ40p53α as compared to p53α (Figure 12H).

However, IP is a semi-quantitative method to assess the protein interactions. Due to the molecular weight of p53 isoforms and PCNA as well as their migrations on SDS gels, the quantification cannot be made properly. The molecular weight of PCNA is 30kDa and the molecular weight of p53 isoforms varies from 31kDa to 53 kDa (Figure 6A), The molecular weight of the IgG heavy chain is 50 kDa and the light chain is 25 kDa. Positions of some p53 isoforms are close to those of IgG heavy chain and the light chain on blots and make quantification being inaccurate and hard. A better way that might carry out in future to help will be proximity ligation assay [182] which visualize the association of proteins through IF analysis that can be easily quantified.

Taken these experiments together, I conclude that N-terminal truncation did not affect PCNA mono-ubiquitination compared to p53α and assembly of POLι-PCNA foci, it also did not completely abrogate the capability of ΔN-isoforms to form complexes with PCNA in the chromatin. However, physical interactions of ΔN-

isoforms with POLι were affected, of Δ133p53α and Δ160p53α already in the chromatin. Interestingly, Δ40p53α still associated with POLι in the chromatin, but no longer in Co-IPs from whole cell extracts. This observation indicated that interactions of Δ40p53α with DNA structures and proteins other than POLι could indirectly stabilize its association with POLι in the chromatin. Such an association would not be fully functional with regard to idling, as can be seen from the DNA fiber spreading results in Saos 2 cells (Figure 8C, D). A likely candidate for such an interaction could be RPA, which binds to p53α between amino acids 40-60 [1, 168] and this region is missing in Δ133p53α and Δ160p53α. Of note, the p53 target gene product MDM2 plays a role in facilitating the protective effect of p53α in DNA replication fork processivity [104] which may attributes to the abilities that MDM2 modify histones and chromatin structures [207]. Moreover, MDM2 was found to prevent the persistent existence of R loops (such as DNA: RNA hybrids) [105] and protect the DNA replication. Therefore, MDM2 may serves as a cofactor of formation of p53-POLι complex and idling events especially for p53 isoforms other than p53α during DNA replication fork processing. Thus, the DNA fiber-spreading assay of K562 cells and Saos 2 cells with MDM2 overexpression as well as p53 isoforms expression can be carried out to test this possibility.

As for Δ133p53α and Δ160p53α, also parts of the DBD from amino acids 94 to 132 and amino acids 94 to 159 are missing in these two isoforms. Moreover, the exonuclease activity of p53 is restricted to this DBD (specifically amino acids 80 - 290) [2, 146]. In addition, Δ133p53α and Δ160p53α are not fully proficient in interacting with POLι (Figure 12D) though the expression of Δ133p53α and Δ160p53α still accumulates POLι-PCNA colocalizing foci (Figure 10C) which likely is due to upregulation of mono-ubiquitinated PCNA levels (Figure 13C). In short, Δ133p53α and Δ160p53α failed to interact with POLι and as a consequence cannot participate in idling events during DNA replication. Since Δ133p53α and Δ160p53α decreased the DNA track lengths, Δ133p53α and Δ160p53α might induce fork reversal via an alternative DDT pathway, which contributes to the deceleration of

DNA replication [202]. Moreover, shortening of DNA track lengths may also attribute to increasing fork stalling [104] and origin firing [151]. Hence, calculation of fork asymmetry and origin firing will be performed in future to verify these possibilities.

Importantly, mono-ubiquitination of PCNA is affected by p53 and its target p21. p21 binds to PCNA via its PCNA-interacting protein (PIP) box and exclude POLδ which provide more space for respective protein to mono-ubiquitinate PCNA and the loading of other TLS-POLs [122]. p53 isoforms other p53α are defective in transcriptional activity in p21 and then might lead to defective in formation of p53-POLι complex and idling. Future DNA fiber-spreading assay could be applied to K562 cells and Saos 2 cells transfected with p21 expression plasmids and p53 isoforms expression plasmids for investigating the role of p21 in POLι dependent DDT.

After cells were treated with MMC, Δ40p53α, Δ133p53α and Δ160p53α isoforms were fully defective in reducing DNA track lengths (Figure 7D, Figure 8D) and accumulation of POLι foci and POLι-PCNA colocalizing foci (Figure 10A, C). Thus, these isoforms are unable to process the DNA lesions induced by MMC via the p53-POLι DDT pathway slowing down replication. Nevertheless, other mechanisms might be that other TLS-POLs are recruited instead of POLι or restart of replication by Primase And DNA Directed Polymerase (PRIMPOL) [13] when MMC-treatment is applied. Future investigation should focus on the involvement of other TLS-POLs and PRIMPOL in DNA replication under cell stress.

Through my results with these ΔN-isoforms, it is obvious that the p53 N-terminal and the DBD are both essential for POLι dependent DDT.

4.4 The effect of p53 isoforms on the p53α-POLι dependent DDT pathway

Dysregulation of the co-expression of different p53 isoforms in cells is known to change the cellular p53 response, thereby driving oncogenesis, while conferring sensitivity to certain cancer treatments [5]. Altered co-expression of p53 isoforms is also observed in many cancers (Table 2). Importantly, p53 hetero-oligomerization

can occur when p53 isoforms are co-expressed. A dominant-negative effect of p53 exerted via hetero-oligomerization has already been reported in 1992 [113]. Therefore, I co-expressed p53α and other five isoforms in the p53-negative cell lines K562 and Saos 2, respectively, to investigate the impact of C-terminally altered and N-terminally truncated p53 isoforms on the p53α-POLι dependent DDT pathway.

First of all, I performed the DNA fiber-spreading assay in K562 and Saos 2 cells. p53α expression led to deceleration of DNA replication in a dose-dependent manner (Figure 15, Figure 16) in both mock and MMC treated cells. Co-expression of p53α together with other isoforms did not affect the DNA replication speed compared to the p53-negative ctrl cells when cells underwent mock-treatment (Figure 15A, Figure 16A). This was also true for cells subjected to MMC-treatment except for K562 cells co-expressing p53α and p53β, where a significant reduction in DNA track length compared to ctrl was observed while this reduction was gone in Saos 2 cells (Figure 15B, Figure 16B). Fork asymmetry analysis by measuring the ratio of longer vs shorter tracks was calculated from the DNA fiber-spreading assay shown in Figure 17 and increased ratios of either CldU/IdU or IdU/CldU indicates replication fork stalling [130]. MMC-treatment at least leads to fork stalling in all transfected K562 cells. In addition, the fork slowing by p53α was the consequence of idling but not increasing fork stalling.

Furthermore, IF analysis of POLι and PCNA was performed in K562 cells (Figure 18, Figure 19). As expected, p53α induced accumulation of POLι foci and POLι-PCNA colocalization foci significantly compared to ctrl cells in a dose-dependent manner and regardless of treatment (Figure 18A, Figure 19A). However, all the co-expression samples except p53α&p53β (MMC-treatment) failed to upregulate POLι foci and POLι-PCNA colocalization foci (Figure 18A, Figure 19A). The accumulation of POLι-PCNA colocalizing foci by p53α&p53β under MMC-treatment was compatible with track length shortening in the same cells indicating functionality of the p53α-POLι complex in DNA replication. Thus, the fiber assay in Figure 15B showing that p53α&p53β reduces the DNA track length under MMC-treatment is

very likely a consequence of upregulated POLι-PCNA colocalization foci.

Altogether, these co-expression data indicate the existence of five other p53 isoforms altering the p53α-POLι dependent DDT in a dominant negative fashion towards p53α. Herein p53β exerted the smallest if any effect, reflecting the phenotype of individual p53β expression (Figure 7, Figure 8), and again only in K562 cells with constitutive MDM2 expression and residual p21 levels.

Possible explanation for the dominant negative effect can be the subcellular localization of isoforms. Δ40p53α, which complexes p53α, has previously been found to predominantly localize in the cytoplasm and therefore shift the localization of p53α from the nucleus to the cytoplasm [72]. The other probable explanation for this dominant negative effect on the p53α-POLι dependent DDT is the hetero-oligomerization of p53α with other isoforms. It was shown that p53β forms a protein complex with p53α [33, 103] and binds DNA, regulates transcription, regulates apoptosis, cell cycle progression and senescence [103]. Δ40p53 was also found to oligomerize with p53α and act in a dominant negative fashion on p53α, which inhibits transactivation activity and impairs growth suppression mediated by p53α [48]. Moreover, Δ133p53α was proven to play a dominant negative effect on apoptosis induction by p53α, which is beneficial for p53α-dependent DNA repair and cell cycle progression [33, 45, 147]. Δ133p53α can interact with p53α and decrease the expression of *p21* mRNA and miR-34a induced by p53α, which further proved the dominant negative effect of Δ133p53α [145]. In addition, protein aggregation may also contribute to the dominant negative effect on p53α. The TAD of p53α was shown to inhibit aggregation of the p53α DBD significantly whereby Δ40p53 possesses a higher aggregation tendency [171]. ∆133p53 aggregates much faster than p53α or p53C (artificial p53 fragment consisting only of the DBD) [109]. Thus, ∆133p53 could exert a dominant negative effect by aggregating with p53α or blocking p53α from binding to the REs of target genes [200]. Δ160p53α, which is similar to ∆133p53α in missing the full TAD and part of the DBD but still possessing the full OD may also form complexes with p53α and play a dominant negative effect

through hetero-oligomerization.

In summary, when p53α is co-expressed with one of the other five isoforms included in this study, the p53α-POLι dependent DDT pathway is inactivated and the reason might be the hetero-oligomerization of different p53 isoforms known to inactivate the canonical functions of p53α in transcription.

4.5 p53 isoforms and POLι dependent DDT in cancer

p53 isoforms are found to be differently expressed in mRNA level or in protein level in many cancers and proven to play important roles in diagnosis as well as prognosis of patients (Table 2). p53α accomplished a “healer” function due to its ability to form complex with POLι and serves as a necessary factor in POLι DDT pathway to protect fast-proliferating cancer cells from DNA replication stress as well as chemotherapy [83].

In my thesis, I studied the roles of different p53 isoforms that are frequently expressed and correlated with tumor (Table 2) in the POLι dependent DDT pathway in order to reveal how p53 isoforms other than p53α and how co-expression of p53 isoforms affecting this POLι dependent DDT pathway which shows protective effect in tumor development. With the results from two p53 C-terminally altered isoforms: p53β and p53γ, they are still able to bind PCNA and POLι to perform idling during DNA replication. However, their abilities to mediate homology-directed DDT are defective due to partial loss of OD and complete loss of CTD. In many cancers, when p53β and p53γ mRNA or protein are found to be co-exist with p53 mutations, increasing p53β and p53γ mRNA or protein level is associated with better OS or DFS (Table 2) [11, 32, 219]. This phenomenon might be explained by that p53β and p53γ activate POLι dependent DDT but are unable to mediate the homology-directed DDT. Thus, the protective function for cancer cells was lost, which might result in fork collapse during the DNA replication and lead to cell death. Additionally, these two isoforms show transcriptional activities of *BAX* which regulate the apoptosis (Table 1)[33, 128] in a p53α independent manner. With these mechanisms, some patients with elevated p53β and p53γ mRNA or protein levels demonstrate

improved OS or DFS when p53α is mutated.

Δ40p53α and Δ133p53α demonstrate some oncogenic properties in Table 2. Δ40p53α is involved in cell cycle regulation and pluripotency shown in Table 1. Cell cycle regulation offer cells the opportunities to repair the DNA damage. The pluripotency of ESCs was found to be maintained by Δ40p53α [196]. There are now more evidence showing that cancer stem cells attribute to cancer development [19]. My hypothesize is that the expression of Δ40p53α maintains the pluripotency of cancer stem cells and facilitates the cancer progression. But this requires more investigation.

Δ133p53α is associates with many biological functions that facilitates the cancer development (Table 2) such as cell cycle regulation, DNA damage repair and cellular invasion. Δ160p53α is less investigated compared to other isoforms and show limited information both in biological functions and tumor (Table 1, Table 2). My study showing that Δ133p53α and Δ160p53α bind to PCNA and regulate DNA replication in cancer cells provide the clue that these two isoforms play important role in DNA replication. However, more details are still required to understand the exact meaning of these observations and mechanisms hidden behind.

Altogether, the expression patterns and roles of p53 isoforms in cancers are complicated and diverse. Additionally, different p53 isoforms are commonly expressed together which increased the difficulty in classifying their interplays. Nevertheless, investigating the roles of p53 isoforms in cancers is helpful in elucidating multiple functions of p53.

5 Summary

The human *tumor protein p53 (TP53)* gene, has been considered to play essential roles in deoxyribonucleic acid (DNA) damage responses (DDR) and DNA damage tolerance (DDT). Additionally, a new p53-Polymerase iota (POLι) dependent DDT pathway which was described in 2016 suggests that p53α is involved in promoting DNA replication fork stability by interacting with POLι to perform idling when the replication fork encounters a replication barrier to protect the fork from collapse and permit safe DNA damage bypass mediated by helicase-like transcription factor (HLTF) and Zinc Finger Ran-Binding Domain-Containing Protein 3 (ZRANB3) or, in case of persistent stress, Meiotic Recombination 11 Homolog (MRE11) dependent DNA resection.

Recently, p53 isoforms have attracted more attention. By utilizing different promotors, alternative splicing and internal ribosome entry site (IRES), 12 different isoforms of the p53 can be generated whereby p53α is one of them which is usually considered full length (FL) p53. All p53 isoforms except p53α have their C-terminal or N-terminal truncated and/or replaced by alternative sequences. These isoforms have their own biological functions which might be different from p53α. Moreover, these isoforms were also found to play important roles in various cancers.

Therefore, it was interesting to elucidate the roles of the p53 isoforms in the p53-POLι dependent DDT pathway as compared with p53α. Moreover, investigating how p53 isoforms affect the role of p53α in the p53-POLι dependent DDT pathway by co-expression of p53α and its isoforms, as this represents a prominent phenotype in cancer and normal cells, was even more appealing.

In my MD thesis, I found that p53 C/N-terminally altered/truncated isoforms dramatically decreased the p21 induction in K562 cells without markedly affecting the constitutively high Mouse Double Minute 2 (MDM2) expression level. The transactivation activities of these isoforms were also found severely defective in Saos 2 cells as compared to p53α. Hence, p53 isoforms other than p53α were devoid of the canonical p53 functions in transcriptional transactivation in the human

p53-negative cell types engaged in this study.

Second, a difference in the characteristics of the proliferating cell nuclear antigen (PCNA) switchboard was noticeable in response to spontaneously generated or Mitomycin C (MMC)-induced replication barriers in the presence of different p53 isoforms other than p53α. More detailed, p53 isoforms stimulate PCNA mono/poly ubiquitination to a different extent at replication barriers, whereby C-terminally altered p53 isoforms failed to upregulate already PCNA mono-ubiquitination when ultimate replication barriers were introduced via MMC-treatment. N-terminally truncated isoforms showed a defect in PCNA poly-ubiquitination even without treatment. These changes in PCNA modification may at least in part also underlie abrogated assembly of POLι and PCNA foci in the nuclei that I noticed via immunofluorescence microscopic colocalization studies after MMC exposure. On the other hand, complex formation of p53 and POLι as well as p53 and PCNA as detected by immunoprecipitation experiments with and without chromatin crosslinking was found to be disturbed in case of the N-terminally truncated p53 isoforms. In my work I could further show that these molecular changes associated with p53 isoforms other than p53α translated into loss of replication-associated recombination, detected by a fluorescence-based assay, and failure to decelerate DNA replication at least after MMC-treatment, as monitored by DNA-fiber spreading assay.

In summary, even partial loss of the oligomerization domain in case of p53β and p53γ and the N-terminal domain in case of Δ40p53α or even DNA-binding domain in case of Δ133p53α and Δ160p53α cause failure to facilitate replication-associated recombination. Strikingly, I found that the presence of other p53 isoforms inactivate the p53α-POLι dependent DDT pathway, which indicates a dominant negative effect that might attributed to hetero-oligomerization of different p53 isoforms and resembles the situation in many cancers.

6 Bibliography

1. Abramova N A, Russell J, Botchan M, Li R: Interaction between replication protein A and p53 is disrupted after UV damage in a DNA repair-dependent manner. Proc Natl Acad Sci U S A 94: 7186–7191 (1997)
2. Ahn J, Poyurovsky M V., Baptiste N, Beckerman R, Cain C, Mattia M, McKinney K, Zhou J, Zupnick A, Gottifredi V, Prives C: Dissection of the sequence-specific DNA binding and exonuclease activities reveals a superactive yet apoptotically impaired mutant p53 protein. Cell Cycle 8: 1603–1615 (2009)
3. Akyüz N, Boehden G S, Süsse S, Rimek A, Preuss U, Scheidtmann K-H, Wiesmüller L: DNA Substrate Dependence of p53-Mediated Regulation of Double-Strand Break Repair. Mol Cell Biol 22: 6306–6317 (2002)
4. Albor A, Kaku S, Kulesz-Martin M: Wild-type and mutant forms of p53 activate human topoisomerase i: A possible mechanism for gain of function in mutants. Cancer Res 58: 2091–2094 (1998)
5. Anbarasan T, Bourdon J C: The emerging landscape of p53 isoforms in physiology, cancer and degenerative diseases. Int J Mol Sci 20: 6257 (2019)
6. Ånensen N, Hjelle S M, Van Belle W, Haaland I, Silden E, Bourdon J C, Hovland R, Taskén K, Knappskog S, Lønning P E, Bruserud O, Gjertsen B T: Correlation analysis of p53 protein isoforms with NPM1/FLT3 mutations and therapy response in acute myeloid leukemia. Oncogene 31: 1533–1545 (2012)
7. Aoubala M, Murray-Zmijewski F, Khoury M P, Fernandes K, Perrier S, Bernard H, Prats A C, Lane D P, Bourdon J C: P53 directly transactivates Δ133p53α, regulating cell fate outcome in response to DNA damage. Cell Death Differ 18: 248–258 (2011)
8. Arsic N, Gadea G, Lagerqvist E L, Bußon M, Cahuzac N, Brock C, Hollande F, Gire V, Pannequin J, Roux P: The p53 isoform Δ133p53β promotes cancer stem cell potential. Stem Cell Reports 4: 531–540 (2015)
9. Arsic N, Ho-Pun-Cheung A, Evelyne C, Assenat E, Jarlier M, Anguille C, Colard M, Pezet M I, Roux P, Gadea G: The p53 isoform delta133p53β regulates cancer cell apoptosis in a RhoB-dependent manner. PLoS One 12: e0172125 (2017)
10. Aurelio O N, Cajot J F, Hua M L H, Khwaja Z, Stanbridge E J: Germ-line-derived hinge domain p53 mutants have lost apoptotic but not cell cycle arrest functions. Cancer Res 58: 2190–2195 (1998)
11. Avery-Kiejda K A, Morten B, Wong-Brown M W, Mathe A, Scott R J: The relative mRNA expression of p53 isoforms in breast cancer is associated with clinical features and outcome. Carcinogenesis 35: 586–596 (2014)
12. Avery-Kiejda K A, Xu D Z, Adams L J, Scott R J, Vojtesek B, Lane D P, Hersey P: Small molecular weight variants of p53 are expressed in human melanoma cells and are induced by the DNA-damaging agent cisplatin. Clin Cancer Res 14: 1659–1668 (2008)
13. Bai G, Kermi C, Stoy H, Schiltz C J, Bacal J, Zaino A M, Hadden M K, Eichman

B F, Lopes M, Cimprich K A: HLTF Promotes Fork Reversal, Limiting Replication Stress Resistance and Preventing Multiple Mechanisms of Unrestrained DNA Synthesis. Mol Cell 78: 1237–1251 (2020)
14. Baker S J, Fearon E R, Nigro J M, Hamilton S R, Preisinger A C, Jessup J M, vanTuinen P, Ledbetter D H, Barker D F, Nakamura Y, White R, Vogelstein B: Chromosome 17 deletions and p53 gene mutations in colorectal carcinomas. Science 244: 217–221 (1989)
15. Baker S J, Preisinger A C, Jessup J M, Paraskeva C, Markowitz S, Willson J K V, Hamilton S, Vogelstein B: p53 Gene Mutations Occur in Combination with 17p Allelic Deletions as Late Events in Colorectal Tumorigenesis. Cancer Res 50: 7717–7722 (1990)
16. Banks D, Wu M, Higa L A, Gavrilova N, Quan J, Ye T, Kobayashi R, Sun H, Zhang H: L2DTL/CDT2 and PCNA interact with p53 and regulate p53 polyubiquitination and protein stability through MDM2 and CUL4A/DDB1 complexes. Cell Cycle 5: 1719–1729 (2006)
17. Baptiste N, Friedlander P, Chen X, Prives C: The proline-rich domain of p53 is required for cooperation with anti-neoplastic agents to promote apoptosis of tumor cells. Oncogene 21: 9–21 (2002)
18. Bargonetti J, Friedman P N, Kern S E, Vogelstein B, Prives C: Wild-type but not mutant p53 immunopurified proteins bind to sequences adjacent to the SV40 origin of replication. Cell 65: 1083–1091 (1991)
19. Batlle E, Clevers H: Cancer stem cells revisited. Nat Med 23: 1124–1134 (2017)
20. Beckerman R, Prives C: Transcriptional regulation by p53. Cold Spring Harb Perspect Biol 2: a000935–a000935 (2010)
21. Beckerman R, Yoh K, Mattia-Sansobrino M, Zupnick A, Laptenko O, Karni-Schmidt O, Ahn J, Byeon I J, Keezer S, Prives C: Lysines in the tetramerization domain of p53 selectively modulate G1 arrest. Cell Cycle 15: 1425–1438 (2016)
22. Bertrand P, Saintigny Y, Lopez B S: p53's double life: Transactivation-independent repression of homologous recombination. Trends Genet 20: 235–243 (2004)
23. Bi X: Mechanism of DNA damage tolerance. World J Biol Chem 6: 48–56 (2015)
24. Bi X, Barkley L R, Slater D M, Tateishi S, Yamaizumi M, Ohmori H, Vaziri C: Rad18 Regulates DNA Polymerase κ and Is Required for Recovery from S-Phase Checkpoint-Mediated Arrest. Mol Cell Biol 26: 3527–3540 (2006)
25. Biber S, Pospiech H, Gottifredi V, Wiesm L: Multiple biochemical properties of the p53 molecule contribute to activation of polymerase iota-dependent DNA damage tolerance. Nucleic Acids Res 48: 12188–12203 (2020)
26. Bischof K, Knappskog S, Hjelle S M, Stefansson I, Woie K, Salvesen H B, Gjertsen B T, Bjorge L: Influence of p53 Isoform Expression on Survival in High-Grade Serous Ovarian Cancers. Sci Rep 9: 5244 (2019)

27. Bischof K, Knappskog S, Stefansson I, McCormack E M, Trovik J, Werner H M J, Woie K, Gjertsen B T, Bjorge L: High expression of the p53 isoform γ is associated with reduced progression-free survival in uterine serous carcinoma. BMC Cancer 18: 1–10 (2018)
28. Blake M S, Johnston K H, Russell-Jones G J, Gotschlich E C: A rapid, sensitive method for detection of alkaline phosphatase-conjugated anti-antibody on Western blots. Anal Biochem 136: 175–179 (1984)
29. Bochkareva E, Kaustov L, Ayed A, Yi G S, Lu Y, Pineda-Lucena A, Liao J C C, Okorokov A L, Milner J, Arrowsmith C H, Bochkarev A: Single-stranded DNA mimicry in the p53 transactivation domain interaction with replication protein A. Proc Natl Acad Sci U S A 102: 15412–15417 (2005)
30. Boldrup L, Bourdon J C, Coates P J, Sjöström B, Nylander K: Expression of p53 isoforms in squamous cell carcinoma of the head and neck. Eur J Cancer 43: 617–623 (2007)
31. Bouaoun L, Sonkin D, Ardin M, Hollstein M, Byrnes G, Zavadil J, Olivier M: TP53 Variations in Human Cancers: New Lessons from the IARC TP53 Database and Genomics Data. Hum Mutat 37: 865–876 (2016)
32. Bourdon J C, Khoury M P, Diot A, Baker L, Fernandes K, Aoubala M, Quinlan P, Purdie C A, Jordan L B, Prats A C, Lane D P, Thompson A M: P53 mutant breast cancer patients expressing p53γ have as good a prognosis as wild-type p53 breast cancer patients. Breast Cancer Res 13: R7 (2011)
33. Bourdon J, Fernandes K, Murray-zmijewski F, Liu G, Diot A, Xirodimas D P, Saville M K, Lane D P: p53 isoforms can regulate p53 transcriptional activity. Genes Dev 19: 2122–2137 (2005)
34. Brady C A, Jiang D, Mello S S, Johnson T M, Jarvis L A, Kozak M M, Kenzelmann Broz D, Basak S, Park E J, McLaughlin M E, Karnezis A N, Attardi L D: Distinct p53 transcriptional programs dictate acute DNA-damage responses and tumor suppression. Cell 145: 571–583 (2011)
35. Branzei D, Foiani M: Maintaining genome stability at the replication fork. Nat Rev Mol Cell Biol 11: 208–219 (2010)
36. Broomfield S, Chow B L, Xiao W: MMS 2, encoding a ubiquitin-conjugating-enzyme-like protein, is a member of the yeast error-free postreplication repair pathway. Proc Natl Acad Sci U S A 95: 5678–5683 (1998)
37. Brosh R, Rotter V: When mutants gain new powers: News from the mutant p53 field. Nat Rev Cancer 9: 701–713 (2009)
38. Buchhop S, Gibson M K, Wang X W, Wagner P, Stürzbecher H W, Harris C C: Interaction of p53 with the human Rad51 protein. Nucleic Acids Res 25: 3868–3874 (1997)
39. Burns J L, Guzder S N, Sung P, Prakash S, Prakash L: An affinity of human replication protein A for ultraviolet-damaged DNA: Implications for damage recognition in nucleotide excision repair. J Biol Chem 271: 11607–11610 (1996)
40. Byun T S, Pacek M, Yee M C, Walter J C, Cimprich K A: Functional uncoupling

of MCM helicase and DNA polymerase activities activates the ATR-dependent checkpoint. Genes Dev 19: 1040–1052 (2005)
41. Campbell H, Fleming N, Roth I, Mehta S, Wiles A, Williams G, Vennin C, Arsic N, Parkin A, Pajic M, Munro F, McNoe L, Black M, McCall J, Slatter T L, Timpson P, Reddel R, Roux P, Print C, Baird M A, Braithwaite A W: Δ133p53 isoform promotes tumour invasion and metastasis via interleukin-6 activation of JAK-STAT and RhoA-ROCK signaling. Nat Commun 9: 254 (2018)
42. Candeias M M, Hagiwara M, Matsuda M: Cancer-specific mutations in p53 induce the translation of Δ160p53 promoting tumorigenesis. EMBO Rep 17: 1542–1551 (2016)
43. Chang D J, Cimprich K A: DNA damage tolerance: When it's OK to make mistakes. Nat Chem Biol 5: 82–90 (2009)
44. Chen J, Marechal V, Levine A J: Mapping of the p53 and mdm-2 interaction domains. Mol Cell Biol 13: 4107–4114 (1993)
45. Chen J, Ng S M, Chang Q, Zhang Z, Bourdon J C, Lane D P, Peng J: P53 isoform Δ113p53 is a p53 target gene that antagonizes p53 apoptotic activity via BclxL activation in zebrafish. Genes Dev 23: 278–290 (2009)
46. Cho Y, Gorina S, Jeffrey P D, Pavletich N P: Crystal structure of a p53 tumor suppressor-DNA complex: Understanding tumorigenic mutations. Science 265: 346–355 (1994)
47. Ciccia A, Elledge S J: The DNA Damage Response: Making It Safe to Play with Knives. Mol Cell 40: 179–204 (2011)
48. Courtois S, Verhaegh G, North S, Luciani M G, Lassus P, Hibner U, Oren M, Hainaut P: ΔN-p53, a natural isoform of p53 lacking the first transactivation domain, counteracts growth suppression by wild-type p53. Oncogene 21: 6722–6728 (2002)
49. D'Abramo M, Bešker N, Desideri A, Levine A J, Melino G, Chillemi G: The p53 tetramer shows an induced-fit interaction of the C-terminal domain with the DNA-binding domain. Oncogene 35: 3272–3281 (2016)
50. Davidson W R, Kari C, Ren Q, Daroczi B, Dicker A P, Rodeck U: Differential regulation of p53 function by the N-terminal Np53 and 113p53 isoforms in zebrafish embryos. BMC Dev Biol 10: 102 (2010)
51. Davies A A, Huttner D, Daigaku Y, Chen S, Ulrich H D: Activation of Ubiquitin-Dependent DNA Damage Bypass Is Mediated by Replication Protein A. Mol Cell 29: 625–636 (2008)
52. Delavaine L, La Thangue N B: Control of E2F activity by p21Waf1/Cip1. Oncogene 18: 5381–5392 (1999)
53. Dippold W G, Jay G, DeLeo A B, Khoury G, Old L J: p53 transformation-related protein: detection by monoclonal antibody in mouse and human cells. Proc Natl Acad Sci U S A 78: 1695–1699 (1981)
54. Donehower L A: The p53-deficient mouse: A model for basic and applied cancer studies. Semin Cancer Biol 7: 269–278 (1996)
55. Donehower L A, Harvey M, Slagle B L, McArthur M J, Montgomery C A J,

Butel J S, Bradley A: Mice deficient for p53 are developmentally normal but susceptible to spontaneous tumours. Nature 356: 215–221 (1992)
56. Donehower L A, Harvey M, Vogel H, McArthur M J, Montgomery C A, Park S H, Thompson T, Ford R J, Bradley A: Effects of genetic background on tumorigenesis in p53-deficient mice. Mol Carcinog 14: 16–22 (1995)
57. Dunker A K, Obradovic Z, Romero P, Garner E C, Brown C J: Intrinsic protein disorder in complete genomes. Genome Inform Ser Workshop Genome Inform 11: 161–171 (2000)
58. Dutta A, Ruppert J M, Aster J C, Winchester E: Inhibition of DNA replication factor RPA by p53. Nature 365: 79–82 (1993)
59. el-Deiry W S, Tokino T, Velculescu V E, Levy D B, Parsons R, Trent J M, Lin D, Mercer W E, Kinzler K W, Vogelstein B: WAF1, a potential mediator of p53 tumor suppression. Cell 75: 817–825 (1993)
60. Eliyahu D, Goldfinger N, Pinhasi-Kimhi O, Shaulsky G, Skurnik Y, Arai N, Rotter V, Oren M: Meth A fibrosarcoma cells express two transforming mutant p53 species. Oncogene 3: 313–321 (1988)
61. Eliyahu D, Michalovitz D, Oren M: Overproduction of p53 antigen makes established cells highly tumorigenic. Nature 316: 158–160 (1985)
62. Eliyahu D, Raz A, Gruss P, Givol D, Oren M: Participation of p53 cellular tumour antigen in transformation of normal embryonic cells. Nature 312: 646–649 (1984)
63. Finlay C A, Hinds P W, Tan T H, Eliyahu D, Oren M, Levine A J: Activating mutations for transformation by p53 produce a gene product that forms an hsc70-p53 complex with an altered half-life. Mol Cell Biol 8: 531–539 (1988)
64. Fischbach A, Krüger A, Hampp S, Assmann G, Rank L, Hufnagel M, Stöckl M T, Fischer J M F, Veith S, Rossatti P, Ganz M, Ferrando-May E, Hartwig A, Hauser K, Wiesmüller L, Bürkle A, Mangerich A: The C-terminal domain of p53 orchestrates the interplay between non-covalent and covalent poly(ADP-ribosyl)ation of p53 by PARP1. Nucleic Acids Res 46: 804–822 (2018)
65. Fischer M: Census and evaluation of p53 target genes. Oncogene 36: 3943–3956 (2017)
66. Fragou A, Tzimagiorgis G, Karageorgopoulos C, Barbetakis N, Lazopoulos A, Papaioannou M, Haitoglou C, Kouidou S: Increased δ133p53 mRNA in lung carcinoma corresponds with reduction of p21 expression. Mol Med Rep 15: 1455–1460 (2017)
67. Fujita K, Mondal A M, Horikawa I, Nguyen G H, Kumamoto K, Sohn J J, Bowman E D, Mathe E A, Schetter A J, Pine S R, Ji H, Vojtesek B, Bourdon J-C, Lane D P, Harris C C: p53 isoforms Delta133p53 and p53beta are endogenous regulators of replicative cellular senescence. Nat Cell Biol 11: 1135–1142 (2009)
68. Gadea G, Arsic N, Fernandes K, Diot A, Joruiz S M, Abdallah S, Meuray V, Vinot S, Anguille C, Remenyi J, Khoury M P, Quinlan P R, Purdie C A, Jordan L B, Fuller-Pace F V, De Toledo M, Cren M, Thompson A M, Bourdon J C,

Roux P: TP53 drives invasion through expression of its Δ133p53β variant. Elife 5: e14734 (2016)
69. Gambino V, De Michele G, Venezia O, Migliaccio P, Dall'Olio V, Bernard L, Minardi S P, Fazia M A Della, Bartoli D, Servillo G, Alcalay M, Luzi L, Giorgio M, Scrable H, Pelicci P G, Migliaccio E: Oxidative stress activates a specific p53 transcriptional response that regulates cellular senescence and aging. Aging Cell 12: 435–445 (2013)
70. Garg P, Stith C M, Sabouri N, Johansson E, Burgers P M: Idling by DNA polymerase delta maintains a ligatable nick during lagging-strand DNA replication. Genes Dev 18: 2764–2773 (2004)
71. Gatz S A, Wiesmüller L: p53 in Recombination and Repair. Cell Death Differ 13: 1003–1016 (2006)
72. Ghosh A, Stewart D, Matlashewski G: Regulation of Human p53 Activity and Cell Localization by Alternative Splicing. Mol Cell Biol 24: 7987–7997 (2004)
73. Gobert C, Skladanowski A, Larsen A K: The interaction between p53 and DNA topoisomerase I is regulated differently in cells with wild-type and mutant p53. Proc Natl Acad Sci U S A 96: 10355–10360 (1999)
74. Gong H, Zhang Y, Jiang K, Ye S, Chen S, Zhang Q, Peng J, Chen J: p73 coordinates with Δ133p53 to promote DNA double-strand break repair. Cell Death Differ 25: 1063–1079 (2018)
75. Gong L, Gong H, Pan X, Chang C, Ou Z, Ye S, Yin L, Yang L, Tao T, Zhang Z, Liu C, Lane D P, Peng J, Chen J: p53 isoform Δ113p53/Δ133p53 promotes DNA double-strand break repair to protect cell from death and senescence in response to DNA damage. Cell Res 25: 351–369 (2015)
76. Goodman M F, Woodgate R: Translesion DNA polymerases. Cold Spring Harb Perspect Biol 5: a010363 (2013)
77. Graupner V, Schulze-Osthoff K, Essmann F, Jänicke R U: Functional characterization of p53β and p53γ, two isoforms of the tumor suppressor p53. Cell Cycle 8: 1238–1248 (2009)
78. Grover R, Ray P S, Das S: Polypyrimidine tract binding protein regulates IRES-mediated translation of p53 isoforms. Cell Cycle 7: 2189–2198 (2008)
79. Guo Y, Rall-Scharpf M, Bourdon J-C, Wiesmüller L, Biber S: p53 isoforms differentially impact on the POLı dependent DNA damage tolerance pathway. Cell Death Dis 12: 941 (2021)
80. Hafsi H, Santos-Silva D, Courtois-Cox S, Hainaut P: Effects of Δ40p53, an isoform of p53 lacking the N-terminus, on transactivation capacity of the tumor suppressor protein p53. BMC Cancer 13: 134 (2013)
81. Halevy O, Rodel J, Peled A, Oren M: Frequent p53 mutations in chemically induced murine fibrosarcoma. Oncogene 6: 1593–1600 (1991)
82. Hamard P J, Lukin D J, Manfredi J J: p53 basic C terminus regulates p53 functions through DNA binding modulation of subset of target genes. J Biol Chem 287: 22397–22407 (2012)
83. Hampp S, Kiessling T, Buechle K, Mansilla S F, Thomale J, Rall M, Ahn J,

Pospiech H, Gottifredi V, Wiesmüller L: DNA damage tolerance pathway involving DNA polymerase ι and the tumor suppressor p53 regulates DNA replication fork progression. Proc Natl Acad Sci U S A 113: E4311–E4319 (2016)
84. Haracska L, Unk I, Prakash L, Prakash S: Ubiquitylation of yeast proliferating cell nuclear antigen and its implications for translesion DNA synthesis. Proc Natl Acad Sci U S A 103: 6477–6482 (2006)
85. He F, Borcherds W, Song T, Wei X, Das M, Chen L, Daughdrill G W, Chen J: Interaction between p53 N terminus and core domain regulates specific and nonspecific DNA binding. Proc Natl Acad Sci U S A 116: 8859–8868 (2019)
86. Hedglin M, Benkovic S J: Regulation of Rad6/Rad18 Activity During DNA Damage Tolerance. Annu Rev Biophys 44: 207–228 (2015)
87. Hibi K, Trink B, Patturajan M, Westra W H, Caballero O L, Hill D E, Ratovitski E A, Jen J, Sidransky D: AIS is an oncogene amplified in squamous cell carcinoma. Proc Natl Acad Sci U S A 97: 5462–5467 (2000)
88. Hoege C, Pfander B, Moldovan G L, Pyrowolakis G, Jentsch S: RAD6-dependent DNA repair is linked to modification of PCNA by ubiquitin and SUMO. Nature 419: 135–141 (2002)
89. Hoffman W H, Biade S, Zilfou J T, Chen J, Murphy M: Transcriptional repression of the anti-apoptotic survivin gene by wild type p53. J Biol Chem 277: 3247–3257 (2002)
90. Hofmann R M, Pickart C M: Noncanonical MMS2-encoded ubiquitin-conjugating enzyme functions in assembly of novel polyubiquitin chains for DNA repair. Cell 96: 645–653 (1999)
91. Hofstetter G, Berger A, Berger R, Zorić A, Braicu E I, Reimer D, Fiegl H, Marth C, Zeimet A G, Ulmer H, Moll U, Zeillinger R, Concin N: The N-terminally truncated p53 isoform Δ40p53 influences prognosis in mucinous ovarian cancer. Int J Gynecol Cancer 22: 372–379 (2012)
92. Hofstetter G, Berger A, Schuster E, Wolf A, Hager G, Vergote I, Cadron I, Sehouli J, Braicu E I, Mahner S, Speiser P, Marth C, Zeimet A G, Ulmer H, Zeillinger R, Concin N: Δ133P53 Is an Independent Prognostic Marker in P53 Mutant Advanced Serous Ovarian Cancer. Br J Cancer 105: 1593–1599 (2011)
93. Huang T, Long M, Huo B: Competitive Binding to Cuprous Ions of Protein and BCA in the Bicinchoninic Acid Protein Assay. Open Biomed Eng J 4: 271–278 (2010)
94. Inoue H, Nojima H, Okayama H: High efficiency transformation of Escherichia coli with plasmids. Gene 96: 23–28 (1990)
95. Jenkins J R, Rudge K, Currie G A: Cellular immortalization by a cDNA clone encoding the transformation-associated phosphoprotein p53. Nature 312: 651–654 (1984)
96. Jiang D, Brady C A, Johnson T M, Lee E Y, Park E J, Scott M P, Attardi L D: Full p53 transcriptional activation potential is dispensable for tumor

suppression in diverse lineages. Proc Natl Acad Sci U S A 108: 17123–17128 (2011)
97. Joruiz S M, Bourdon J C: p53 isoforms: Key regulators of the cell fate decision. Cold Spring Harb Perspect Med 6: a026039 (2016)
98. Jost C A, Marin M C, Kaelin W G: P73 Is a Human P53-Related Protein That Can Induce Apoptosis. Nature 389: 191–194 (1997)
99. Kazantseva M, Eiholzer R A, Mehta S, Taha A, Bowie S, Roth I, Zhou J, Joruiz S M, Royds J A, Hung N A, Slatter T L, Braithwaite A W: Elevation of the TP53 isoform Δ133p53β in glioblastomas: an alternative to mutant p53 in promoting tumor development. J Pathol 246: 77–88 (2018)
100. Kazantseva M, Mehta S, Eiholzer R A, Gimenez G, Bowie S, Campbell H, Reily-Bell A L, Roth I, Ray S, Drummond C J, Reid G, Joruiz S M, Wiles A, Morrin H R, Reader K L, Hung N A, Baird M A, Slatter T L, Braithwaite A W: The Δ133p53β isoform promotes an immunosuppressive environment leading to aggressive prostate cancer. Cell Death Dis 10: 631 (2019)
101. Kern S E, Kinzler K W, Bruskin A, Jarosz D, Friedman P, Prives C, Vogelstein B: Identification of p53 as a sequence-specific DNA-binding protein. Science 252: 1708–1711 (1991)
102. Khoury M P, Bourdon J-C: The isoforms of the p53 protein. Cold Spring Harb Perspect Biol 2: a000927–a000927 (2010)
103. Khoury M P, Bourdon J C: P53 isoforms: An intracellular microprocessor? Genes and Cancer 2: 453–465 (2011)
104. Klusmann I, Rodewald S, Müller L, Friedrich M, Wienken M, Li Y, Schulz-Heddergott R, Dobbelstein M: p53 Activity Results in DNA Replication Fork Processivity. Cell Rep 17: 1845–1857 (2016)
105. Klusmann I, Wohlberedt K, Magerhans A, Teloni F, Korbel J O, Altmeyer M, Dobbelstein M: Chromatin modifiers Mdm2 and RNF2 prevent RNA:DNA hybrids that impair DNA replication. Proc Natl Acad Sci U S A 115: E11311–E11320 (2018)
106. Knezović Florijan M, Ozretić P, Bujak M, Pezzè L, Ciribilli Y, Kaštelan Ž, Slade N, Hudolin T: The role of p53 isoforms' expression and p53 mutation status in renal cell cancer prognosis. Urol Oncol Semin Orig Investig 37: 578.e1-578.e10 (2019)
107. Kondo T, Oka T, Sato H, Shinnou Y, Washio K: Behind the scenes: Unravelling the molecular mechanisms of p53 target gene selectivity (Review). Int J Oncol 35: 547–557 (2009)
108. Kong X T, Gao H, Stanbridge E J: Mechanisms of Differential Activation of Target Gene Promoters by p53 Hinge Domain Mutants with Impaired Apoptotic Function. J Biol Chem 276: 32990–33000 (2001)
109. Kovachev P S, Banerjee D, Rangel L P, Eriksson J, Pedrote M M, Martins-Dinis M M D C, Edwards K, Cordeiro Y, Silva J L, Sanyal S: Distinct modulatory role of RNA in the aggregation of the tumor suppressor protein p53 core domain. J Biol Chem 292: 9345–9357 (2017)

110. Kress M, May E, Cassingena R, May P: Simian virus 40-transformed cells express new species of proteins precipitable by anti-simian virus 40 tumor serum. J Virol 31: 472–483 (1979)
111. Kussie P H, Gorina S, Marechal V, Elenbaas B, Moreau J, Levine A J, Pavletich N P: Structure of the MDM2 oncoprotein bound to the p53 tumor suppressor transactivation domain. Science 274: 948–953 (1996)
112. Laemmli U K: Cleavage of structural proteins during the assembly of the head of bacteriophage T4. Nature 227: 680–685 (1970)
113. Lane D P: p53, guardian of the genome. Nature 358: 15–16 (1992)
114. Lane D P, Crawford L V: T antigen is bound to a host protein in SV40-transformed cells. Nature 278: 261–263 (1979)
115. Lehmann A R, Niimi A, Ogi T, Brown S, Sabbioneda S, Wing J F, Kannouche P L, Green C M: Translesion synthesis: Y-family polymerases and the polymerase switch. DNA Repair (Amst) 6: 891–899 (2007)
116. Lei J, Qi R, Tang Y, Wang W, Wei G, Nussinov R, Ma B: Conformational stability and dynamics of the cancer-associated isoform Δ133p53β are modulated by p53 peptides and p53-specific DNA. FASEB J 33: 4225–4235 (2019)
117. Lerner L K, Francisco G, Soltys D T, Rocha C R R, Quinet A, Vessoni A T, Castro L P, David T I P, Bustos S O, Strauss B E, Gottifredi V, Stary A, Sarasin A, Chammas R, Menck C F M: Predominant role of DNA polymerase eta and p53-dependent translesion synthesis in the survival of ultraviolet-irradiated human cells. Nucleic Acids Res 45: 1270–1280 (2017)
118. Leung W, Baxley R M, Moldovan G L, Bielinsky A K: Mechanisms of DNA damage tolerance: post-translational regulation of PCNA. Genes 10: 10 (2019)
119. Levine A J, Oren M: The first 30 years of p53: growing ever more complex. Nat Rev Cancer 9: 749-758 (2009)
120. Linzer D I, Levine A J: Characterization of a 54K dalton cellular SV40 tumor antigen present in SV40-transformed cells and uninfected embryonal carcinoma cells. Cell 17: 43–52 (1979)
121. Liu G, Chen X: DNA polymerase eta, the product of the xeroderma pigmentosum variant gene and a target of p53, modulates the DNA damage checkpoint and p53 activation. Mol Cell Biol 26: 1398–1413 (2006)
122. Livneh Z: Keeping mammalian mutation load in check: Regulation of the activity of error-prone DNA polymerases by p53 and p21. Cell Cycle 5: 1918–1922 (2006)
123. Lupardus P J, Byun T, Yee M C, Hekmat-Nejad M, Cimprich K A: A requirement for replication in activation of the ATR-dependent DNA damage checkpoint. Genes Dev 16: 2327–2332 (2002)
124. Maier B, Gluba W, Bernier B, Turner T, Mohammad K, Guise T, Sutherland A, Thorner M, Scrable H: Modulation of mammalian life span by the short isoform of p53. Genes Dev 18: 306–319 (2004)
125. Makridakis N M, Reichardt J K V: Translesion DNA polymerases and cancer.

Front Genet 3: 174 (2012)
126. Malkin D, Li F P, Strong L C, Fraumeni J F J, Nelson C E, Kim D H, Kassel J, Gryka M A, Bischoff F Z, Tainsky M A: Germ line p53 mutations in a familial syndrome of breast cancer, sarcomas, and other neoplasms. Science 250: 1233–1238 (1990)
127. Mansilla S F, Bertolin A P, Bergoglio V, Pillaire M J, González Besteiro M A, Luzzani C, Miriuka S G, Cazaux C, Hoffmann J S, Gottifredi V: Cyclin Kinase-independent role of p21CDKN1A in the promotion of nascent DNA elongation in unstressed cells. Elife 5: e18020 (2016)
128. Marcel V, Fernandes K, Terrier O, Lane D P, Bourdon J C: Modulation of p53β and p53γ expression by regulating the alternative splicing of TP53 gene modifies cellular response. Cell Death Differ 21: 1377–1387 (2014)
129. Matlashewski G, Lamb P, Pim D, Peacock J, Crawford L, Benchimol S: Isolation and characterization of a human p53 cDNA clone: expression of the human p53 gene. EMBO J 3: 3257–3262 (1984)
130. Maya-Mendoza A, Moudry P, Merchut-Maya J M, Lee M, Strauss R, Bartek J: High speed of fork progression induces DNA replication stress and genomic instability. Nature 559: 279–284 (2018)
131. Mazouzi A, Velimezi G, Loizou J I: DNA replication stress: Causes, resolution and disease. Exp Cell Res 329: 85-93 (2014)
132. McIntyre J: Polymerase iota - an odd sibling among Y family polymerases. DNA Repair (Amst) 86: 102753 (2020)
133. McKinney K, Mattia M, Gottifredi V, Prives C: p53 linear diffusion along DNA requires its C terminus. Mol Cell 16: 413–424 (2004)
134. Meek D W, Anderson C W: Posttranslational modification of p53: cooperative integrators of function. Cold Spring Harb Perspect Biol 1: a000950 (2009)
135. Melero J A, Stitt D T, Mangel W F, Carroll R B: Identification of new polypeptide species (48-55K) immunoprecipitable by antiserum to purified large T antigen and present in SV40-infected and -transformed cells. Virology 93: 466–480 (1979)
136. Michael W M, Ott R, Fanning E, Newport J: Activation of the DNA replication checkpoint through RNA synthesis by primase. Science 289: 2133–2137 (2000)
137. Milićević Z, Bajić V, Živković L, Kasapović J, Andjelković U, Spremo-Potparević B: Identification of p53 and its isoforms in human breast carcinoma cells. Sci World J 2014: 618698 (2014)
138. Mobaraki R N, Karimi M, Alikarami F, Farhadi E, Amini A, Bashash D, Paridar M, Kokhaei P, Rezvani M R, Kazemi A, Safa M: RITA induces apoptosis in p53-null K562 leukemia cells by inhibiting STAT5, Akt, and NF-κB signaling pathways. Anticancer Drugs 29: 847–853 (2018)
139. Moldovan G L, Pfander B, Jentsch S: PCNA, the Maestro of the Replication Fork. Cell 129: 665-679 (2007)
140. Moll U M, Petrenko O: The MDM2-p53 Interaction. Mol Cancer Res 1: 1001–

1008 (2003)
141. Mondal A M, Horikawa I, Pine S R, Fujita K, Morgan K M, Vera E, Mazur S J, Appella E, Vojtesek B, Blasco M a, Lane D P, Harris C C: p53 isoforms regulate aging- and tumor-associated replicative senescence in T lymphocytes. J Clin Invest 123: 5247–5257 (2013)
142. Mondal A M, Zhou H, Horikawa I, Suprynowicz F A, Li G, Dakic A, Rosenthal B, Ye L, Harris C C, Schlegel R, Liu X: Δ133P53α, a Natural P53 Isoform, Contributes To Conditional Reprogramming and Long-Term Proliferation of Primary Epithelial Cells. Cell Death Dis 9: 750 (2018)
143. Morten B C, Scott R J, Avery-Kiejda K A: Comparison of the QuantiGene 2.0 assay and real-time RT-PCR in the detection of p53 isoform mRNA expression in formalin-fixed paraffin-embedded tissues- A preliminary study. PLoS One 11: e0165930 (2016)
144. Motegi A, Liaw H J, Lee K Y, Roest H P, Maas A, Wu X, Moinova H, Markowitz S D, Ding H, Hoeijmakers J H J, Myung K: Polyubiquitination of proliferating cell nuclear antigen by HLTF and SHPRH prevents genomic instability from stalled replication forks. Proc Natl Acad Sci U S A 105: 12411–12416 (2008)
145. von Muhlinen N, Horikawa I, Alam F, Isogaya K, Lissa D, Vojtesek B, Lane D P, Harris C C: p53 isoforms regulate premature aging in human cells. Oncogene 37: 2379–2393 (2018)
146. Mummenbrauer T, Janus F, Müller B, Wiesmüller L, Deppert W, Grosse F: P53 Protein Exhibits 3'-To-5' Exonuclease Activity. Cell 85: 1089–1099 (1996)
147. Murray-Zmijewski F, Lane D P, Bourdon J C: p53/p63/p73 isoforms: An orchestra of isoforms to harmonise cell differentiation and response to stress. Cell Death Differ 13: 962–972 (2006)
148. Murray-Zmijewski F, Slee E A, Lu X: A complex barcode underlies the heterogeneous response of p53 to stress. Nat Rev Mol Cell Biol 9: 702–712 (2008)
149. Natan E, Baloglu C, Pagel K, Freund S M V, Morgner N, Robinson C V, Fersht A R, Joerger A C: Interaction of the p53 DNA-binding domain with its n-terminal extension modulates the stability of the p53 tetramer. J Mol Biol 409: 358–368 (2011)
150. Navarro F, Gutman D, Meire E, Cáceres M, Rigoutsos I, Bentwich Z, Lieberman J: miR-34a contributes to megakaryocytic differentiation of K562 cells independently of p53. Blood 114: 2181–2192 (2009)
151. Nieminuszczy J, Schwab R A, Niedzwiedz W: The DNA fibre technique – tracking helicases at work. Methods 108: 92–98 (2016)
152. Nutthasirikul N, Limpaiboon T, Leelayuwat C, Patrakitkomjorn S, Jearanaikoon P: Ratio disruption of the Δ133p53 and TAp53 isoform equilibrium correlates with poor clinical outcome in intrahepatic cholangiocarcinoma. Int J Oncol 42: 1181–1188 (2013)
153. Ohki R, Kawase T, Ohta T, Ichikawa H, Taya Y: Dissecting functional roles of p53 N-terminal transactivation domains by microarray expression analysis.

Cancer Sci 98: 189–200 (2007)
154. Opitz R, Müller M, Reuter C, Barone M, Soicke A, Roske Y, Piotukh K, Huy P, Beerbaum M, Wiesner B, Beyermann M, Schmieder P, Freund C, Volkmer R, Oschkinat H, Schmalz H-G, Kühne R: A modular toolkit to inhibit proline-rich motif-mediated protein-protein interactions. Proc Natl Acad Sci U S A 112: 5011–5016 (2015)
155. Ou Z, Yin L, Chang C, Peng J, Chen J: Protein interaction between p53 and δ113p53 is required for the anti-apoptotic function of δ113p53. J Genet Genomics 41: 53–62 (2014)
156. Owen-Schaub L B, Zhang W, Cusack J C, Angelo L S, Santee S M, Fujiwara T, Roth J A, Deisseroth A B, Zhang W W, Kruzel E: Wild-type human p53 and a temperature-sensitive mutant induce Fas/APO-1 expression. Mol Cell Biol 15: 3032–3040 (1995)
157. Ozretić P, Hanžić N, Proust B, Sabol M, Trnski D, Radić M, Musani V, Ciribilli Y, Milas I, Puljiz Z, Bosnar M H, Levanat S, Slade N: Expression profiles of p53/p73, NME and GLI families in metastatic melanoma tissue and cell lines. Sci Rep 9: 12470 (2019)
158. Parada L F, Land H, Weinberg R A, Wolf D, Rotter V: Cooperation between gene encoding p53 tumour antigen and ras in cellular transformation. Nature 312: 649–651 (1984)
159. Park J-H, Zhuang J, Li J, Hwang P M: p53 as guardian of the mitochondrial genome. FEBS Lett 590: 924–934 (2016)
160. Pavletich N P, Chambers K A, Pabo C O: The DNA-binding domain of p53 contains the four conserved regions and the major mutation hot spots. Genes Dev 7: 2556–2564 (1993)
161. Pcna P, Recognized G, Zeman M K, Cimprich K A: Finally, Polyubiquitinated PCNA Gets Recognized. Mol Cell 333–334 (2012)
162. Pilzecker B, Buoninfante O A, Jacobs H: DNA damage tolerance in stem cells, ageing, mutagenesis, disease and cancer therapy. Nucleic Acids Res 47: 7163–7181 (2019)
163. Pluta A, Nyman U, Joseph B, Robak T, Zhivotovsky B, Smolewski P: The role of p73 in hematological malignancies. Leukemia 20: 757–766 (2006)
164. Prakash S, Johnson R E, Prakash L: EUKARYOTIC TRANSLESION SYNTHESIS DNA POLYMERASES: Specificity of Structure and Function. Annu Rev Biochem 74: 317–353 (2005)
165. Raj N, Attardi L D: The Transactivation Domains of the p53 Protein. Cold Spring Harb Perspect Med 7: a026047 (2017)
166. Restle A, Färber M, Baumann C, Böhringer M, Scheidtmann K H, Müller-Tidow C, Wiesmüller L: Dissecting the role of p53 phosphorylation in homologous recombination provides new clues for gain-of-function mutants. Nucleic Acids Res 36: 5362–5375 (2008)
167. Riley K J L, Maher L J: p53-RNA interactions: New clues in an old mystery. RNA 13: 1825–1833 (2007)

168. Romanova L Y, Willers H, Blagosklonny M V., Powell S N: The interaction of p53 with replication protein A mediates suppression of homologous recombination. Oncogene 23: 9025–9033 (2004)
169. Rosenbluth J M, Mays D J, Jiang A, Shyr Y, Pietenpol J A: Differential regulation of the p73 cistrome by mammalian target of rapamycin reveals transcriptional programs of mesenchymal differentiation and tumorigenesis. Proc Natl Acad Sci U S A 108: 2076–2081 (2011)
170. Sale J E, Lehmann A R, Woodgate R: Y-family DNA polymerases and their role in tolerance of cellular DNA damage. Nat Rev Mol Cell Biol 13: 141–152 (2012)
171. Dos Santos N M, De Oliveira G A P, Rocha M R, Pedrote M M, Da Silva Ferretti G D, Rangel L P, Morgado-Diaz J A, Silva J L, Gimba E R P: Loss of the p53 transactivation domain results in high amyloid aggregation of the δ40p53 isoform in endometrial carcinoma cells. J Biol Chem 294: 9430–9439 (2019)
172. Sauer M, Bretz A C, Beinoraviciute-Kellner R, Beitzinger M, Burek C, Rosenwald A, Harms G S, Stiewe T: C-terminal diversity within the p53 family accounts for differences in DNA binding and transcriptional activity. Nucleic Acids Res 36: 1900–1912 (2008)
173. Sawhney S, Hood K, Shaw A, Braithwaite A W, Stubbs R, Hung N A, Royds J A, Slatter T L: Alpha-enolase is upregulated on the cell surface and responds to plasminogen activation in mice expressing a Δ133p53α mimic. PLoS One 10: e0116270 (2015)
174. Schindelin J, Arganda-Carreras I, Frise E, Kaynig V, Longair M, Pietzsch T, Preibisch S, Rueden C, Saalfeld S, Schmid B, Tinevez J-Y, White D J, Hartenstein V, Eliceiri K, Tomancak P, Cardona A: Fiji: an open-source platform for biological-image analysis. Nat Methods 9: 676–682 (2012)
175. Sengupta S, Harris C C: p53: Traffic cop at the crossroads of DNA repair and recombination. Nat Rev Mol Cell Biol 6: 44–55 (2005)
176. Sharathchandra A, Katoch A, Das S: IRES mediated translational regulation of p53 isoforms. Wiley Interdiscip Rev RNA 5: 131–139 (2014)
177. Shiloh Y, Ziv Y: The ATM protein kinase: regulating the cellular response to genotoxic stress, and more. Nat Rev Mol Cell Biol 14: 197–210 (2013)
178. Silden E, Hjelle S M, Wergeland L, Sulen A, Andresen V, Bourdon J C, Micklem D R, McCormack E, Gjertsen B T: Expression of TP53 Isoforms p53β or p53γ Enhances Chemosensitivity in TP53null Cell Lines. PLoS One 8: e56276 (2013)
179. Slatter T L, Hung N, Bowie S, Campbell H, Rubio C, Speidel D, Wilson M, Baird M, Royds J A, Braithwaite A W: Δ122P53, a Mouse Model of Δ133P53A, Enhances the Tumor-Suppressor Activities of an Attenuated P53 Mutant. Cell Death Dis 6: e1783 (2015)
180. Slatter T L, Hung N, Campbell H, Rubio C, Mehta R, Renshaw P, Williams G, Wilson M, Engelmann A, Jeffs A, Royds J A, Baird M A, Braithwaite A W:

Hyperproliferation, cancer, and inflammation in mice expressing a Δ133p53-like isoform. Blood 117: 5166–5177 (2011)
181. Smith A E, Smith R, Paucha E: Characterization of different tumor antigens present in cells transformed by simian virus 40. Cell 18: 335–346 (1979)
182. Söderberg O, Leuchowius K J, Gullberg M, Jarvius M, Weibrecht I, Larsson L G, Landegren U: Characterizing proteins and their interactions in cells and tissues using the in situ proximity ligation assay. Methods 45: 227–232 (2008)
183. Sogo J M, Lopes M, Foiani M: Fork reversal and ssDNA accumulation at stalled replication forks owing to checkpoint defects. Science 297: 599–602 (2002)
184. Song W, Huo S W, Lü J J, Liu Z, Fang X L, Jin X B, Yuan M Z: Expression of p53 isoforms in renal cell carcinoma. Chin Med J (Engl) 122: 921–926 (2009)
185. Speroni J, Federico M B, Mansilla S F, Soria G, Gottifredi V: Kinase-independent function of checkpoint kinase 1 (Chk1) in the replication of damaged DNA. Proc Natl Acad Sci U S A 109: 7344–7349 (2012)
186. Srivastava S, Zou Z Q, Pirollo K, Blattner W, Chang E H: Germ-line transmission of a mutated p53 gene in a cancer-prone family with Li-Fraumeni syndrome. Nature 348: 747–749 (1990)
187. Stelter P, Ulrich H D: Control of spontaneous and damage-induced mutagenesis by SUMO and ubiquitin conjugation. Nature 425: 188-191 (2003)
188. Stenger J E, Tegtmeyer P, Mayr G A, Reed M, Wang Y, Wang P, Hough P V, Mastrangelo I A: p53 oligomerization and DNA looping are linked with transcriptional activation. EMBO J 13: 6011–6020 (1994)
189. Sullivan K D, Galbraith M D, Andrysik Z, Espinosa J M: Mechanisms of transcriptional regulation by p53. Cell Death Differ 25: 133–143 (2018)
190. Takahashi R, Giannini C, Sarkaria J N, Schroeder M, Rogers J, Mastroeni D, Scrable H: p53 isoform profiling in glioblastoma and injured brain. Oncogene 32: 3165–3174 (2013)
191. Takahashi R, Markovic S N, Scrable H J: Dominant effects of Δ40p53 on p53 function and melanoma cell fate. J Invest Dermatol 134: 791–800 (2014)
192. Toledo F, Krummel K A, Lee C J, Liu C-W, Rodewald L-W, Tang M, Wahl G M: A mouse p53 mutant lacking the proline-rich domain rescues Mdm4 deficiency and provides insight into the Mdm2-Mdm4-p53 regulatory network. Cancer Cell 9: 273–285 (2006)
193. Towbin H, Staehelin T, Gordon J: Electrophoretic transfer of proteins from polyacrylamide gels to nitrocellulose sheets: procedure and some applications. Proc Natl Acad Sci U S A 76: 4350–4354 (1979)
194. Tu Q, Gong H, Yuan C, Liu G, Huang J, Li Z, Luo J: Δ133p53/FLp53 Predicts Poor Clinical Outcome in Esophageal Squamous Cell Carcinoma. Cancer Manag Res 12: 7405–7417 (2020)
195. Ulrich H D: Two RING finger proteins mediate cooperation between ubiquitin-conjugating enzymes in DNA repair. EMBO J 19: 3388–3397 (2000)
196. Ungewitter E, Scrable H: Δ40p53 controls the switch from pluripotency to

differentiation by regulating IGF signaling in ESCs. Genes Dev 24: 2408–2419 (2010)
197. Unk I, Hajdú I, Blastyák A, Haracska L: Role of yeast Rad5 and its human orthologs, HLTF and SHPRH in DNA damage tolerance. DNA Repair (Amst) 9: 257–267 (2010)
198. Vaughan C, Pearsall I, Yeudall A, Deb S P, Deb S: p53: Its mutations and their impact on transcription. Subcell Biochem 85: 71–90 (2014)
199. Venot C, Maratrat M, Dureuil C, Conseiller E, Bracco L, Debussche L: The requirement for the p53 proline-rich functional domain for mediation of apoptosis is correlated with specific PIG3 gene transactivation and with transcriptional repression. EMBO J 17: 4668–4679 (1998)
200. Vieler M, Sanyal S: p53 Isoforms and Their Implications in Cancer. Cancers (Basel) 10: 288 (2018)
201. Vousden K H, Prives C: Blinded by the Light: The Growing Complexity of p53. Cell 137: 413–431 (2009)
202. Vujanovic M, Krietsch J, Raso M C, Terraneo N, Zellweger R, Schmid J A, Taglialatela A, Huang J W, Holland C L, Zwicky K, Herrador R, Jacobs H, Cortez D, Ciccia A, Penengo L, Lopes M: Replication Fork Slowing and Reversal upon DNA Damage Require PCNA Polyubiquitination and ZRANB3 DNA Translocase Activity. Mol Cell 67: 882–890 (2017)
203. Walker K K, Levine A J: Identification of a novel p53 functional domain that is necessary for efficient growth suppression. Proc Natl Acad Sci U S A 93: 15335–15340 (1996)
204. Walter J, Newport J: Initiation of eukaryotic DNA replication: Origin unwinding and sequential chromatin association of Cdc45, RPA, and DNA polymerase α. Mol Cell 5: 617–627 (2000)
205. Warbrick E: The puzzle of PCNA's many partners. Bioessays 22: 997–1006 (2000)
206. Weston R, Peeters H, Ahel D: ZRANB3 is a structure-specific ATP-dependent endonuclease involved in replication stress response. Genes Dev 26: 1558–1572 (2012)
207. Wienken M, Dickmanns A, Nemajerova A, Kramer D, Najafova Z, Weiss M, Karpiuk O, Kassem M, Zhang Y, Lozano G, Johnsen S A, Moll U M, Zhang X, Dobbelstein M: MDM2 Associates with Polycomb Repressor Complex 2 and Enhances Stemness-Promoting Chromatin Modifications Independent of p53. Mol Cell 61: 68–83 (2016)
208. Williams A B, Schumacher B: p53 in the DNA-damage-repair process. Cold Spring Harb Perspect Med 6: a026070 (2016)
209. Wolf D, Harris N, Goldfinger N, Rotter V: Isolation of a full-length mouse cDNA clone coding for an immunologically distinct p53 molecule. Mol Cell Biol 5: 127–132 (1985)
210. Wolf D, Harris N, Rotter V: Reconstitution of p53 expression in a nonproducer Ab-MuLV-transformed cell line by transfection of a functional p53 gene. Cell

38: 119–126 (1984)
211. Wolf D, Rotter V: Major deletions in the gene encoding the p53 tumor antigen cause lack of p53 expression in HL-60 cells. Proc Natl Acad Sci U S A 82: 790–794 (1985)
212. Wright P E, Dyson H J: Intrinsically disordered proteins in cellular signalling and regulation. Nat Rev Mol Cell Biol 16: 18–29 (2015)
213. Xie N, Chen M, Dai R, Zhang Y, Zhao H, Song Z, Zhang L, Li Z, Feng Y, Gao H, Wang L, Zhang T, Xiao R P, Wu J, Cao C M: SRSF1 promotes vascular smooth muscle cell proliferation through a Δ133p53/EGR1/KLF5 pathway. Nat Commun 8: 16016 (2017)
214. Xiong Y, Hannon G J, Zhang H, Casso D, Kobayashi R, Beach D: p21 is a universal inhibitor of cyclin kinases. Nature 366: 701–704 (1993)
215. Xue Y, Wang S, Feng X: Influence of magnesium ion on the binding of p53 DNA-binding domain to DNA-response elements. J Biochem 146: 77–85 (2009)
216. Yin Y, Stephen C W, Luciani M G, Fåhraeus R: P53 Stability and Activity Is Regulated By Mdm2-Mediated Induction of Alternative P53 Translation Products. Nat Cell Biol 4: 462–467 (2002)
217. Yu H, Chen J K, Feng S, Dalgarno D C, Brauer A W, Schreiber S L: Structural basis for the binding of proline-rich peptides to SH3 domains. Cell 76: 933–945 (1994)
218. Zang Y, Shi Y, Liu K, Qiao L, Guo X, Chen D: Δ40p53 is involved in the inactivation of autophagy and contributes to inhibition of cell death in HCT116-Δ40p53 cells. Oncotarget 8: 12754–12763 (2017)
219. Zhang H, Zhao Y, Sun P, Zhao M, Su Z, Jin X, Song W: p53β: A new prognostic marker for patients with clear-cell renal cell carcinoma from 5.3 years of median follow-up. Carcinogenesis 39: 368–374 (2018)
220. Zhao L, Todd Washington M: Translesion synthesis: Insights into the selection and switching of DNA polymerases. Genes (Basel) 8: 24 (2017)
221. Zhou J, Ahn J, Wilson S H, Prives C: A role for p53 in base excision repair. EMBO J 20: 914–923 (2001)
222. Zou L, Elledge S J: Sensing DNA damage through ATRIP recognition of RPA-ssDNA complexes. Science 300: 1542–1548 (2003)
223. Zou L, Liu D, Elledge S J: Replication protein A-mediated recruitment and activation of Rad17 complexes. Proc Natl Acad Sci U S A 100: 13827–13832 (2003)

7 Appendix

7.1 List of figure/table citations

Figure 1 is based on Bi X: Mechanism of DNA damage tolerance. World J Biol Chem 6: 48–56 (2015) [23].

Figure 2 is based on Bi X: Mechanism of DNA damage tolerance. World J Biol Chem 6: 48–56 (2015) [23] and Pilzecker B, Buoninfante O A, Jacobs H: DNA damage tolerance in stem cells, ageing, mutagenesis, disease and cancer therapy. Nucleic Acids Res 47: 7163–7181 (2019) [162].

Figure 3 is based on Hampp S, Kiessling T, Buechle K, Mansilla S F, Thomale J, Rall M, Ahn J, Pospiech H, Gottifredi V, Wiesmüller L: DNA damage tolerance pathway involving DNA polymerase ι and the tumor suppressor p53 regulates DNA replication fork progression. Proc Natl Acad Sci U S A 113: E4311–E4319 (2016) [83].

Figure 4 is based on Vieler M, Sanyal S: p53 Isoforms and Their Implications in Cancer. Cancers (Basel) 10: 288 (2018) [200] and Anbarasan T, Bourdon J C: The emerging landscape of p53 isoforms in physiology, cancer and degenerative diseases. Int J Mol Sci 20: 6257 (2019) [5].

Table 1 is based on Anbarasan T, Bourdon J C: The emerging landscape of p53 isoforms in physiology, cancer and degenerative diseases. Int J Mol Sci 20: 6257 (2019) [5].

Table 2 is based on Vieler M, Sanyal S: p53 Isoforms and Their Implications in Cancer. Cancers (Basel) 10: 288 (2018) [200] and Anbarasan T, Bourdon J C: The emerging landscape of p53 isoforms in physiology, cancer and degenerative diseases. Int J Mol Sci 20: 6257 (2019) [5].

Figure 6-16,18,19 were published in Guo Y, Rall-Scharpf M, Bourdon J-C, Wiesmüller L, Biber S: p53 isoforms differentially impact on the POLι dependent DNA damage tolerance pathway. Cell Death Dis 12: 941 (2021) [79].

8 Acknowledgement

During my study in Ulm and my research for MD degree, I would like to appreciate a lot of people who have ever helped me, their support and understanding are the bases of my work here. Though four years are a long time, the most important things are whom I met, what I did and what I have learnt.

First of all, I would like to show gratitude to my supervisor Prof. Dr. Lisa Wiesmüller who offered me the opportunity to do research and finish my MD thesis in this lab with adequate facilities and guidance. During my study here, I was able to learn a lot of things including knowledge on p53, DNA replication and DNA repair. And with her knowledge, I was able to be more understandable in my project. All these qualities of her made her an outstanding professor and a great supervisor.

Subsequently, I would like to say thanks to Dr. Stephanie Biber. She offered me lots of assistance in my study and work. In my whole study period, she helped me a lot in student affairs. Moreover, she taught me how to perform experiments and knowledge related to the project as well as helping me elucidate my results. When I had some obstacles, she was willing to help in time. I think she is a good teacher and a scientist with potential.

In addition, thanks to my lab members who offered me a lot of help. Whenever I was in trouble, I can always find people who are willing to help me and solve my questions. I am very sorry that I could not mention all your names in person. But thanks to all of you, for all your help, for your patience, for your understanding.

Thanks for Dr. Jean-Christophe Bourdon from University of Dundee who provided the expression plasmids of p53 isoforms.

Thanks China Scholarship Council for offering me the scholarships to support my life and work.

Finally, thanks to my family, my friends, they gave me a lot of power and we have great time in Germany.

All of you who helped me in life, in work, deserve my appreciation, thank you!

9 Curriculum vitae

For protection of author’s privacy, this part is not published.